RAINDROP SIZE DISTRIBUTION RETRIEVAL AND EVALUATION USING AN S-BAND RADAR PROFILER

by

FANG FANG

B.S.E.E. University of Central Florida, 2003

A thesis submitted in partial fulfillment of the requirements
for the degree of Master of Science
in the Department of Electrical and Computer Engineering
in the College of Engineering and Computer Science
at the University of Central Florida
Orlando, Florida

Summer Term

2004

ABSTRACT

Vertical pointing Doppler radar profilers are used to explore the vertical structure of precipitation cloud systems and to provide validation information for use in weather research. In this thesis, a theoretical radar rain-backscatter model was developed to simulate profiler Doppler spectra as a function of assumed rain parameters, of which the raindrop size distribution (DSD) is the fundamental quantity used to describe the characteristics of rain. Also, profiler observations during stratiform rain are analyzed to retrieve the corresponding rain DSD's. In particular, a gamma distribution model is introduced, which uses Rayleigh scattering portion of the Doppler velocity spectrum to estimate the raindrop size distribution.

This theoretical scattering model was validated by simulating atmospheric profiles of precipitation Doppler spectra and three moments (reflectivity, mean Doppler velocity and spectral width) and then comparing these with the corresponding measurements from an S-band radar profiler during a NASA conducted Tropical Rainfall Measuring Mission (TRMM) field experiment in Central Florida in 1998. Also, the results of my analysis yielding precipitation retrievals are validated with an independent, simultaneous Joss-Waldvogel Disdrometer rain DSD observations that were collocated with the radar profiler.

ACKNOWLEDGMENTS

First of all, I would like to thank my advisor Dr. Linwood Jones for his guidance and support on this project. Secondly, I give thanks to the members of my committee, Dr. Takis Kasparis and Dr. Brian Lail for their interests in my work. This thesis project has heavily relied upon the guidance from NOAA Aeronomy Laboratory CIRES Research Scientist, Dr. Christopher R. Williams. He has provided me with necessary resources and program code for this project. Here I would like to express my sincere gratitude to him. Without Dr. Williams, this thesis would not be possible. Finally, I would like to thank my friends and families, especially to my husband Bob for his great support, encouragement and patient love throughout the years.

This research was partially funded under a grant with the Tropical Rainfall Measuring Mission Project at the NASA Goddard Space Flight Center.

TABLE OF CONTENTS

LIST OF FIGURES

LIST OF TABLES

CHAPTER 1 INTRODUCTION

Beginning in the 1950s, meteorologists began using Doppler radar to make weather observations. Weather radar exploits backscattered energy from hydrometeors (rain droplets, ice and snow) and Doppler effects from their motion to detect severe weather conditions such as thunderstorms, tornadoes, and snow storms. Accurate weather forecasting using meteorological radar has significant importance in our life; and in the 1980's, the US National Weather Service installed a Doppler radar network across the country, which is known as the Next Generation Weather Radars (NEXRAD). These ground based scanning radars track weather systems on a synoptic scale, but it is increasingly clear that improvements are needed to get reliable local measurements to properly present and validate numerical models of hydrological cycle [1]. In the early 1960s, radar meteorologists acknowledged the potential of retrieving cloud and precipitation properties from Doppler spectra collected from vertically pointing radars [2]. The vertical pointing radars, known as Doppler radar profilers, provide spatial and temporal information of precipitation vertical profiles that can be used as calibration tools for scanning radars.

This thesis is organized as follows:

1. Chapter 1 begins with a tutorial on meteorological radars and Doppler measurements.
2. Chapter 2 introduces the S-band radar profiler used in this thesis and scattering theory.
3. Chapter 3 discusses rain**d**rop **s**ize **d**istribution (DSD), which is the parameter that is of most interest.

4. Chapter 4 explains how the three parameters of a fitted gamma distribution are determined and how they are used to calculate the rain DSD.

5. In chapter 5, the calculated rain parameters such as rain rate, mean rain diameters, and reflectivity from the lowest range gate are compared with simulated reflectivity from simultaneous collocated surface disdrometer observations.

1.1 Radar Basics

The simplified block diagram of a meteorological radar system is shown in Figure 1.1. The transmitter produces a series of pulses of electromagnetic radiation that propagate through space at the speed of light. The radiation is concentrated into a narrow beam by the large aperture antenna that usually scans in the manner of a searchlight beam to search the surrounding air volume for hydrometeors. When the radar beam encounters a volume of water droplets, the transmitted signal (pulse) is reflected back to the antenna, and this is known as a "radar echo". Antenna collects the echoes from individual targets and sends these time-delayed pulses to the receiver. After down-converting the received radio energy to intermediate frequency signals, the echo's frequency is compared to the transmitted frequency to determine the Doppler frequency shift. Using Fourier transform techniques, the Doppler power spectrum is obtained and is used to derive the hydrometeor properties. By measuring the round-trip propagation delay time for each echo, the distance to the target (known as range, R) is determined:

$$\mathrm{R} = \frac{cT_p}{2}, \text{ m} \qquad (1.1)$$

where c is the speed of light in m/s and T_p is the round trip delay time in seconds.

The radar profiler configuration is shown in Figure 1.2 with a parabolic reflector antenna pointed vertically. The beam of radar antenna spread as a conical volume as transmitted pulses propagate. As range increases, the diameter of the cone cross section increases forming a larger pulse volume. The scattering volume is related to the range by:

$$V = p\,(Rb_1/2)(Rb_2/2) \times dR\text{, m}^3 \qquad (1.2)$$

where b_1, b_2 (radian) are the half power beam widths for the orthogonal planes of the antenna and $d\,\mathrm{R}$ is the range gate, or range resolution:

$$d\,\mathrm{R} = \frac{ct}{2}\text{, m} \qquad (1.3)$$

where τ is the transmit pulse width in seconds. The $d\,\mathrm{R}$ is a specified range interval over which the backscattered energy is measured within the scattering volume. Target cross section is calculated using the scattering volume multiplied by the backscattering cross section per unit volume. The radar equation in terms of the target radar cross section is discussed in Chapter 2.

In radar systems, range gates are contiguous intervals of range resolution given by equation 1.3. Also, this equation establishes the minimum range where targets can be detected that is refers to as the first range gate. By measuring the backscattered energy from contiguous range gates, weather radar makes spatial observations in polar coordinates (range versus azimuth).

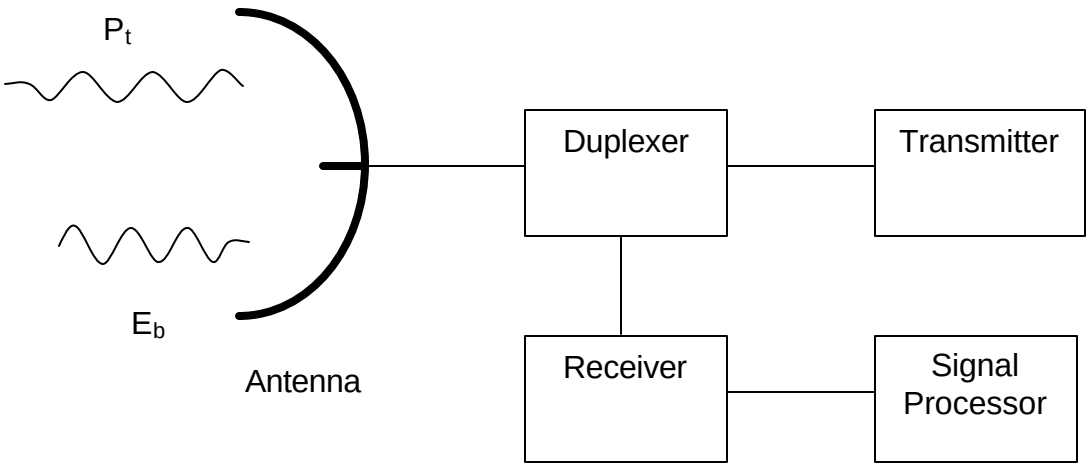

Figure 1.1 Simplified block diagram of a meteorological radar

1.2 Doppler Measurement

In radar meteorology, the targets usually refer to raindrops, snows, ice particles and other cloud systems. Because these targets are in motion from both advection by a moving air mass and vertical velocity (falling) due to the action of gravity, their echoes are measured using pulsed Doppler radar techniques. Doppler radar compares the frequency of the received echo signal with the transmitted signal, and the difference in frequency called Doppler shift is due to the radial velocity of the moving target relative to the radar. As a target moves towards the antenna, the frequency increases; and when a target moves away from the antenna, the frequency decreases. Doppler frequency shift f_D is calculated by:

$$f_D = \frac{2V}{l}, \mathrm{s}^{-1} \qquad (1.4)$$

where V is the radial velocity of the target in m/s (direct away or towards radar), and l is the radar wavelength in meters. Since frequency is the time derivative of phase, Doppler is measured by observing the rate of change of the echo phase. To accomplish this, received signal is split into the two channels, which are synchronously detected by multiplying by sine and cosine signals that are coherently related to the transmitter frequency. These outputs known as in-phase and quadrature (I and Q) channels are the real and imaginary parts of the complex echo phasor. Using these I and Q signals, the echo phase shift relative to the transmitter is determined, and the relative radial velocity of the target can be found. The sum of $I^2 + Q^2$ equals the echo power averaged over the cycle of the signal [3]:

$$A = \sqrt{I^2 + Q^2}, \mathrm{W} \qquad (1.5)$$

where A is the voltage amplitude. The successive values of I and Q pairs measured at equally spaced time intervals (range gates) create a time series sample of the Doppler-shifted signal. Fourier analysis of the time series extracts the backscattered power as a function of Doppler shift frequency. Such a function is the power density spectrum, and also called Doppler spectrum represented by $S(f)$ or in terms of the radial velocity, $S(v)$. It is calculated in the digital processor. The radar profiler Doppler spectrum and spectrum moments are discussed in the next chapter.

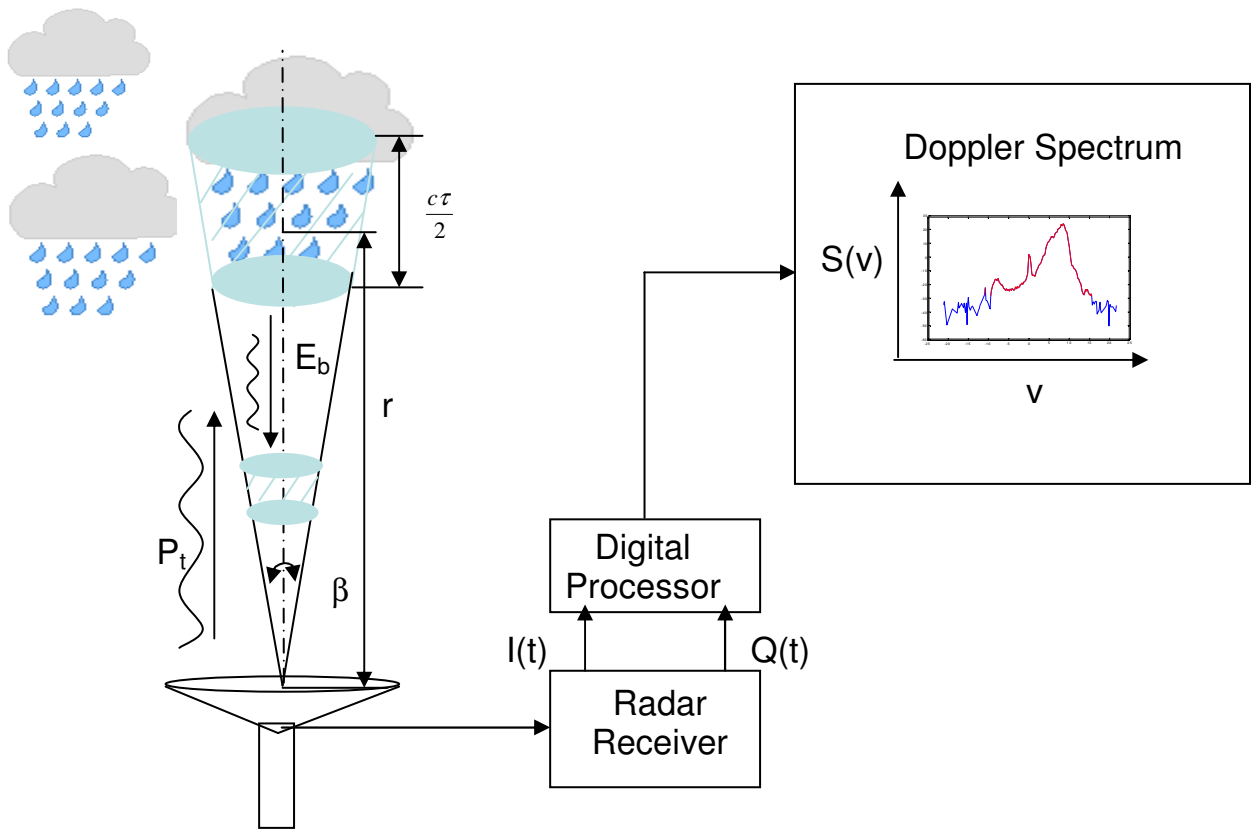

Figure 1.2 Radar profiler configuration

CHAPTER 2 RADAR PROFILER

2.1 Vertical Pointing Profiler

The profiler is a ground based Doppler profiling radar with a fixed antenna beam pointing vertically. The operational frequencies of vertical pointing profilers are usually in the very high frequency (VHF), ultra high frequency (UHF) and low-microwave frequency bands. VHF profilers observe ambient air motion characteristics caused by energy backscattered from perturbations in the radio refractive index (Bragg scattering); but because of their long wavelength, they are quite insensitive to the motion of the hydrometeors due to the weak Rayleigh scattering [4]. Thus, the VHF profiler has the ability to measure air motion in nearly all meteorological conditions. In clear air, the signal power is less than the noise power, so profilers often use relatively longer integration time than scanning meteorological radars. On the other hand, UHF and low-microwave frequency profilers are most sensitive to hydrometers and provide a highly resolved time-height cross section of precipitating cloud system [5]. Profilers retrieve cloud and precipitation properties by processing Doppler spectra to yield three spectral moments including the (zeroth moment) reflectivity, (first moment) mean Doppler velocity of the hydrometers in ambient air and the (second moment about the mean) spectral width. The details on Doppler moments are discussed in section 2.2. In the next section, the S-band profiler used in this thesis is introduced.

2.1.1 S-band Profiler

The S-band profiler used in this study is a low powered Doppler radar operating at a frequency of 2.835 GHz. It has a vertically pointing shrouded-dish antenna to measure Doppler motion of precipitation directly above it and up to a maximum altitude of 10.6 km. A photograph of the S-band profiler antenna is given in Figure 2.1, which shows the antenna half enclosed by a clutter screen, which is used to mitigate the effects of ground clutter to improve the profiler performance. Further, Figure 2.2 shows a simplified conceptual block diagram of the entire system. The transmitter is located in the transmit-receive (T/R) module mounted on the edge of the antenna dish. A 60 MHz local oscillator carrier, derived coherently from the transmitter frequency, is mixed with the received signal; and the received phase coherent signal is converted to baseband and the resulting Q-channels are filtered, amplified and range sampled with 12-bit digitizers. At each sampled range gate, the echo is averaged, sampled and stored to produce a time series of echo amplitude and phase. The S-band profiler operates in two range gate modes, alternating between 60 meters and 105 meters pulse length resolution approximately every 30 seconds of dwell time; but in this research, I have analyzed only the 105 meter observations. The averaged time series are further processed using a Fast Fourier Transform to produce Doppler power spectra of 256 points. The first three spectra moments are produced and stored on disk and displayed in real time. Because of its low-microwave frequency, the S-band profiler is insensitive to hydrometeor attenuation. Further, because of well-understood Rayleigh EM scattering from rain droplets, the profiler interpretation provides a reasonably accurate estimation of rain intensity and provides spatial and temporal information on hydrometeors without using empirical result, such as Z-R relations.

The characteristics of the S-band profiler used in this study are summarized in Table 1.

Table 1.1 S-Band profiler characteristics

Peak power	5 watts
Antenna	3m shrouded dish
Wavelength	10.6 cm
Frequency	2.835 GHz
Beam width	5 degrees
Height resolution delta R	60 m and 105 m
Max height sampled	10.6 km
Spectral points (resolution)	256
Dwell time	30 seconds

Figure 2.1 Photograph of S-band profiler (NOAA Aeronomy Laboratory's S-band profiler during a joint field experiment with the University of Iowa, in Iowa City, Iowa)

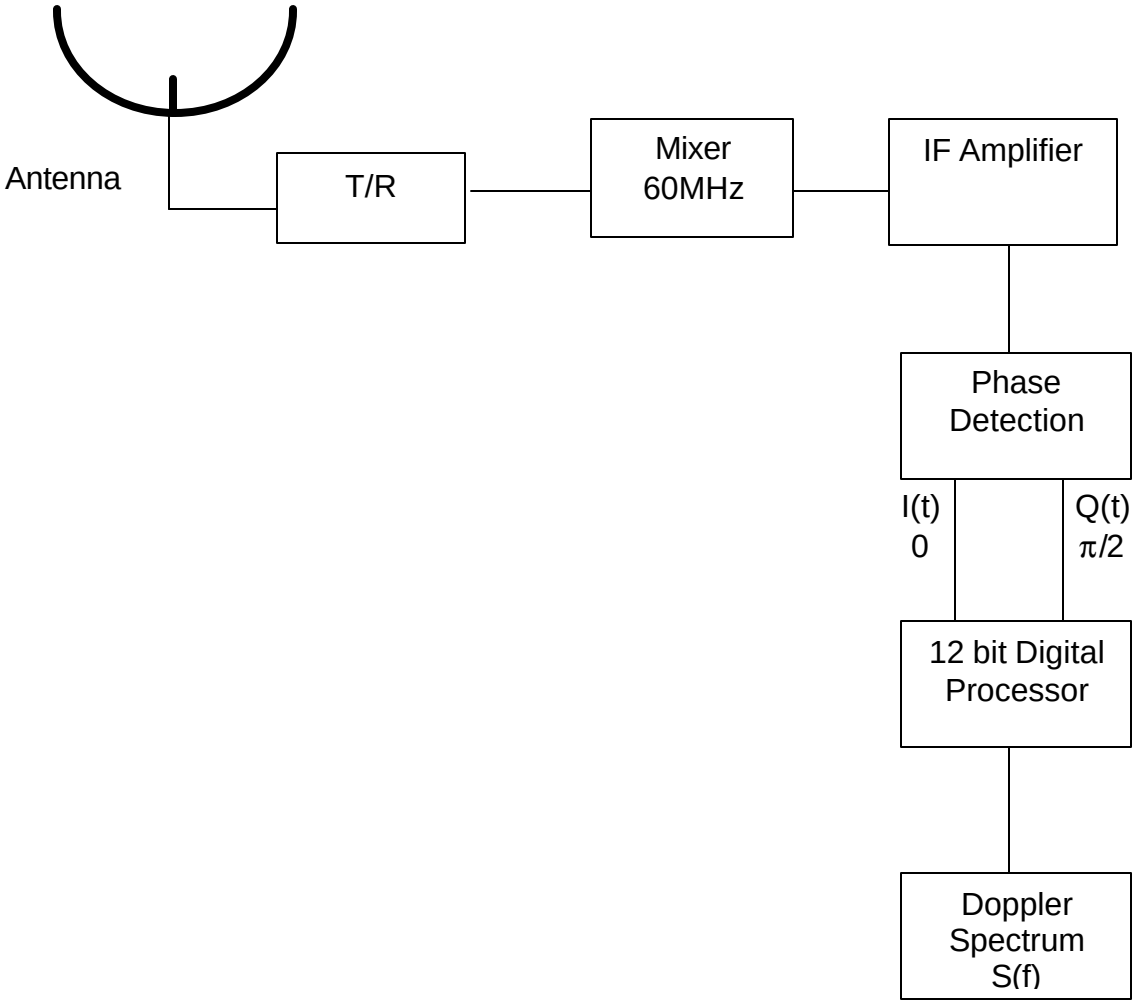

Figure 2.2 Simplified conceptual block diagram of the S-band profiler system.

2.2 Doppler Moments

The Doppler velocity spectrum $S(v)$ is a power-weighted distribution of the radial velocities of the precipitation scatterers [6]. If the Doppler velocity spectrum is scaled correctly, the received power can be estimated as the area under the spectral curve within a frequency range of $v1$ to $v2$ [7]. This is the zeroth moment of the spectrum.

$$p_r = \int_{v1}^{v2} S(v)dv \text{ , W} \qquad (2.1)$$

The mean Doppler velocity is the first moment of the spectra or the first moment of the power-normalized spectra. It can be obtained from:

$$\bar{v} = \frac{\int_{v1}^{v2} vS(v)dv}{\int_{v1}^{v2} S(v)dv} \text{ , m/s} \qquad (2.2)$$

The variance is an important indicator of the spread of Doppler Spectrum. It is the second moment of the spectra (calculated about the mean):

$$s^2 = \frac{\int_{v1}^{v2} (v - \bar{v})^2 S(v) dv}{\int_{v1}^{v2} S(v) dv}, \text{ (m/s)}^2 \qquad (2.3)$$

The spectral width is defined as twice of s :

$$w = 2s \text{ , m/s} \qquad (2.4)$$

2.2.1 Doppler Moment Observations

The next three figures are the three moments produced using S-band profiler data provided by Dr. Chris Williams from NOAA Aronomy Laboratory [8]. These data were obtained during the Tropical Rainfall Measuring Mission (TRMM) **Te**xas and **F**Lorida **Un**derflights (TEFLUN) experiment conducted in Central Florida during 1998. A 5-hour time series of profiler measurements from day 234 (August 22) was selected for use in my thesis. These measurements were obtained during stratiform rain where the vertical air motions were believed to be small, which satisfies the assumptions of the DSD retrieval model developed as a part of my thesis.

The rain reflectivity profile observed by the S-band profiler is shown in Figure 2.3 as a plot of height versus time with reflectivity (dBZ) shown in color. The profiler observations are obtained from a total of 100 range gates, and the altitude goes up to 10 kilometers in vertical. There appears a bright band around 4 kilometers that is the melting level where ice starts to melt

into water. Above melting level, most precipitation is ice or snow particles. As they fall to warmer temperature in the atmosphere approaching the melting level, the ice surface starts melting into liquid water. Radar sees melting ice crystals as large raindrops and reflectivity is associated with the wet ice dielectric constant. The dielectric constant of water is much higher than that of ice, which causes a strong reflectivity at melting level and appears to be a bright band. Also, rain below the melting level can be seen for times between hour 2 and 3. Here the reflectivity of rain is higher than the reflectivity of ice crystals above the melting level. The existence of the melting level is one of the distinguishing characteristic of stratiform rainfall, which separates it from other types of rain as discussed in chapter 3.

The profiler derived mean Doppler velocity is shown in Figure 2.4 as a plot of altitude-time with false-color for the mean Doppler velocity. Doppler velocity results from the terminal fall-speed of the hydrometeors and the vertical air motion (assumed to be negligible in this thesis). The sign convention is that positive is upward velocity. The melting level can also be seen in the Doppler where ice and snow particles, falling into the warmer atmosphere, melt into liquid at around 4 kilometers. It appears to be a bright band indicating the transition from slow fall velocity of ice crystals (1 to 2 m/s) at high altitudes to higher fall velocity of raindrops (5m/s to 8 m/s) below 4 kilometers. The terminal velocity varies with raindrop diameter which causes the observed change in color (velocity) in time as the intensity of rain changes the drop sizes.

Spectral Width (Figure 2.5) represents the variability of the Doppler velocity. Small values indicate that the particle size distribution is relatively narrow, while large values of spectrum width indicate a broad particle size distribution or possibly atmospheric air motion turbulence. Above the freezing level the spectral width is small, the ice and snow particles fall at a lower rate. Below the melting level rain exists, and there are larger variations in velocities due

to the raindrop sizes present. Spectral width can be used as a discriminator to separate rain from frozen precipitation regions.

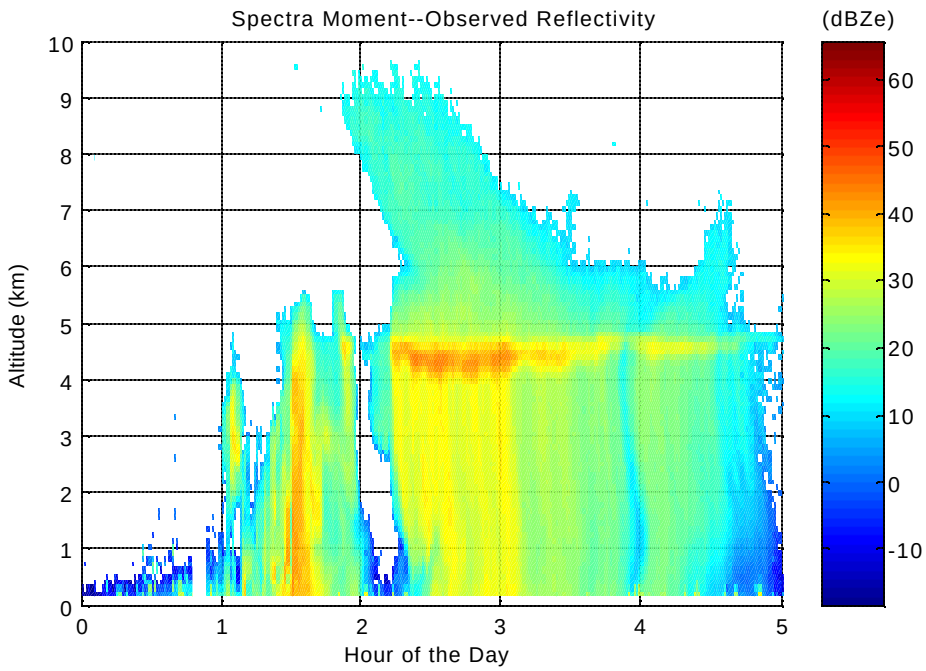

Figure 2.3 Observed spectral reflectivity moment from S-band profiler

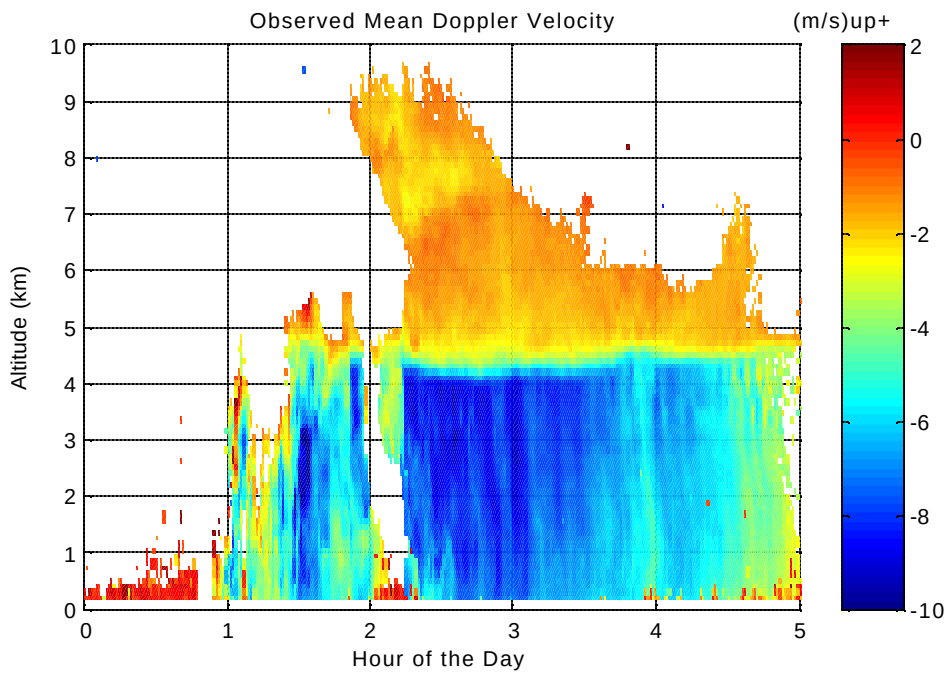

Figure 2.4 Observed spectral mean Doppler velocity moment from S-band profiler

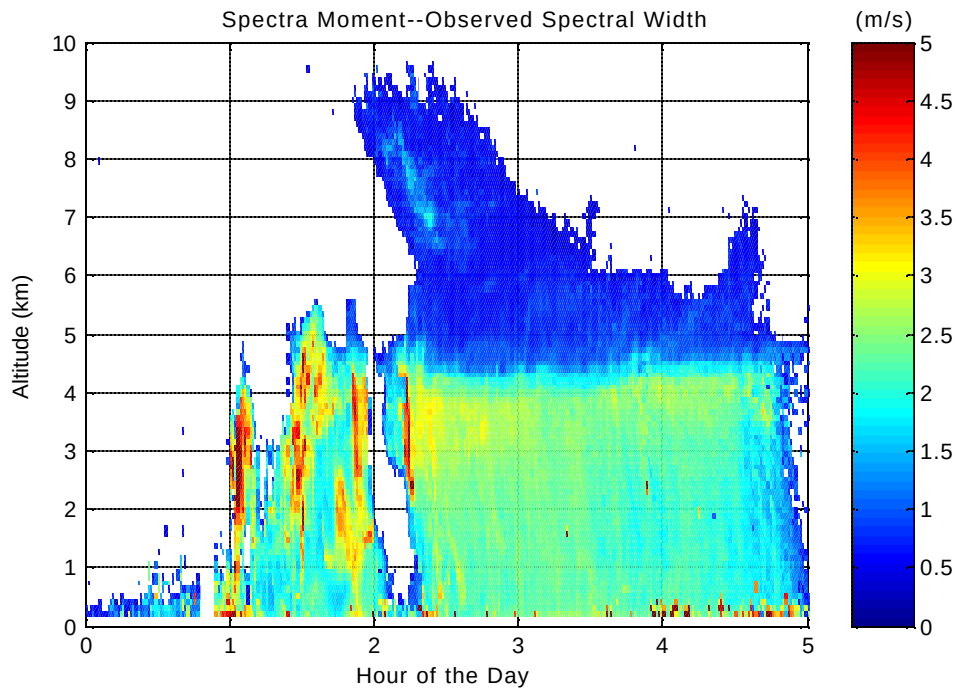

Figure 2.5 Observed spectral width moment from S-band profiler

2.3 EM Scattering Theory

When EM radiation encounters an object (or medium), it will be absorbed, scattered or transmitted. Electromagnetic waves can transmit energy through atmosphere comprised of gas molecules with little or no attenuation, but when it encounters precipitation particles, some of the energy is absorbed and some is scattered. If we assume an arbitrary particle is a single dipole, the incident electromagnetic field induces dipole oscillations at the frequency of the field causing the particle to scatter radiation in all directions. Rayleigh approximation explains the nature of the backscattered radar signal if the target size is much smaller than the incident wave wavelength (e.g., $D \leq l/16$). For a single scatterer, the amount of Rayleigh scattering that occurs is dependent upon the EM wavelength, particle size, and the dielectric constant of the particle. At the wavelength of the S-band profiler, liquid water precipitation (rain droplets) are Rayleigh scatterers. Next section describes how radar equation is used in Rayleigh region for volume backscattering and how the forward model developed in this thesis is related to rain reflectivity.

2.4 The Weather Radar Equation

A simple form of radar equation for a "point target" [9] is used to relate the dependence of the received echo power (P_r) on the radar parameters; transmit power (P_t), antenna gain (G) and effective aperture (A_e), and the target range (R) and the target radar cross section (σ_i)

$$P_r = \frac{P_t G A_e s_i}{(4p)^2 R^4} \text{ , W} \qquad (2.5)$$

The effective area of the receiving antenna can be related to antenna gain $G = \frac{4pA_e}{l^2}$, then equation 2.5 becomes:

$$P_r = \frac{P_t G^2 l^2 s_i}{(4p)^3 R^4} \text{ , W} \qquad (2.6)$$

However, for the meteorological target, such as rainfall the target is not a single scatterer; rather, the radar beam illuminates a volume containing a large group of raindrops. Thus, the range gate defines the measurement volume V in terms of the antenna beam widths (in orthogonal planes) and the transmit pulse length τ of the radar [7],

$$V = p\,(\frac{Rb_1}{2})(\frac{Rb_2}{2})(\frac{ct}{2}) \text{ , m}^3 \qquad (2.7)$$

Within this volume, each raindrop backscatters some energy, and if we assume raindrops are randomly distributed and do not interact (no multiple scattering), the total backscattering cross section is the sum of the individual cross section of rain drops. Thus, the backscattering cross section per unit volume is defined. It is also called radar reflectivity η, in units of $m^2 m^{-3}$. Since Rayleigh scattering applies, η is related to the summation of the sixth power of the diameters over a unit volume [7]:

$$h = 10^{-10} \frac{p^5}{l^4} |K_w|^2 \sum_{vol.} D^6 \text{ , m}^2/\text{m}^3 \qquad (2.8)$$

where $|K_w|^2$ is a coefficient related to the dielectric constant of water

$$K_w = \frac{n^2 - 1}{n^2 + 2} \qquad (2.9)$$

where n is the complex index of refraction of the droplet relative to the air background; taken n=8.87-j 0.628 at 3GHz from [10], $|K_w|^2 \approx$ 0.93 for liquid water.

$\sum_{vol.} D^6$ in equation 2.8 is the summation of the sixth power of all drop diameters per unit volume. It defines the radar reflectivity factor Z, in unit of $mm^6 m^{-3}$. We can rewrite radar reflectivity as [10]:

$$h = 10^{-10} \frac{p^5}{l^4} |K_w|^2 Z \text{ , m}^2/\text{m}^3 \qquad (2.10)$$

If reflectivity is approximately uniform over the backscattering volume V, the backscattered cross section of scattering volume can be defined as

$$s = hV \text{ , m}^2 \qquad (2.11)$$

Now we can replace the σ_i in equation 2.5 with σ to express the received power due to backscattering from volume-distributed scatterers as radar equation:

$$P_r = \frac{P_t G^2 l^2 s}{(4p)^3 R^4} \text{ , W} \qquad (2.12)$$

Let X be a constant in radar equation, such that

$$X = \frac{P_t G^2 l^2}{(4p)^3} \qquad (2.13)$$

Based equation 2.11, we can replace σ in radar equation 2.12 with the product of equation 2.7 and 2.10 to get a proportionality between the received power and reflectivity factor

$$P_r \propto X \frac{|K_w|^2 Z}{R^2} \qquad (2.14)$$

Equation 2.14 can be rewrite as the weather radar equation [7],

$$P_r = C|K_w|^2 \frac{Z}{R^2} \text{, W} \qquad (2.15)$$

where C is the radar constant depending on the characteristics of the radar.

2.4.1 Effective Radar Reflectivity Factor

The use of radar reflectivity factor Z is only valid for Rayleigh scattering and spherical raindrops, but this is not always the case. Hence, it is common to replace Z with the effective radar reflectivity factor Z_e [7]. It is more appropriate to express the actual observed P_r as:

$$P_r = C\left|K_w\right|^2 \frac{Z_e}{R^2}, \text{W} \qquad (2.16)$$

Z_e has the same unit as Z ($mm^6 m^{-3}$), but practical radar reflectivity may span several orders of magnitude, so a logarithmic scale of Z_e is introduced [3] and is expressed in unit of dBZ.

$$dBZ = 10\log_{10}\left(\frac{Zmm^6 m^{-3}}{1mm^6 m^{-3}}\right) \qquad (2.17)$$

Reflectivity Z and Z-R relationship are discussed in the next chapter.

CHAPTER 3 RAINDROP SIZE DISTRIBUTION

DSD describes the number and size of the precipitation particles, and it can relate rain rate to reflectivity. These parameters are important in understanding the development and evolution of precipitation.

3.1 Rain

Rain is formed by a very complex process, which involves the condensation of water vapor and the coalescence of tiny droplets from clouds. Raindrops are typically two orders of magnitude larger in diameter than cloud droplets [10]. During their fall from clouds to earth's surface, small droplets may coalesce with each other forming bigger drops. Sometimes droplets are surrounded by warm and dry air, and they may evaporate before reaching ground. In general, rain consists of a distribution of drop sizes in the range of 0.5 mm to 8 mm.

3.2 Types of Rain

There are different types of rain with different spatial scales that range from a few kilometers in diameter to a few ten's of kilometers. Among these types, two major ones are convective and stratiform rain. Their characteristics primarily differ in spatial extent, rain drop sizes and in vertical air motion that is instrumental in the rain formation process.

Convective rainfall is usually formed from convective clouds (precipitation cells) in the tropics that are associated with strong up-drafts that carry moisture quickly to high altitudes well above the freezing level. Rain drops form rapidly through collision and accretion with other droplets. Because these rain cells contain frozen precipitation (above the freezing level where the air temperature is < 0 C), they are usually associated with strong electrical activity and lightning; therefore they are commonly called thunder storms, which are characterized by high spatial and temporal intensity gradients [11].

As opposed to the vertical development of convective rain, stratiform rain is formed from stably stratified clouds. Stratiform clouds are horizontally widespread in character, and its rain has extensive horizontal development. In stratiform clouds, precipitation grows in a widespread forced updraft of low magnitude. Raindrops form in stratiform clouds primarily by condensation. Because of a lack of a strong updraft to keep droplets aloft, stratiform rain falls out of the cloud with lower rain rate. Stratiform rain is more uniform in intensity and consists of relatively small raindrops.

Although most rain consists of a combination of the two, identifying the characteristics of rain help the study of rain intensity and raindrop size distribution. Convective rain is generally heavy due to large drop size and high rain intensity. Stratiform rain is a gentle, long lasting rain with no lightning. High reflectivity and reflectivity gradient separate the convective rain from the stratiform rain [11].

3.3 Raindrop Size Distribution (DSD)

Rain comprises drops of many different diameters, which are characterized by a particular rain**d**rop **s**ize **d**istribution (DSD) that provides information on the number and size of

raindrops in a sample. Because the DSD is a unity area distribution, calculated at different resolutions gives different distribution curves, which can be seen in Figure 3.1. Choosing the same rain rate, different scale of drop size interval defines a different probability density function (pdf) of DSD within a unit volume. Thus DSD, usually denoted by $N(D)$ with units of m^{-4}, is a fundamental quantity used to describe the characteristic of rain.

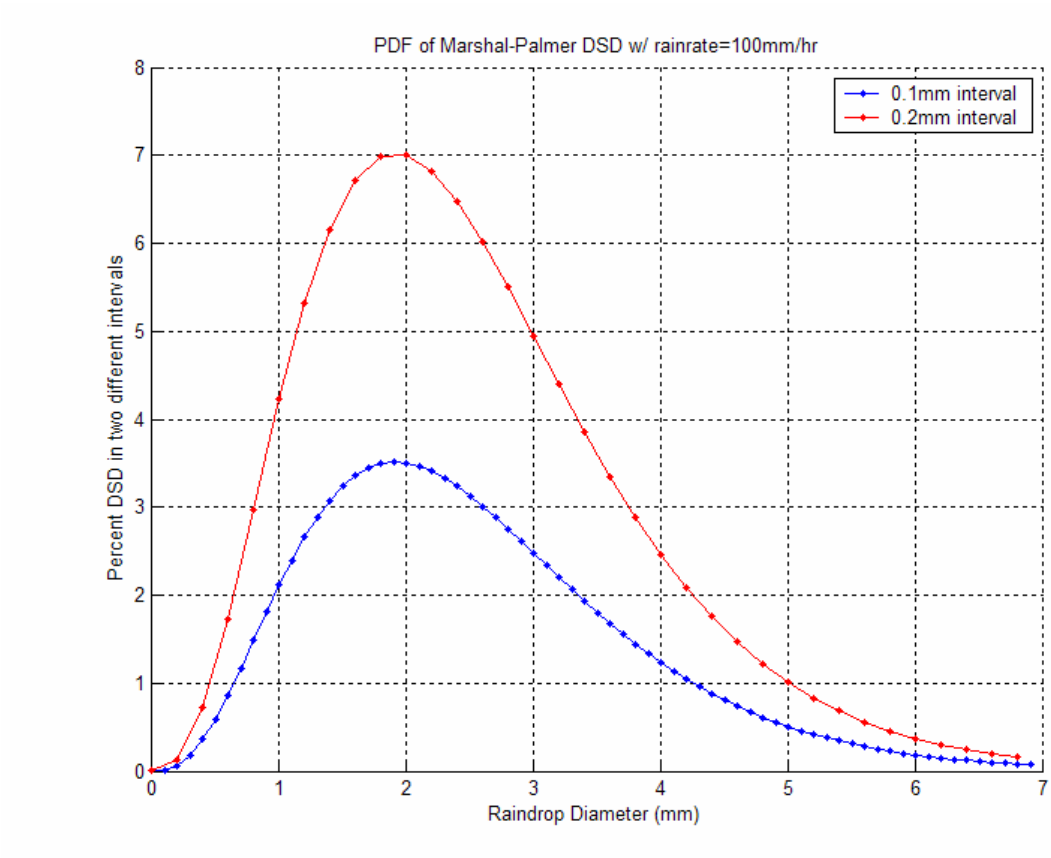

Figure 3.1 PDF of Marshal-Palmer DSDs with diameter interval 0.1 mm and 0.2mm

3.3.1 Marshall-Palmer DSD

The raindrop size distribution has been studied by many investigators and generally modeled as an exponential distribution. The most widely used DSD in scientific literature is Marshall and Palmer [12], which is a special case of the exponential distribution with two fitting parameters N_0 and Λ. Marshall-Palmer DSD is defined as:

$$N(D) = N_0 e^{-\Lambda D}, \text{ m}^{-4} \qquad (3.1)$$

where $N_0 = 8\times10^6 m^{-4}$, D is the drop diameter in unit of meters and Λ is the slope parameter. It is related to rain rate R (mm/hr) as:

$$\Lambda = 4100 R^{-0.21}, \text{ m}^{-1} \qquad (3.2)$$

In many radar studies, Marshall-Palmer DSD are assumed for lack of better information; but in my thesis, I use the modified gamma DSD that will be described later in chapter-4.

3.4 Rain Rate R

Rain rate R is a measure of the intensity of rain by calculating the volume of rain that falls to ground in a given interval of time. The rain rate is expressed in units of length (depth) per unit time (mm/hr), which is the depth of rain captured in a collection vessel per unit time. Figure 3.2 shows a graphical representation of the pdf of Marshall-Palmer DSD with three different rain

rates. As rain intensity increase, the drop size increases. Under stratiform rainfall conditions, the vertical air motion is weak and is usually neglected because its value is generally not known. The error introduced is believed to be small compared to the terminal velocity of most rain drops. Rainfall rate R is related to $N(D)$ [4]:

$$R = \frac{6p}{10^4}\int_0^\infty v(D)D^3 N(D)dD \text{, mm/hr} \qquad (3.3)$$

Where $v(D)$ represents the relationship between the raindrop terminal fall velocity in still air and the equivalent spherical raindrop diameter D (mm). An exponential expression of fall speed to diameter relationship is derived as [13]:

$$v\ (D) = [a_1 - a_2 \exp(-a_3 D)]\left(\frac{r_0}{r}\right)^{0.4} \text{, m/s} \qquad (3.4)$$

where α_1 = 9.65 m/s , α_2 = 10.3 m/s, and α_3 = 0.6 m/s. $\left(\frac{r_0}{r}\right)^{0.4}$ is a density ratio factor adjusting terminal fall speed due to air density change with altitude. Equation 3.4 can be used to estimate the diameter of the raindrops from Doppler motion (when vertical air motion is not present). As drop size increases, the fall velocity increases rapidly and following an exponential curve as shown in Figure 3.3. In my forward model, I have taken the raindrops diameter sizes from 0 to 7mm with 0.1mm size interval as input to calculate the terminal fall velocity. Due to aerodynamic forces, at larger drop diameters surface tension is insufficient to overcome drag

forces. As a result, raindrops larger than 7mm tend to flatten out and break apart into smaller droplets; therefore these diameters do not exist in the DSD.

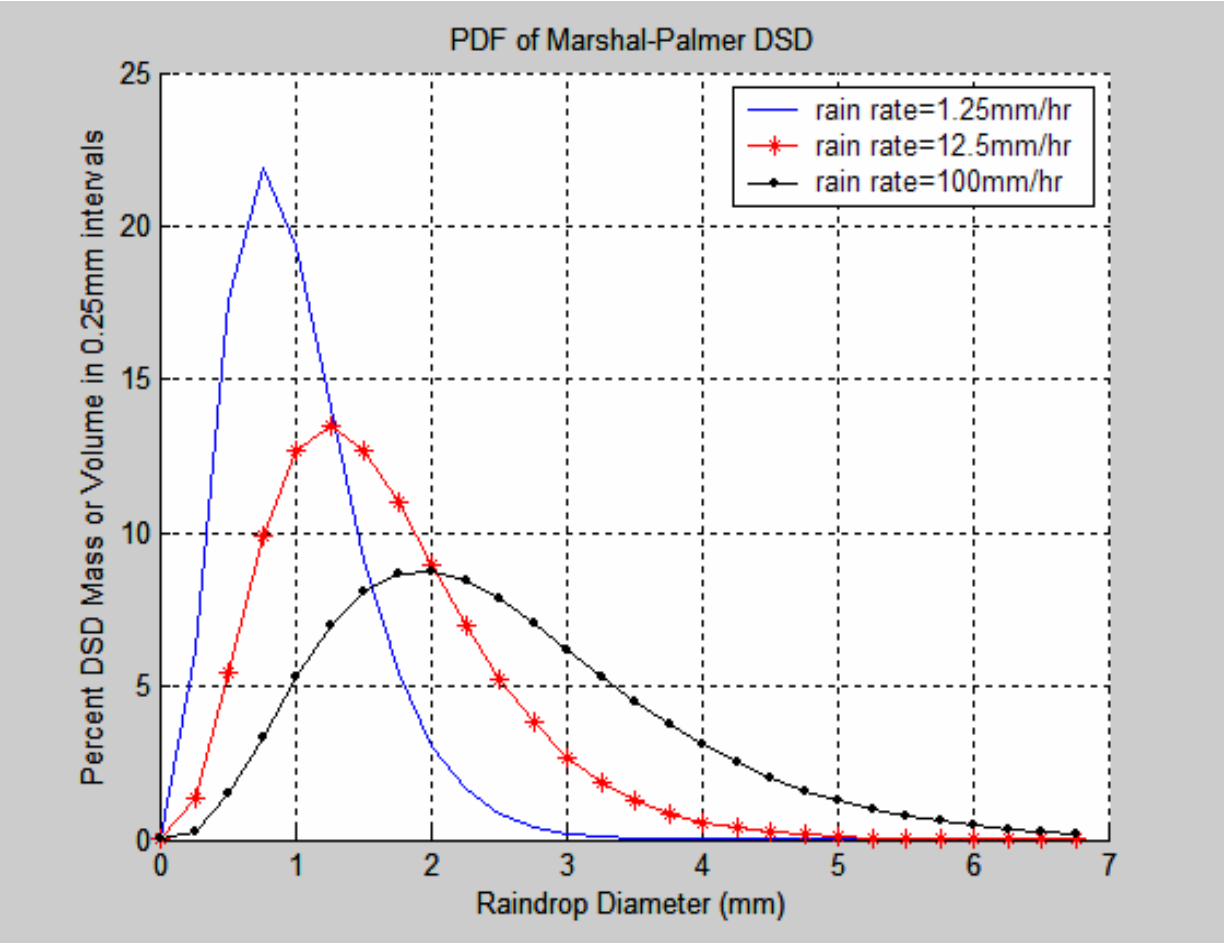

Figure 3.2 PDF of Marshall-Palmer DSDs with Three Different Rain Rates

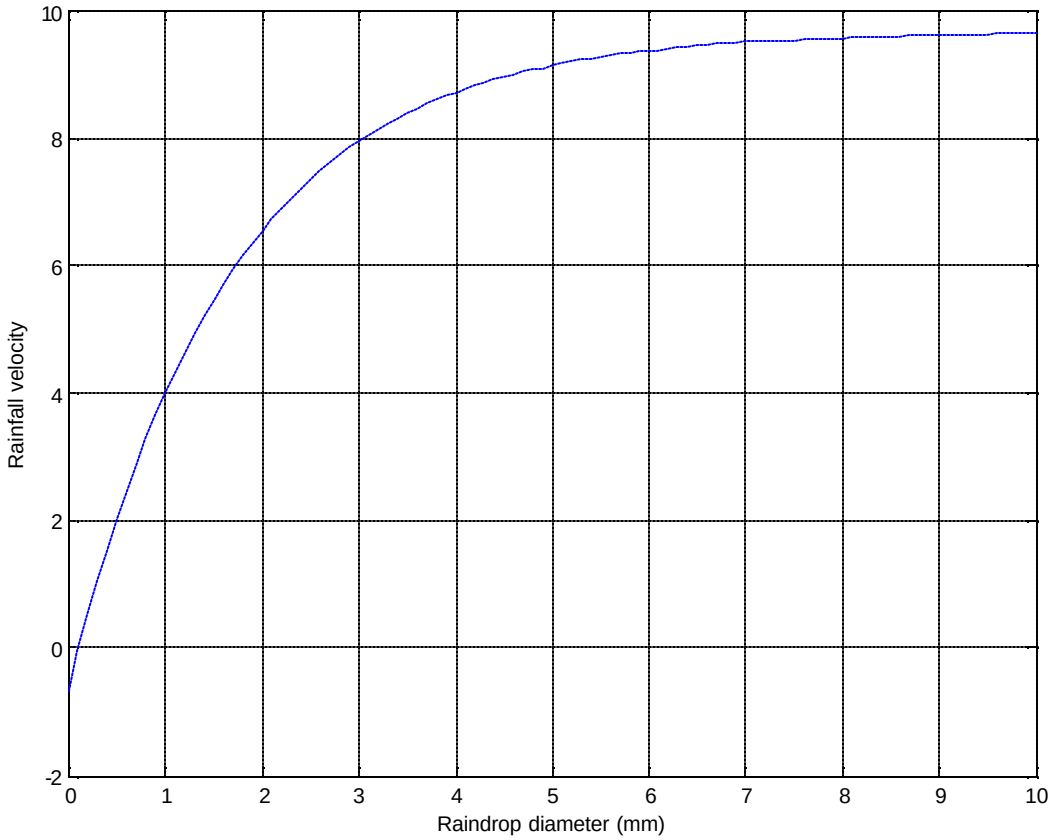

Figure 3.3 Rainfall velocity related to raindrop diameters

3.5 Reflectivity Z

As mentioned earlier, the radar reflectivity, Z, is defined as the summation of the sixth power of the drop size diameters in a unit volume. It is also related to raindrop size distribution $N(D)$ in the radar sample volume [7]:

$$Z = \int_0^\infty D^6 N(D) dD, \text{ mm}^6/\text{m}^3 \qquad (3.5)$$

Based on Marshal-Palmer DSD (equation 3.1), at a given rain rate, the reflectivity Z values can be obtained. In the forward model, I have chosen three different rain rates to calculate the reflectivity. Using weather radar equation introduced in chapter 2, the spectrum powers (received power for a given raindrop size) are obtained. Figure 3.4 shows the simulate profiler Doppler spectra as a function of assumed rain parameters.

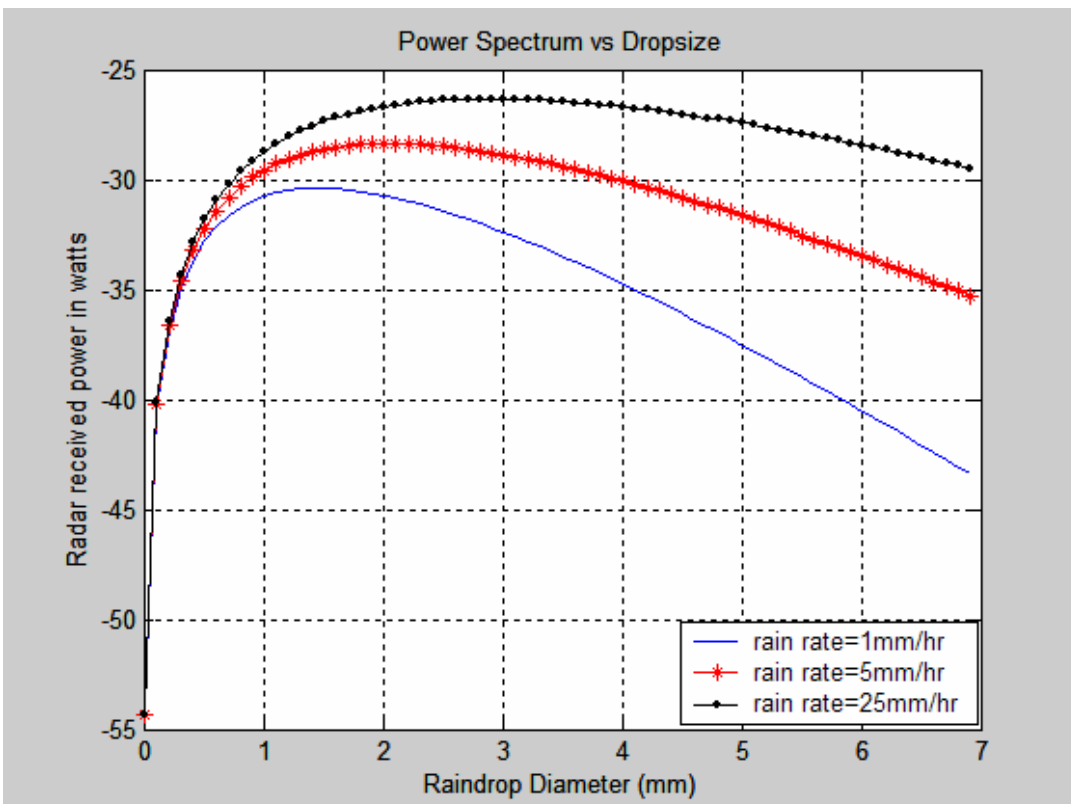

Figure 3.4 Simulated Doppler spectrum as a function of rain diameters

3.6 Z-R relations

Equations 3.3 and 3.5 show that Z and R are related by $N(D)$ and $v(D)$. Given the information on DSD, Z-R relationship can be calculated using regression analysis [14], but in practice, empirical results are used. Often time it is in the form of a power law expression [7]:

$$Z = aR^b \text{, dBZ} \qquad (3.6)$$

where a and b are coefficients that vary in geographically and seasonally and depend on the type of rain. Table 3.1 listed some commonly used Z-R relationships from NOAA Radar Operations Center (ROC). In next chapter, the Gamma distribution model is discussed and we will see the advantage of using Gamma DSDs.

Table 3.1 Z-R Recommendations used in NOAA ROC

Relationship:	Optimum for:	Also recommended for:
Marshall-Palmer ($Z=200R^{1.6}$)	General stratiform precipitation	
East-Cool Stratiform ($Z=130R^{2.0}$)	Winter stratiform precipitation - east of continental divide	Orographic rain - East
West-Cool Stratiform ($Z=75R^{2.0}$)	Winter stratiform precipitation - west of continental divide	Aerographic rain - West
WSR-88D Convective ($Z=300R^{1.4}$)	Summer deep convection	Other non-tropical convection
Rosenfeld Tropical ($Z=250R^{1.2}$)	Tropical convective systems	

CHAPTER 4 PROFILER SIMULATION METHODOLOGY

In the past, lack of detailed knowledge on DSDs has limited the utilization of radar to accurately detect rainfall intensities. Frequently, rainfall rate was estimated using empirical models, such as reflectivity to rain rate (Z-R) relations derived from rain gage measurements and regression or numerical simulation analyses [15]. The ability of profilers to estimate DSD has been demonstrated by several research groups using various techniques [16].

In this thesis, I have validated a theoretical backscatter model by simulating measured precipitation Doppler spectra from an S-band radar profiler during TEFLUN field experiment in Central Florida in 1998. Given these time series of Doppler spectra, I used a fitted Gamma distribution model to estimate DSD under the condition of near-surface (low altitude) stratiform rainfall with no vertical air motion. My analysis program compares the profiler observed moments with calculated moments from a set of estimated gamma parameters and assumed Gaussian measurement noise. The smallest difference between the measured and theoretical spectra moments determines the best estimates for these rain parameters. Occasionally, the observed profiler spectra do not satisfy the assumptions of stratiform rain (and no vertical air motion). For these cases, I have developed a quality control procedure to eliminate these cases from my analysis, which is discussed in Appendix D.

4.1 Gamma Distribution

Marshall-Palmer DSD introduced in Chapter 3 specifies that the distribution has an exponential shape with explicit fitting parameters ($N_0 = 8\times10^6 m^{-4}$ and $\Lambda = 4100R^{-0.21}$ m^{-1}). Many experimental results have shown that Marshall-Palmer distribution is a good approximation to the DSD in similar conditions with sufficient averaging in space and time performed [17], but not all rainfall types follow this relationship because DSD varies geographically and seasonally. In particular, N_0 and Λ have been found to vary considerably over short time scales within given rainfall events [18]. Therefore, it is necessary to account for deviations of N_0 and Λ from the constant values derived by Marshall-Palmer. To specify variable precipitation DSD's, a Gamma distribution [17] is proposed, and expressed as:

$$N(D) = N_0 D^m \exp[-\Lambda D], \text{ m}^{-4} \tag{4.1}$$

The Gamma distribution has three fitting parameters N_0 , m , and Λ, where N_0 represent the scale. The exponent m is the shape and can take any positive values to give a concave down distribution curve, and Λ is the slope parameter [4]. The three parameters are capable of describing the composite DSD over a broader range of diameters resolved by the S-band profiler.

Although there are other exponential shapes that can be used to determine the slope parameter, one reason to use the gamma function is that it better represents the shape of observed DSD at the small drop size range. Another reason for using the gamma function (or any function

that has more than two variables) is that the distribution can be narrower than the exponential distribution. The gamma function is one of the functional forms to describe the shape of the DSD.

4.2 Description of Profiler Moments

The three parameters of the Gamma distribution N_0, m, and Λ uniquely define the three moments of the Doppler velocity spectrum [4]:

$$Z = \frac{N_0 \Gamma(7+m)}{\Lambda^{7+m}}, \text{ mm}^6/\text{m}^3 \tag{4.2}$$

where Γ is the complete gamma operator.

$$V_{Doppler} = \frac{\int_{D_{\min}}^{D_{\max}} v_{fallspeed}(D) D^{6+m} \exp[-\Lambda D] dD}{\int_{D_{\min}}^{D_{\max}} D^{6+m} \exp[-\Lambda D] dD}, \text{ m/s} \tag{4.3}$$

$v_{fallspeed}(D)$ is defined in equation 3.4. It relates the terminal fall speed to raindrop diameter D.

By setting the integration limits of reflectivity weighted mean Doppler velocity to $D_{\min} = 0$ and $D_{\max} = \infty$, the $V_{Doppler}$ can be expressed by the shape (m) and slope parameters (Λ) of the Gamma function [19]:

$$V_{Doppler} = V_{fallspeed} - \overline{v} = a_1 - a_2\left[1+\frac{a_3}{\Lambda}\right]^{-(7+m)}\left(\frac{r_0}{r}\right)^{0.4} - \overline{v} \quad \text{, m/s} \qquad (4.4)$$

$\overline{v}$ is the mean ambient vertical air motion. It causes a shift in the Doppler spectrum consistent with the chosen sign convention, where meteorological convention defines upward motion as positive [4]. It also can be seen from the second moment plots in Figure 2.2, negative mean Doppler velocities represent precipitations falling downward.

The spectral width is a measure of the variability of the Doppler velocity. It is rated to the reflectivity-weighted Doppler velocity variance σ_{vel}^2 (equation 2.4). The variance can also be expressed as fall speed to diameter relationship calculated from equation 2.3 and 4.3:

$$\sigma_{vel}^2 = \frac{\int_{D_{min}}^{D_{max}} \left[v_{fallspeed}(D) - V_{fallspeed}\right]^2 D^{6+m} \exp\left[-\Lambda D\right] dD}{\int_{D_{min}}^{D_{max}} D^{6+m} \exp\left[-\Lambda D\right] dD} \quad \text{, (m/s)}^2 \qquad (4.5)$$

By inverting equation 4.2, N_0 can be calculated using observed reflectivity:

$$N_0 = \frac{\Lambda^{7+m} Z_{obs}}{\Gamma(7+m)} \qquad (4.7)$$

The mathematical expressions to relate profiler moment observations to Gamma parameters form the basis of the DSD retrieval program. Program methodology and program description is discussed in the following sections.

4.3 Simulation Mathematical Basis

To make the simulated Doppler spectra more representative of the profiler observed spectra and its moment's, a normalized atmospheric turbulent probability density function is included in the simulated Doppler spectra to represent the variations in velocity due to a turbulent atmosphere [20]. The clear air turbulence is modeled as a normalized (zero-mean) Gaussian distribution function that is convolved with the simulated Doppler spectra [4]:

$$S_{Rayleigh} = S_{hyd}(v) * S_{air}(v) = S_{hyd}(v) * \frac{1}{\sqrt{2p}\, s_{air}} \exp \frac{\left[-v^2\right]}{2s_{air}^{\ 2}} \qquad (4.8)$$

This equation introduces the σ_{air} parameter into the Doppler spectra and is used to calculate the three profiler moments. The variable v is the independent Doppler velocity at each spectral point and S_{hyd} (v) represents the hydrometer spectrum in stationary air. S_{hyd}(v) can be related to $N(D)$ by [4]:

$$S_{hyd}(v) = N(D) D^6 \frac{dD}{dv} \qquad (4.9)$$

where D is the raindrop diameter, and $\frac{dD}{dv}$ represents a coordinate transformation from terminal fall velocity to diameter domain. Multiplying both sides by dv:

$$S_{hyd}(v) dv = N(D) D^6 dD \qquad (4.10)$$

By integrating both sides of equation 4.10, and based on equation 3.5, the reflectivity is related to hydrometer spectrum:

$$\int_{V_{\min}}^{V_{\max}} S_{hyd}(v)dv = \int_{D_{\min}}^{D_{\max}} N(D)D^6 dD = Z \qquad (4.11)$$

where v_{min} and v_{max} defines the observed Doppler velocity range and D_{min} and D_{max} are the corresponding mean diameter range for stratiform rain. Equation 4.11 relates the Doppler spectra in velocity domain to reflectivity in the diameter domain.

4.4 Program Methodology

In this thesis, all the input measured profiler spectra are obtained from observations made on 22nd of August (day 234) 1998 during the TEFLUN field campaigns. The simulation program compares the profiler observed moments with calculated moments from a set of estimated gamma parameters: μ, Dm (Dm is related to shape parameter Λ) and spectral broadening Gaussian noise standard deviation, σ_n. The difference between the moments is the metric used to determine the best Gamma parameter values and noise σ_n which are then used to retrieve the profiler DSD.

In the program, the best-fit gamma and sigma parameters are determined sequentially for each range gate using the procedure shown in the simplified program flow chart given in Figure 4.1. The inputs to the program are measured Doppler velocity spectra from the profiler at 40

range gates. The first subroutine "**VD_relationship**" finds the raindrop diameters D_i corresponding to the Doppler velocities in the input spectrum for each range gate. Using the transformed input spectrum S(D) and the assumed 22 possible μ integer values (0 – 21) as inputs, the "**find** m" routine calls two other subroutine functions. The first, "**find Dm**", inputs one μ integer and a range of mass-weighted mean diameter Dm values to calculate the first moment (mean Doppler velocity) using equation 4.3, where Λ is related to Dm by $\Lambda = \frac{4+m}{D_m}$. For each assumed Dm, the difference (error) is taken between the calculated mean Doppler velocity with the observed Doppler velocity, and the best Dm value is found.

Using this Dm as an input to the subroutine "**find sigma**", zero-mean Gaussian noise is convolved with the first calculated moment (mean Doppler velocity). Next, this noisy first moment is used to calculate the second moment (spectral variance). The best value of noise is found by incrementing the standard deviation in small steps and finding the smallest squared error between the calculated and observed second moment. By calling these two subroutines, every input μ value returns an associated Dm and noise sigma value. These values are returned to the "**find mu**" subroutine, where the zeroth moment (reflectivity) is calculated for each of the 22 μ inputs. The next step is to compare the 22 calculated zeroth moments with profiler observed zeroth moments. Again, the least error determines the best set of μ, Dm and noise sigma values. The final step is to calculate the scale parameter N_0 using equation 4.7. These retrieved parameters are used to produce the N(D), reflectivity and rain rate. Detailed program descriptions are explained in Appendix A.

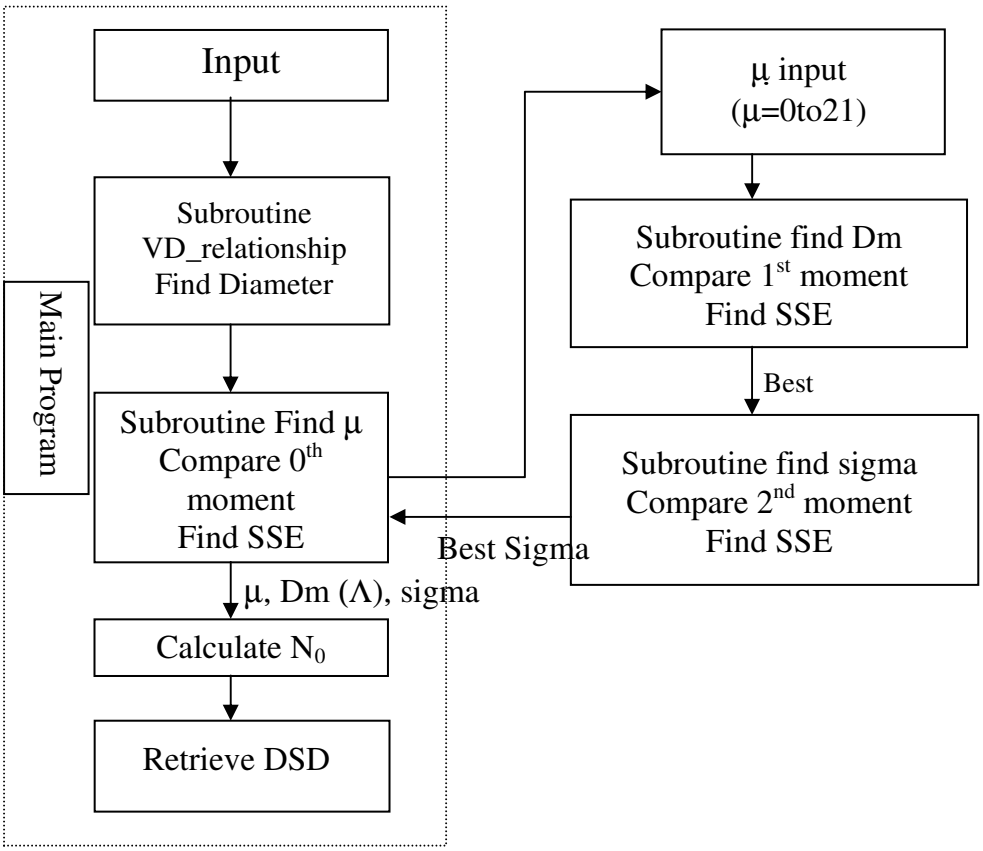

Figure 4.1 Program flowchart

4.5 Spectral points relate to reflectivity

Based on equation 4.11, the area under the spectral curve yields the total reflectivity. To validate that the simulated spectra satisfy this relationship, I have added the 256 observed spectral points of each range gate at a given minute, and compared with profiler recorded reflectivity moment data. Table 4.1 listed one minute compared results for the first 40 range gates, and Fig 4.2 shows the resulting scatter plot.

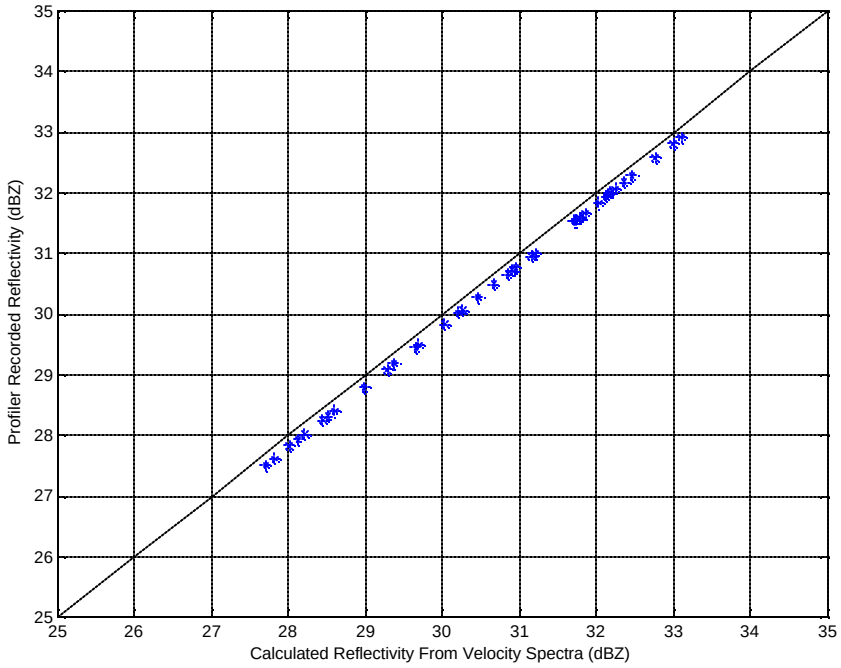

Figure 4.2 Scatter plot of calculated reflectivity vs. profiler recorded reflectivity

Notice from the scatter plot that the sum results (sum of the spectra points) are greater than recorded reflectivity. This is because calculated reflectivity uses all 256 data points in one spectrum and the profiler recorded reflectivity values use only the points above the noise floor. The summed result gives good estimation of the total reflectivity for that range gate at a given time, and as seen from the last column in the table the two agree within 1 dBZ.

Table 4.1 Reflectivity calculated from velocity spectra vs. profiler recorded reflectivity

Range Gate Number	Altitude [m]	Pzdb [dBZ]	Sum(pspc) [dBZ]	Sum(pspc) – pzdb [dBZ]
1	203	32.56	32.77	0.21
2	308	32.91	33.11	0.20
3	413	32.27	32.48	0.21
4	518	32.17	32.37	0.20
5	623	31.98	32.18	0.20
6	728	31.93	32.14	0.20
7	833	31.51	31.71	0.20
8	938	31.66	31.86	0.21
9	1043	31.58	31.78	0.21
10	1148	31.57	31.78	0.21
11	1253	31.99	32.19	0.20
12	1358	31.82	32.03	0.21
13	1463	31.92	32.13	0.21
14	1568	32.05	32.25	0.21
15	1673	31.52	31.73	0.21
16	1778	30.95	31.16	0.21
17	1883	31.00	31.21	0.21
18	1988	30.76	30.97	0.21
19	2093	30.47	30.68	0.21
20	2198	30.64	30.85	0.21
21	2303	30.72	30.91	0.20
22	2408	30.26	30.47	0.21
23	2513	30.01	30.22	0.21
24	2618	30.05	30.27	0.22
25	2723	29.81	30.03	0.22
26	2828	29.49	29.69	0.21
27	2933	29.17	29.38	0.21
28	3038	29.08	29.29	0.21
29	3143	28.78	28.99	0.21
30	3248	28.31	28.52	0.21
31	3353	28.00	28.22	0.22
32	3458	27.51	27.72	0.21
33	3563	27.81	28.02	0.21
34	3668	27.93	28.13	0.20
35	3773	28.39	28.60	0.21
36	3878	27.60	27.84	0.23
37	3983	28.24	28.45	0.22
38	4088	29.43	29.66	0.23
39	4193	32.80	33.00	0.21
40	4298	36.55	36.75	0.20

4.6 Power Spectrum

In the profiler Doppler velocity spectrum, the spectral resolution is determined by the radar pulse-repetition-frequency and the number of spectral lines in the FFT. A logarithmic scaled plot of the Doppler power spectrum for the lowest range gate, obtained during hour 3 and minute 5, is shown in Figure 4.3. Only the spectral points with positive signal to noise ratio above the threshold detectability (shown in red) are selected for analysis. The threshold value is estimated for each time and range gate based on equation 4.12 [21]:

$$threshold = 10\log\left(\frac{25\sqrt{NFFT - 2.3125 + \frac{170}{NPTS}}}{(NPTS)(NFFT)}\right), \text{dB} \qquad (4.12)$$

where NPTS is number of points in each spectra , and NFFT is the number of FFTs averaged to produce the final spectra. In Fig 4.3, the threshold value is -11.50 dBZ.

In the next chapter, selected hours of profiler spectra are compared with the Gamma parameters calculated spectra. Also, a total of 5 hours of calculated reflectivity are compared with the profiler observed reflectivity.

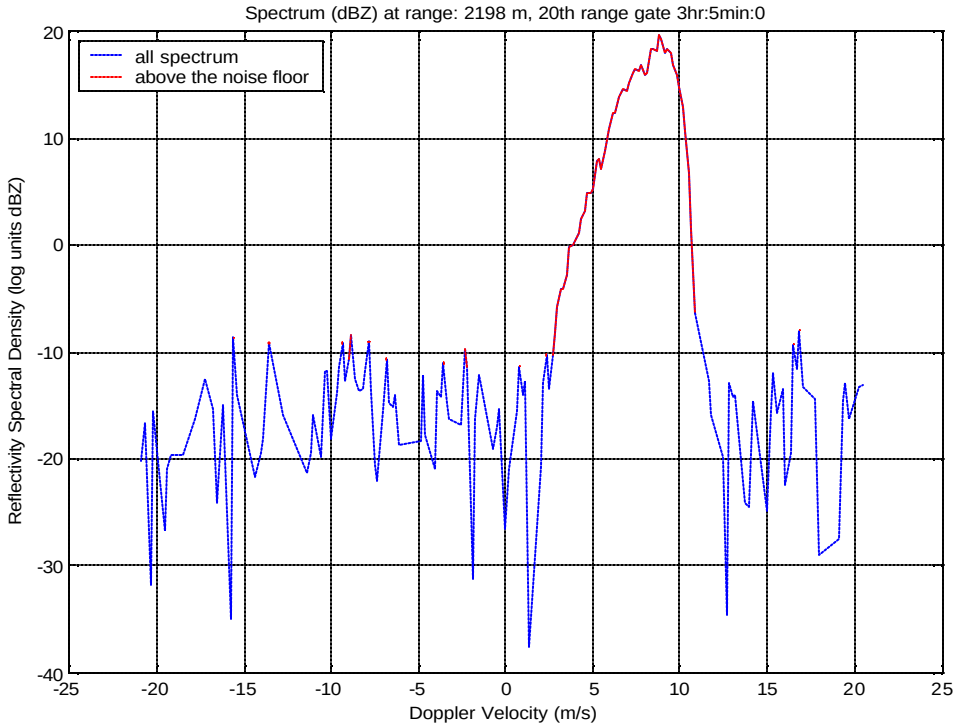

Figure 4.3 Measured profiler spectrum at hour 3, minute 5.

CHAPTER 5 RESULTS AND CONCLUSIONS

5.1 Program Results

Five-hours of S-band profiler data, obtained on August 22nd in 1998 during the TRMM TEFLUN campaign, were used to produce the moments of the Doppler spectra including reflectivity, mean Doppler velocity and spectral width. These were saved as vertical profiles of observed moments of precipitation spectra. An analysis program was developed, which derives the corresponding precipitation DSD using a modified Gamma distribution for rain. The Gamma distribution was determined by three Gamma parameters: N_0 , m , and Λ . The best value of Gamma parameters and Gaussian noise standard deviation were found by matching the calculated Doppler moments with profiler observed moments. The smallest error determined the best set Gamma values and sigma value for each spectrum. A typical example is shown in Figure 5.1 of the observed one minute average Doppler spectrum (black line) for the lowest-altitude range gate. Also shown are the corresponding calculated Doppler velocity spectra produced by Gamma fitting parameters (blue line) and the model spectrum convolved with Gaussian noise (red line), which is based on equation 4.8 discussed in Chapter 4. Within the Gamma parameter retrieval program, the moment calculations are convolved with noise before comparing with the profiler observed moments to minimized the errors (differences). As seen from Figure 5.1, the red curve (convolved with noise) is a much better representation of the observed Doppler spectrum. During profiler data processing for hour 3, some anomalies resulted in that several measured spectra appear to be bimodal, and the “best fit” Gamma parameters used to produce the

calculated Doppler spectra are invalid i.e., my theoretical model cannot produce bimodal spectra. Figure 5.2 is an example of one minute average profiler spectrum for the 59th minute of hour 3. The calculated Doppler spectra (red and blue curves) are not a good representation the profiler observed spectrum; thus I developed a quality control (QC) test (Appendix D) to reject these measured spectra, which cannot be accommodated in my theoretical model. All Doppler spectra, for the first range gate location from hour 3, are presented in Appendix C (C.2); and the calculated Gamma parameters, rain parameters and QC flags are summarized in Table 5.1. Profiler spectra, which fail the QC test, are shown in red fonts.

Table 5.1 Calculated Gamma parameters and rain parameters for hour 1

Hour 3 (minute)	No	μ	σ	Z	R	Dm	λ	QC(Y/N)
1	2493.2	2	0.27	31.44	1.86	1.73	3.47	Y
2	2096	2	0.44	31.93	1.92	1.79	3.36	Y
3	1314.3	2	0.33	34.21	2.49	2.00	3.01	Y
4	1947.9	3	0.39	33.91	2.49	1.99	3.51	Y
5	951.16	3	0.54	32.96	1.77	2.09	3.34	Y
6	1634.8	2	0.40	32.77	2.07	1.88	3.20	Y
7	5917.1	0	1.55	31.82	3.28	1.29	3.11	N
8	2634.9	0	0.59	29.44	1.74	1.34	2.99	Y
9	4171.6	2	0.10	28.29	1.24	1.51	3.98	Y
10	19348	3	0.51	27.85	1.48	1.38	5.08	Y
11	5281.2	3	0.33	27.74	1.07	1.56	4.48	Y
12	23911	4	0.45	27.05	1.19	1.43	5.60	Y
13	7673.9	2	0.50	26.19	1.01	1.34	4.49	Y
14	13931	3	0.38	26.16	1.01	1.37	5.11	Y
15	3951.8	2	0.40	25.73	0.79	1.42	4.22	Y
16	2405.8	1	0.21	24.77	0.68	1.33	3.77	Y
17	1958.7	1	0.43	25.02	0.67	1.37	3.64	Y
18	2521.8	2	0.30	25.28	0.65	1.48	4.06	Y
19	2897.9	2	0.50	25.54	0.71	1.46	4.10	Y
20	3427.3	2	0.33	25.74	0.76	1.44	4.15	Y
21	6931	3	0.34	25.46	0.76	1.44	4.85	Y
22	2626.5	1	0.26	25.58	0.80	1.34	3.72	Y
23	2726.1	1	0.10	25.53	0.80	1.34	3.74	Y
24	6491.7	2	0.24	24.79	0.76	1.31	4.57	Y
25	3428.6	1	0.39	24.37	0.70	1.26	3.98	Y
26	4246	2	0.39	25.32	0.75	1.40	4.30	Y
27	5236.2	2	0.27	25.72	0.85	1.38	4.36	Y
28	7355.3	3	0.32	26.31	0.90	1.46	4.78	Y
29	11649	3	0.43	25.96	0.94	1.39	5.05	Y
30	4949.2	2	0.20	25.34	0.78	1.37	4.37	Y
31	6450.2	2	0.30	25.06	0.80	1.32	4.54	Y
32	5130	1	0.27	24.68	0.83	1.20	4.15	Y
33	7592.1	2	0.38	23.98	0.69	1.26	4.75	Y
34	7986.8	1	0.98	23.03	0.71	1.09	4.60	N
35	2.02E+05	8	0.71	21.42	0.40	1.38	8.71	Y
36	8.41E+05	12	1.01	21.27	0.34	1.49	10.76	Y
37	2.84E+13	4	2.99	27.30	42.59	0.21	37.25	N
38	1.83E+06	12	0.83	21.01	0.36	1.42	11.24	Y
39	1.08E+07	0	2.99	24.37	8.28	0.34	11.62	N
40	6356.2	3	0.17	21.28	0.36	1.32	5.29	Y
41	6359.2	2	0.12	21.93	0.46	1.22	4.91	Y
42	7981	3	0.34	22.96	0.51	1.34	5.21	Y
43	16217	4	0.32	22.49	0.48	1.34	5.95	Y
44	9591.3	3	0.33	22.73	0.51	1.31	5.33	Y

45	11280	4	0.10	24.07	0.59	1.44	5.57	Y
46	66856	6	0.39	23.12	0.56	1.38	7.26	Y
47	3409.9	0	1.21	22.01	0.59	1.01	3.97	N
48	1.89E+05	8	0.14	23.65	0.61	1.43	8.38	Y
49	1.44E+05	6	0.88	23.00	0.63	1.30	7.72	Y
50	2.41E+08	19	0.88	20.70	0.36	1.41	16.28	Y
51	18274	5	0.17	20.79	0.32	1.38	6.54	Y
52	61227	6	0.50	19.85	0.30	1.31	7.64	Y
53	1.05E+09	20	0.89	18.32	0.23	1.34	17.85	Y
54	1.61E+07	13	0.73	17.19	0.20	1.26	13.45	Y
55	3.90E+08	16	1.12	14.31	0.12	1.19	16.85	Y
56	1.57E+41	21	0.94	29.00	-12.06	0.11	233.93	N
57	3.09E+09	2	2.50	14.49	1.80	0.24	25.42	N
58	1.08E+41	21	1.05	27.35	-8.26	0.11	233.93	N
59	1.92E+13	14	2.42	15.75	0.56	0.66	27.11	N
60	9.46E+15	9	1.24	28.60	33.91	0.34	37.76	Y

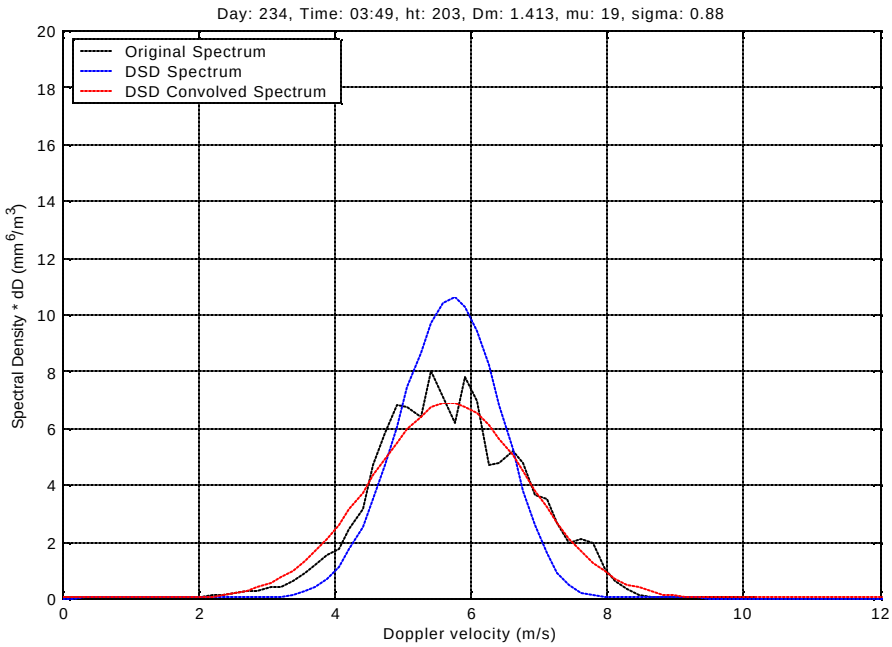

Figure 5.1 Calculated and observed spectrum comparison for time 3:49, @ 203m.

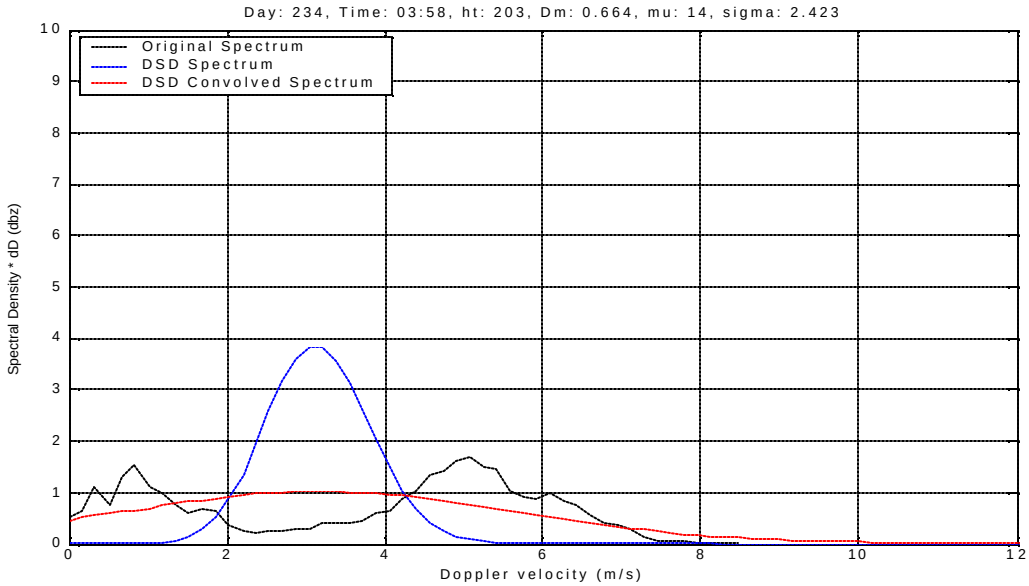

Figure 5.2 Calculated and observed spectrum comparison for time 3:58, @ 203m. The observed bimodal spectrum can not be modeled and is therefore rejected by the quality control test.

Using the valid spectra from Table 5.1, the log-log Z-R relationship is plotted in Figure 5.3, which demonstrates the expected linear relationship between these two quantities. Figure 5.4 is the hour 3 time series of retrieved Gamma parameters μ, No, and Λ, with invalid spectra removed.

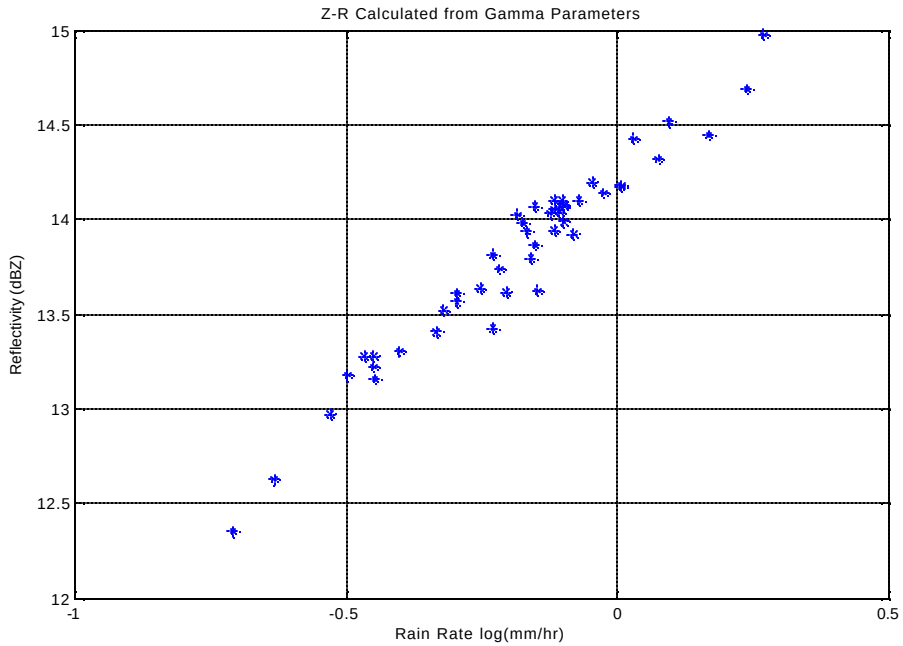

Figure 5.3 (log-log) Z-R retrievals for hour 3

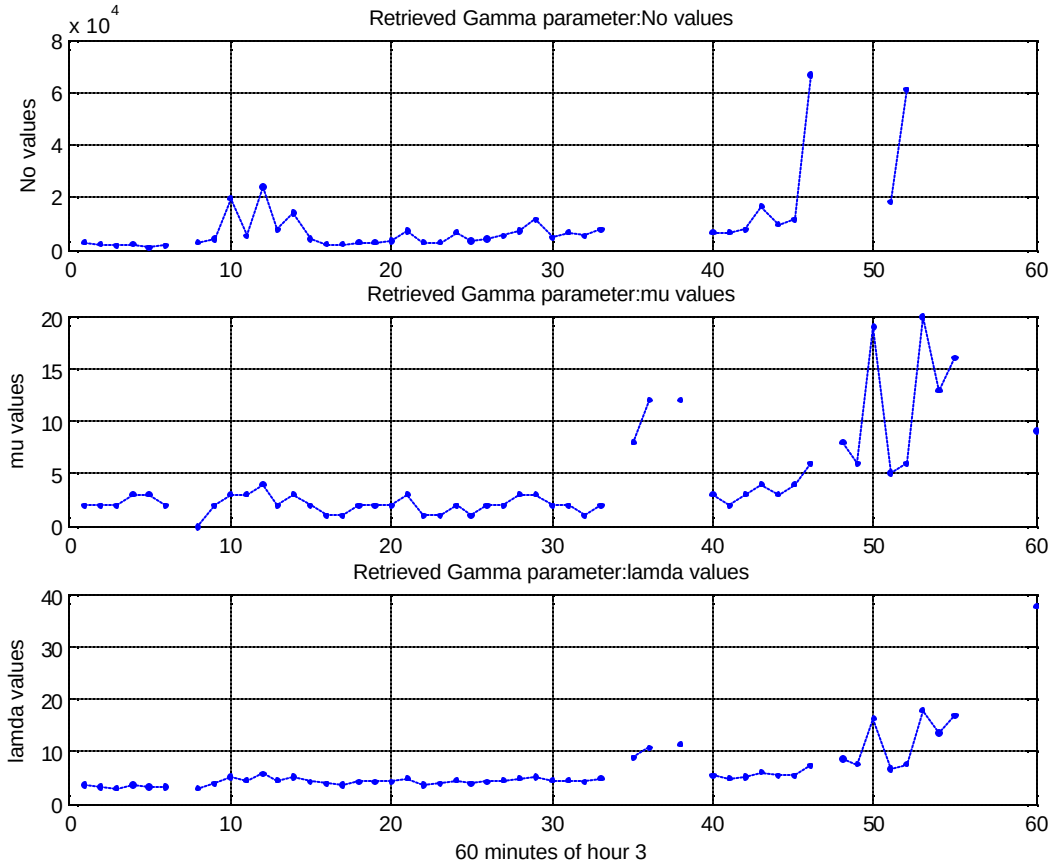

Figure 5.4 Time series of calculated Gamma parameters for hour 3

The principal advantage of the radar profiler is that it provides vertical profiles of precipitation parameters directly above the profiler. Figure 5.5 compares one minute of profiler observed reflectivity with calculated reflectivity for all 40 range gates with 105m pulse length for each range gate below the melting level. It shows good correlation in reflectivity between the observed and calculated values. The bottom panel of Figure 5.6 is the S-band profiler observed reflectivity profile below melting level for the entire 5-hour period. There are a total of 12000 reflectivity points, where each color represents the 40 range gates. For comparison, the top panel displays the corresponding reflectivity data calculated using the retrieved Gamma parameters;

and this is presented Figure 5.7 as a scatter plot. These results demonstrate that given a set of observed profiler spectra, it is possible to find reasonable corresponding gamma distributions to solve for the precipitation DSD and then use these to calculate the resulting reflectivity. As seen by the scatter diagram, this can be performed without any significant error. While this result is pleasing, it is not sufficient to prove that the DSD's are correct. This issue will be addressed in another comparison with an independent DSD measurement at the surface using simultaneous disdrometer in the next section.

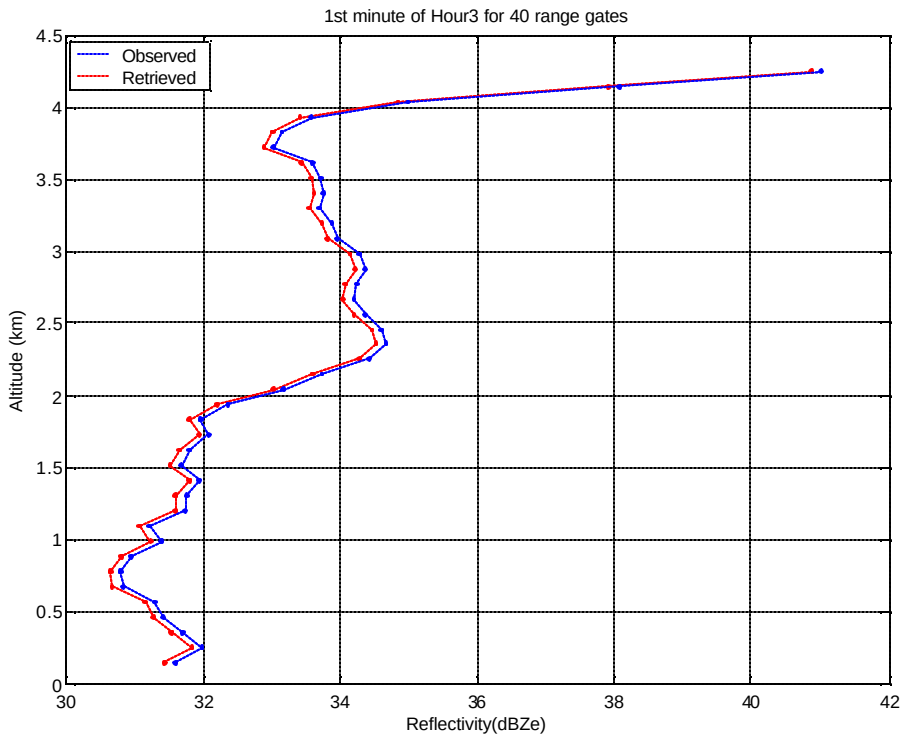

Figure 5.5 One minute profiler reflectivity observations vs. retrievals with altitude variations.

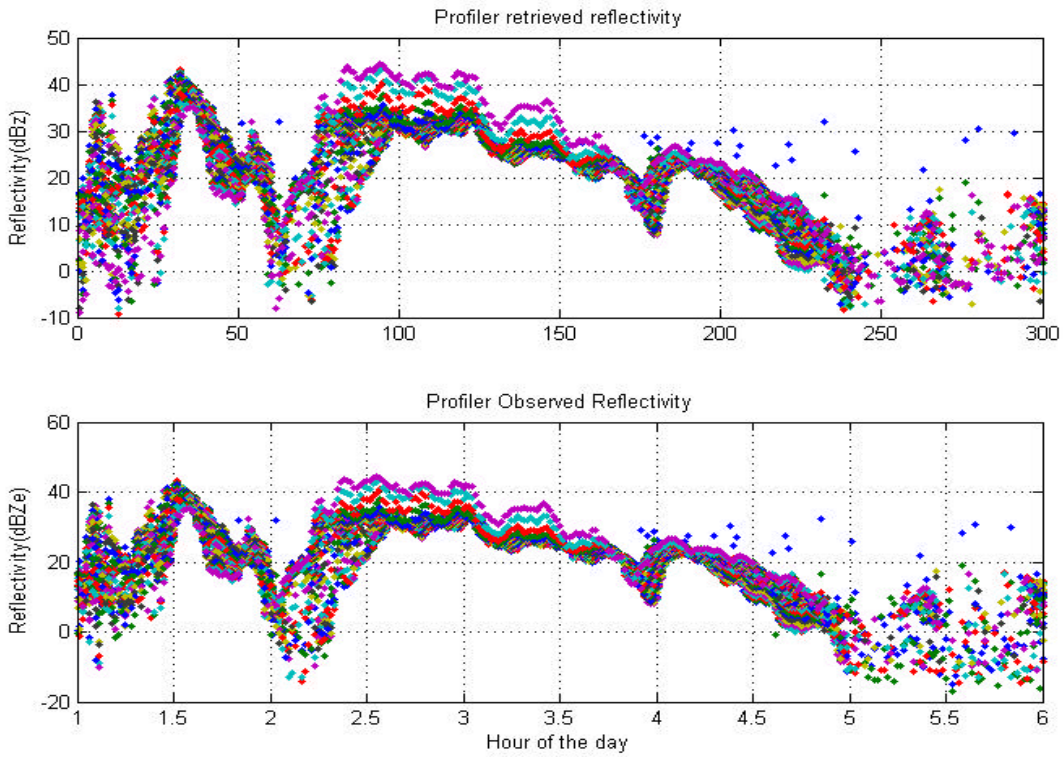

Figure 5.6 Calculated reflectivity and observed reflectivity (40range gate)

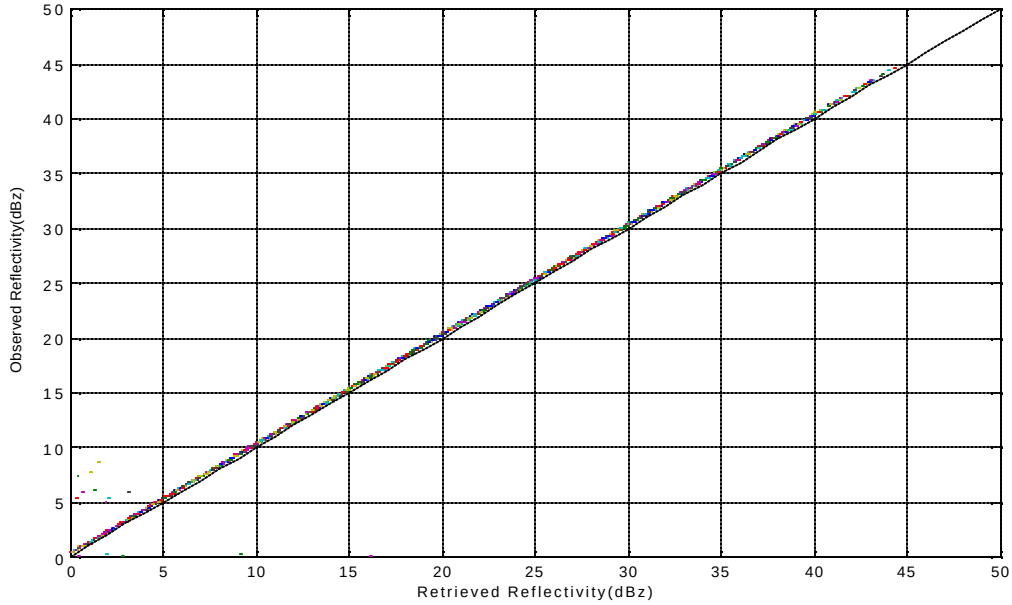

Figure 5.7 Comparison between calculated reflectivity and observed reflectivity

5.2 Inter-Comparison with Disdrometer

In support of the TRMM ground validation field campaign, a collocated RD-69 Joss-Waldvogel disdrometer (JWD) was used as "surface truth" to validate the S-band profiler measurement of rain DSD. In this thesis, to evaluate profiler near ground retrievals, the profiler retrieved rain parameters including rain rate, reflectivity, and mean raindrop diameter from the first range gate at 203 meters above ground level were compared with corresponding disdrometer derived data. Given that the comparison is to be made at two different altitudes (203 m versus surface), one could question the validity of these comparisons. Given the humid atmospheric conditions in Central Florida during this experiment, evaporation is not an issue, so only the gravity sorting of raindrops by their fall velocity should be a concern. This problem was analyzed by Lane [22] and his conclusions were that these comparisons should be reasonable. Figure 5.8 to 5.10 show comparisons of mass weighted mean diameter, rain rate, and reflectivity for hour 3 of the five-hour time series.

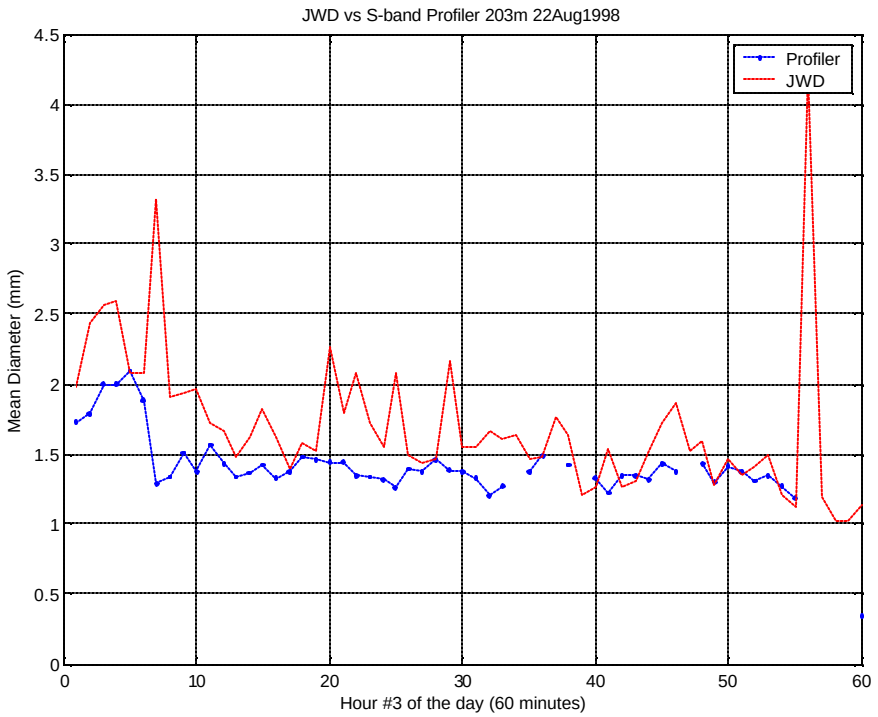

Figure 5.8 Mean diameters comparison between profiler and JWD for hour 3

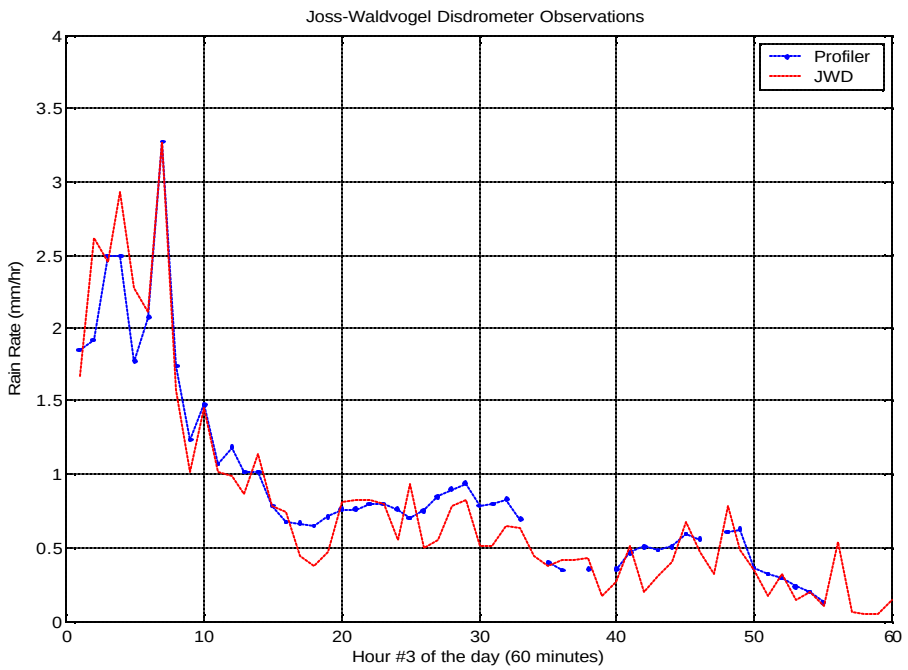

Figure 5.9 Rain rates comparison between profiler and JWD for hour 3

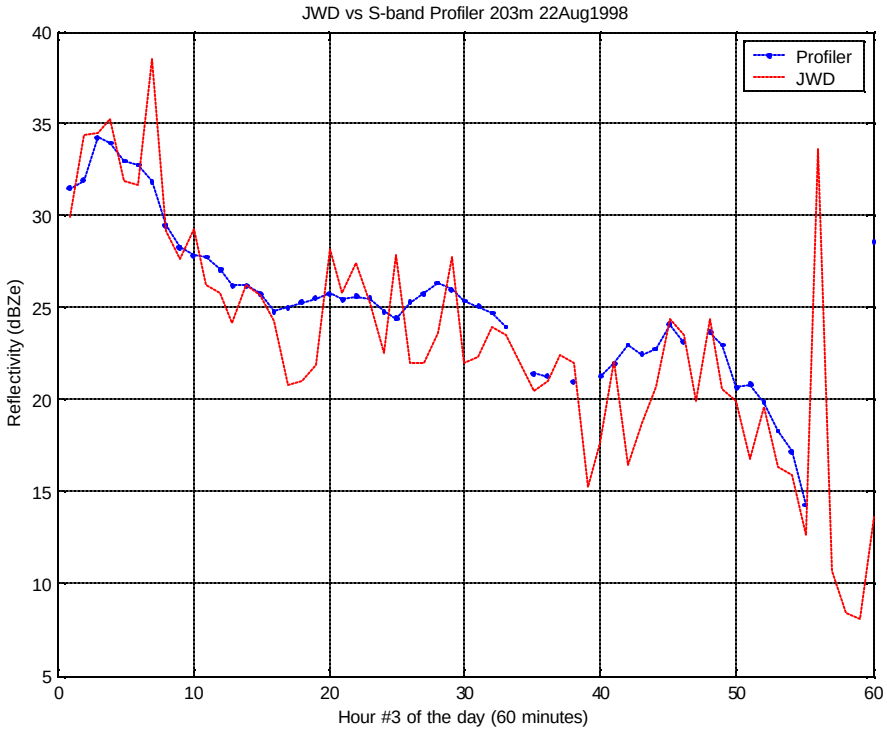

Figure 5.10 Reflectivities comparison between profiler and JWD observations for hour 3

The JWD measurements of mean diameter are slightly larger than the profiler retrieved values. Table 5.2 shows the calculated the mean and standard deviation (STD) of the differences between diameters and their cross-correlation values. The cross correlation improves significantly, from 0.15 to 0.67, by removing the outliers found by the quality control test.

In general, the first five hours rain parameters observed from the JWD compare very well with profiler retrievals, and the time series of profiler retrieved mean diameter, Z, R, and D_m with corresponding JWD observations are shown in Appendix C (C.1).

Table 5.2 Comparison of Dm between JWD and profiler retrievals

Hour 3 Mean Diameter	mean	STD	Cross-Correlation
Before removing outliers	0.42	0.62	0.15
After removing outliers	0.26	0.26	0.67

5.3 Conclusions and Future Studies

In this thesis a theoretical radar rain-backscatter model was developed to simulate profiler Doppler spectra as a function of assumed rain parameters. This theoretical Rayleigh scattering model was validated by duplicating measured precipitation Doppler spectra (and 3 moments) from an S-band radar profiler during a field experiment in Central Florida in 1998. Further, the profiler Doppler spectrum was used to retrieve the precipitation parameters below the melting level during stratiform rain with assumed negligible vertical air motion. Given these time series of Doppler spectra, I have determined the best-fit Gamma distribution model by comparing calculated and measured Doppler moments to estimate the corresponding rain DSD. Results from my radar rain-backscatter model reflectivity profiles compare well with the observed reflectivity, and precipitation retrievals showed good agreement with disdrometer surface observations.

In the future, an extended study should be conducted using collocated VHF or UHF and S-band radar profilers. Because the lower frequency profilers are sensitive to Bragg scattering of atmospheric inhomogeneities, they can be used to retrieve precipitation and vertical air motion simultaneously. This would remove the restriction imposed in my theoretical radar rain-

backscatter model of measuring only stratiform rain where the vertical air motion is negligible and would permit retrieving rain DSD's for other types of rain including convective conditions.

APPENDIX A

PROFILER DATA

Five hours of s-band profiler observations are used in this study. Each hour of observation data is saved in a separate file with root name “spc_p_”. Each input file contains 11 double array variables listed in Table 4.1. Detailed descriptions of these variables are discussed next.

Table A.1 Input profiler spectra data

Name	Size
pV	60x256
phed	60x17
pnos	60x100
prange	60x100
precip_gain	1x1
ps2n	60x100
pspc	60x100x256
pthr	60x100
pvel	60x100
pwid	60x100
pzdb	60x100

Pspc (size 60x100x256) is a three dimensional array representing the power density spectrum. For each minute, there are 256 spectra points observed for each range gate.

The spectral data are two-dimensional arrays. The row defines the time of the profile (60 minutes), and the column defines the range gate (100 grange gates). The following variables have unique values for each profile and range gate. All variables have size 60x100:

pnos: noise value

prange: distance to center of the range gate (m)

ps2n: signal to noise value (dB)

pthr: noise threshold for spectra in pspc ($mm^6/m^3/(m/s)$)

pvel: profiler recorded mean Doppler velocity (m/s)

pwid: profiler recorded spectral width (m/s)

pzdb: profiler recorded reflectivity (dBZ)

The following variables have unique values for each profile. They are independent of range.

pV: (60x256) velocity of each spectral point in spectra (m/s). It is independent of height (range gate).

phed: (60x17) header of an hour information for each profile. The column number corresponds to the following information:

1. radar id code (146)
2. radar frequency (283500 Hz)
3. radar altitude (20m)
4. radar longitude (-81.01 degrees)
5. radar latitude (28.13 degrees)

6. year (1998)

7. day of the year (234)

8. seconds into day (i.e. 3601-7140 seconds for hour number 1)

9. number of coherent integration (NCI = 10)

10. number of spectra(44)

11. number of points in each spectra (NPTS = 256)

12. elevation angle (90 degrees)

13. azimuth angle (zero)

14. pulse width (700ns)

15. number of code bits (0-zero for not coded)

16. inter pulse period (IPP=122000ns)

17. valley threshold (3dB)

precip_gain is the radar calibration constant used to estimate pzdb for all profiles and range gates.

APPENDIX B

PROGRAM DISCRIPTION

The main program retrieves Gamma parameters and uses them to calculate rain parameters and displays the profiler observed power Doppler spectrum and the retrieved Doppler spectrum. In the main program (see Appendix A Main Program Code), five hours worth of data can be processed by the following schemes:

(a) Select any minute of the five hours (choose i between 0 and 60) and a fixed range gate (j between 0 and 40)

(b) Process all 40 range gates of data for one minute, an hour, or five hours.

(c) Select one fixed range gate, process any hour or a total of five hours of data.

In the main program, the following Subroutine functions are called to calculate reflectivity Z and rain rate R using estimated gamma parameter mu and sigma. See below for program methods on gamma parameter estimation.

B.1 VD_Relationship Subroutine

Inputs:

Vd -- Velocity in each spectral bin (256 points)

Outputs:

Ds -- Diameters for this altitude and for each velocity bin

dDs -- Delta diameter

Terminal fall velocities of raindrops can be related to their diameters through empirical relations. In “VD_relationship_test” program, the terminal fall velocity to diameter size relation is calculated using Atlas equation 3.4. A table look up procedure is performed to relate terminal velocity to raindrop diameter. The following steps give the velocity corresponding raindrop diameters:

1. Assume 2000 diameters [xD] ranging from 0.01mm to 20mm with size interval of 0.01mm, and use equation 3.4 to calculate 2000 corresponding terminal fall velocities Vdoppler.

2. Perform a table lookup procedure (interp1 function) using the results from step 1 and the velocity of each spectral point [Vd] to calculate Vd's corresponding mean diameters [Ds]. Similar procedure is used to calculate the [dDs], a variable used in equation 4.10 as the coordinate transformation parameter from velocity domain to diameter space.

B.2 Clean Peak Subroutine

Subroutine "clean_spk_v1_test" cleans the spectra assuming only Rayleigh components are presented. This subroutine is called at the beginning of the program to ensure only the Rayleigh region is to our study interests. The program sets NaN's in all locations that are below the noise threshold

B.3 Find mu Subroutine

"find_mu_Dm_D6_test" routine finds the best mu (μ) value of the gamma DSD. The outputs Ds and dDs from the "VD relationship" subroutine are the inputs of this subroutine.

Inputs:

Ds -- Diameters for this altitude and for each velocity bin

dDs -- Delta diameter

spk -- D^6 weighted spectrum

Outputs:

mu -- Shape parameter of gamma DSD

Dm -- Mass-weighted mean diameter

SSE -- Sum of the Squared Errors in Log space

The following steps explain how to find gamma parameter mu:

1. Using equation 4.3 and 4.5 to calculate the profiler observed first and second moment of spectra: [Vdoppler_obs] and [Wdoppler_obs].

2. Assume 22 different values of mu ranging from 0 to 21 with step size 1. Within the find mu routine, two more subroutines are performed:

a) Call function "find_Dz_v6"

Assume a range of estimated mass-weighted mean diameter [Dm] (0.1mm to 5mm), using equation 4.3 to estimate the first moment [Vdoppler_est], where Λ is substitute with Dm values using relationship:

$$\Lambda = \frac{4+m}{D_m} \qquad \text{(A.1)}$$

Compare the estimated first moment with the observed mean Doppler velocity. Find the Sum of the Squared Errors (SSE). SSE is renamed [SSE_Dm_z] in routine "find_mu_Dm_D6_test." The smallest SSE determines the best estimated mean diameter [Dm] in each range gate. The best Dm value is renamed in "find_mu_Dm_D6_test" as [Dm_z].

b) Call function "find_sigma_z_test"

Similar to the routine of finding the best mean diameter estimation, assume a range of sigma(σ) values from 0.1 to 3. To make the SSE the smallest possible, the first moment is convolved with Gaussian noise [Sv] based on equation 4.8 and it is used to calculated the second moment Spectral Width [Wdoppler_est] using equation 4.5. The smallest value of SSE between the observed and estimated spectral width determines the best sigma value. The best estimated sigma value is saved as [sigma_z] in "find_mu_Dm_D6_test" routine.

APPENDIX C

JWD VS PROFILER RETRIEVALS AND DOPPLER SPECTRA PLOTS

APPENDIX C

JWD VS PROFILER RETRIEVALS AND DOPPLER SPECTRA PLOTS

C.1 JWD Observations vs. Profiler Retrievals (Hours 1 to 5)

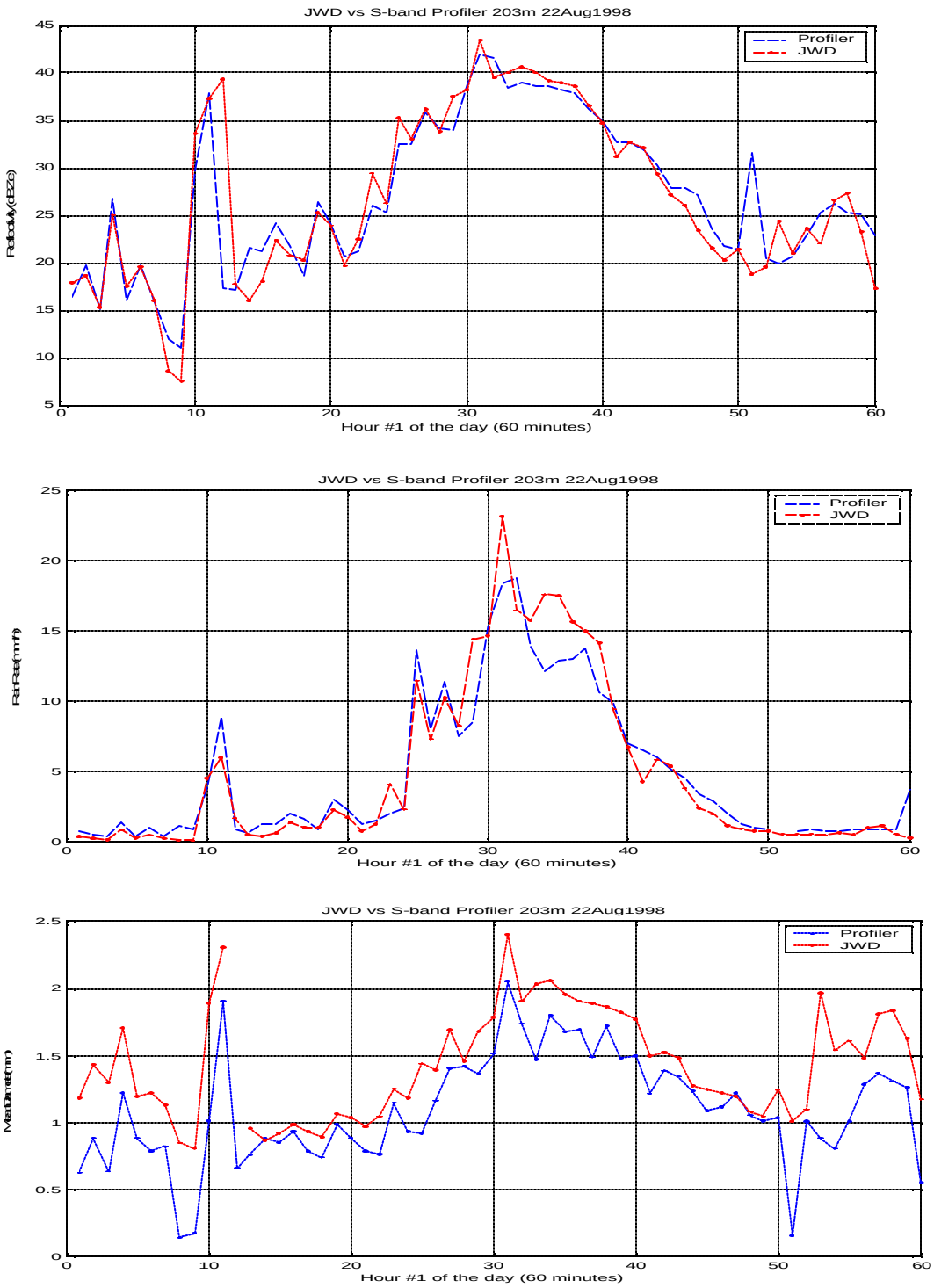

Figure C.1.1 Profiler observations vs. JWD observations for hour 1
(Top: Reflectivity. Middle: Rain Rate. Bottom: Mass Weighted Mean Diameter.)

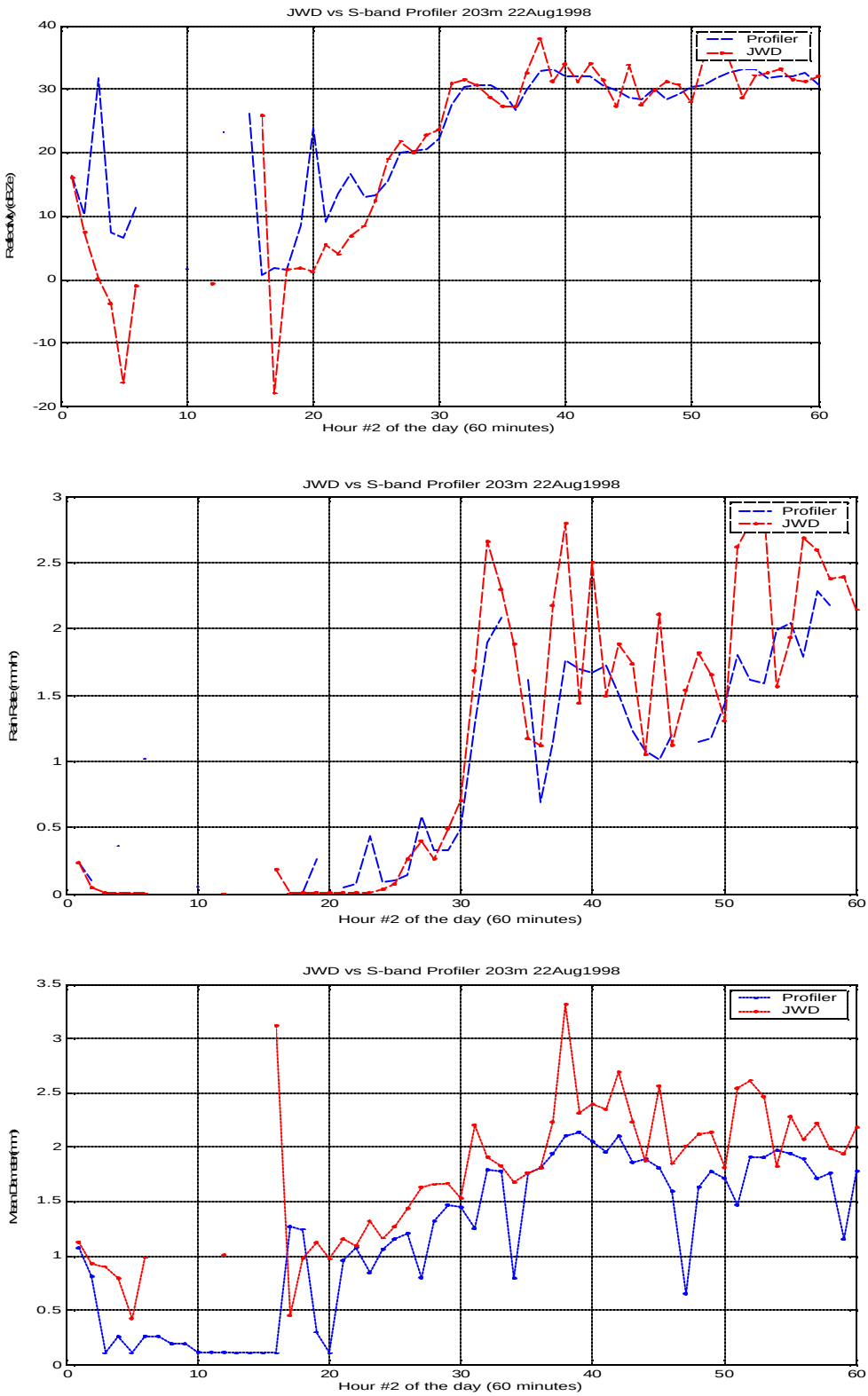

Figure C.1.2 Profiler observations vs. JWD observations for hour 2

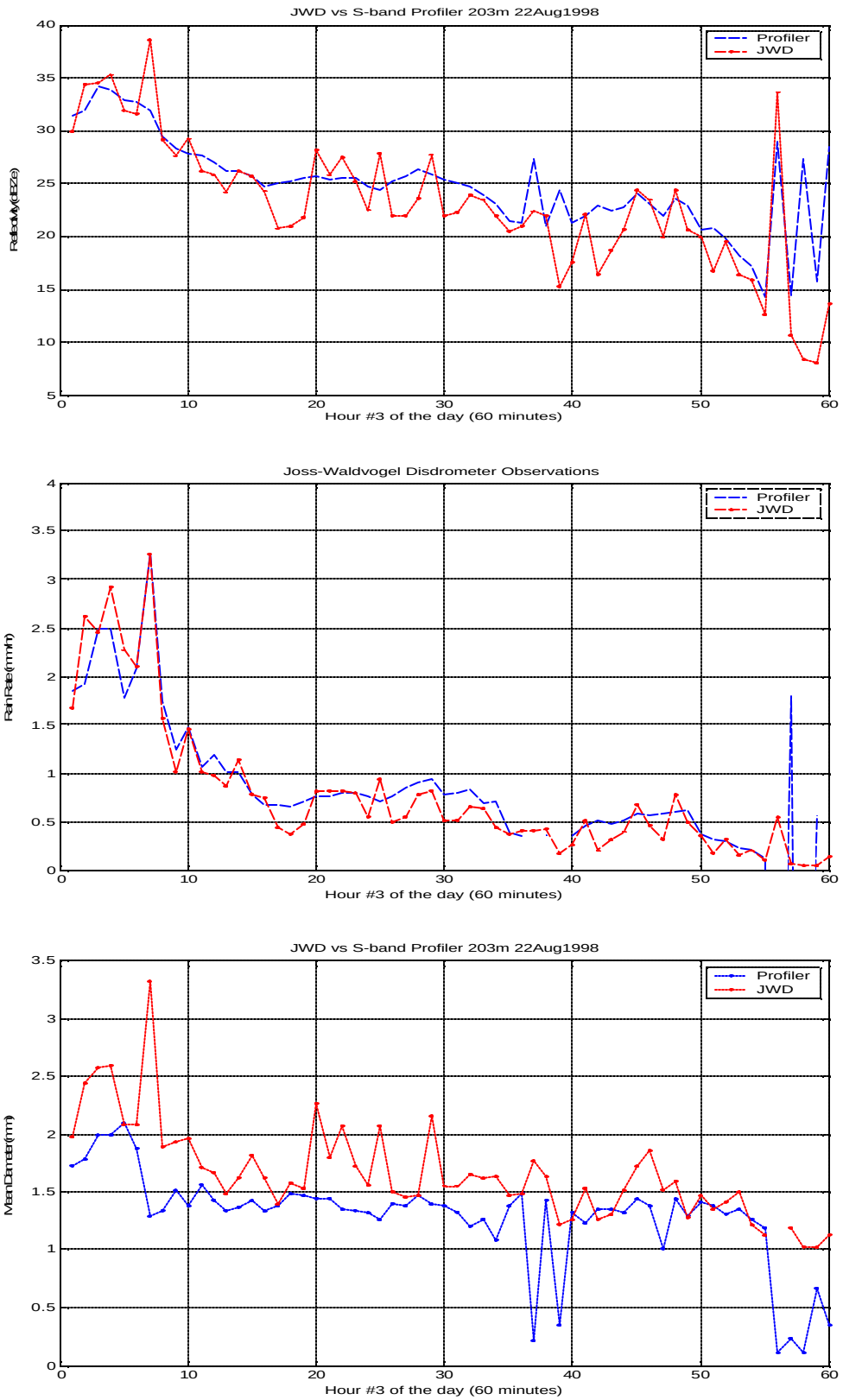

Figure C.1.3 Profiler observations vs. JWD observations for hour 3

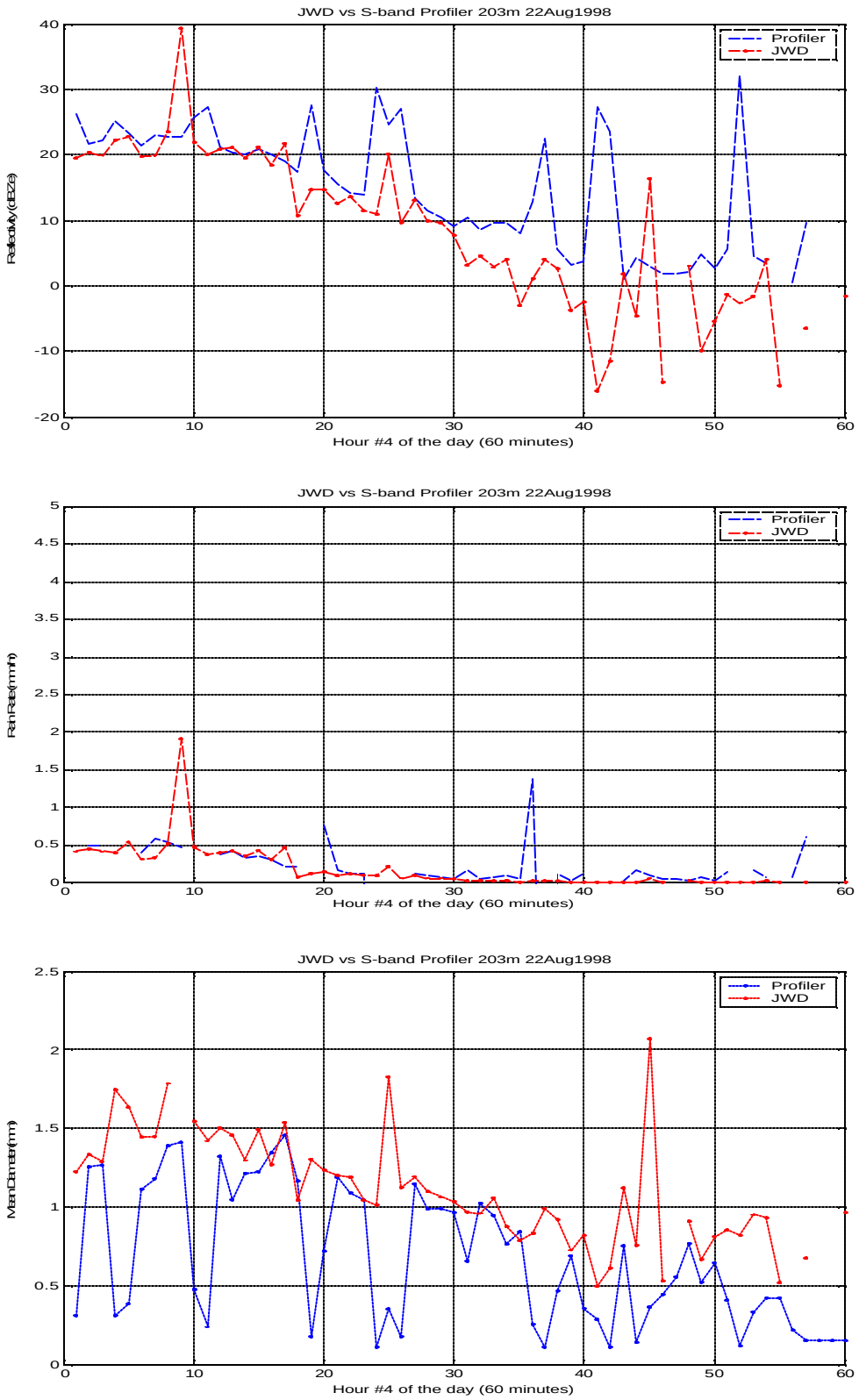

Figure C.1.4 Profiler observations vs. JWD observations for hour 4

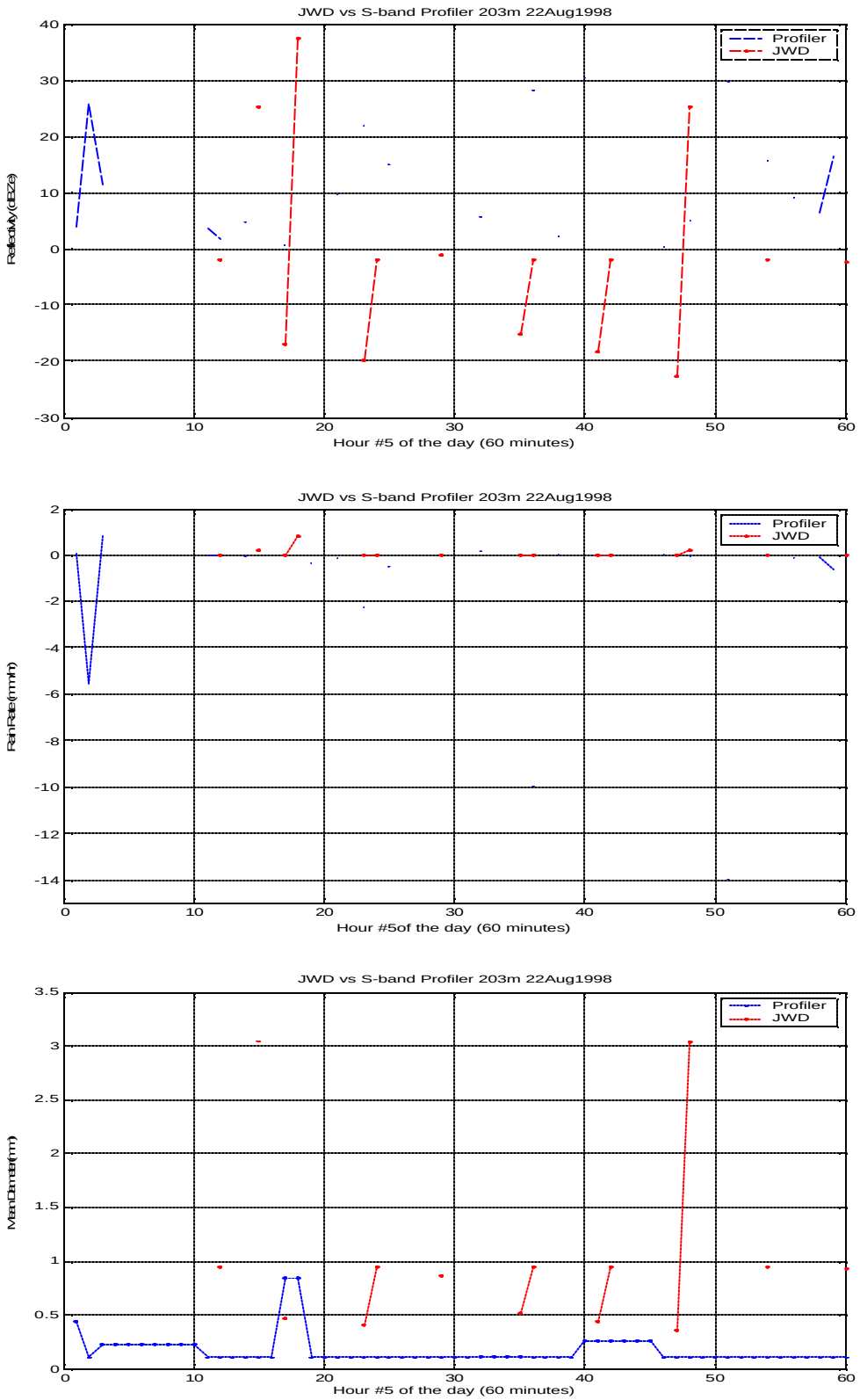

Figure C.1.5 Profiler observations vs. JWD observations for hour 5

C.2 Simulated Profiler Doppler Spectra For Hour 3

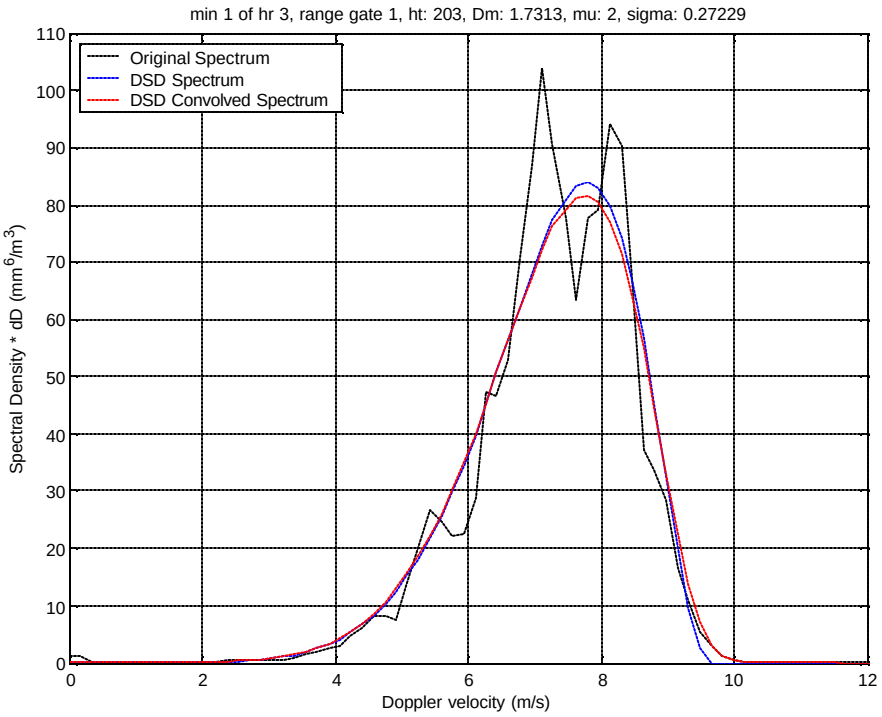

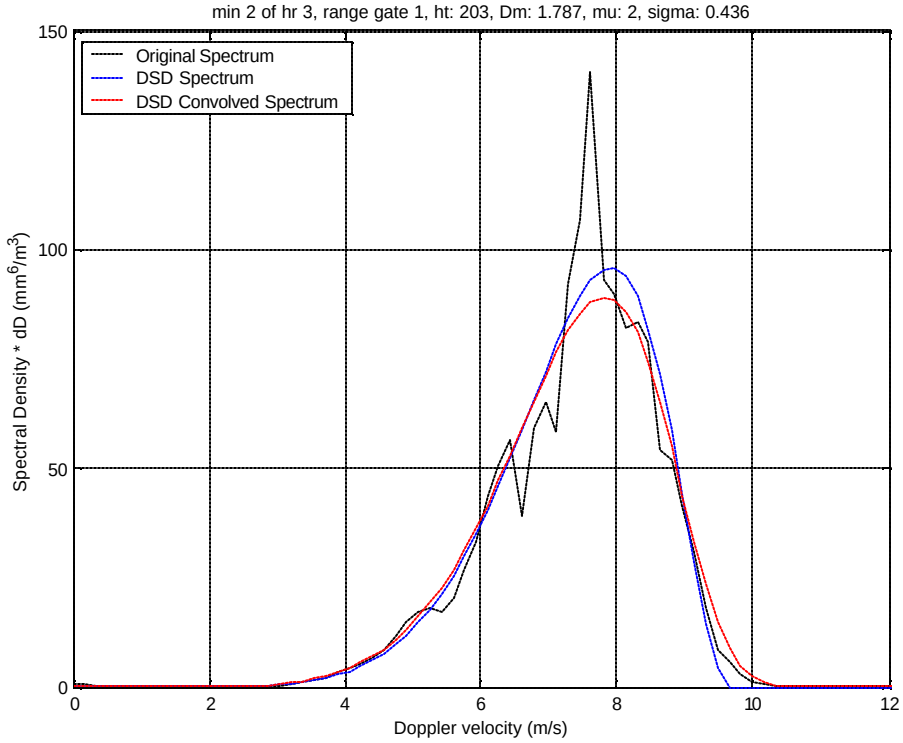

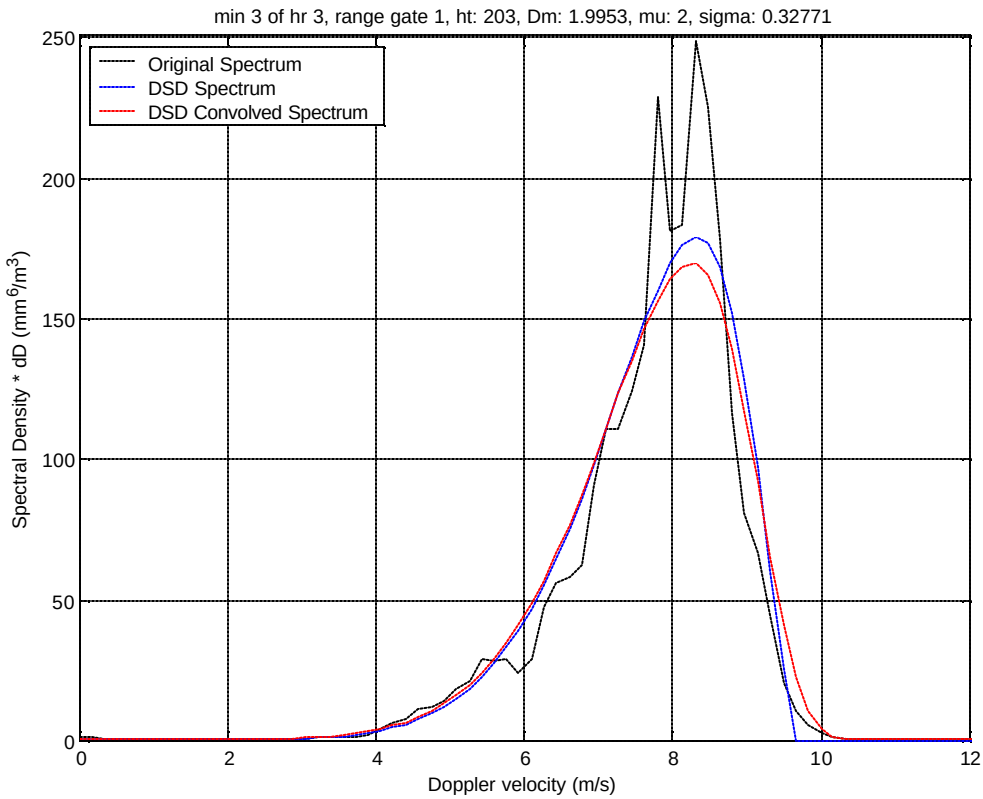
min 3 of hr 3, range gate 1, ht: 203, Dm: 1.9953, mu: 2, sigma: 0.32771
Original Spectrum
DSD Spectrum
DSD Convolved Spectrum
Spectral Density * dD (mm6/m3)
Doppler velocity (m/s)
0
50
100
150
200
250
0
2
4
6
8
10
12

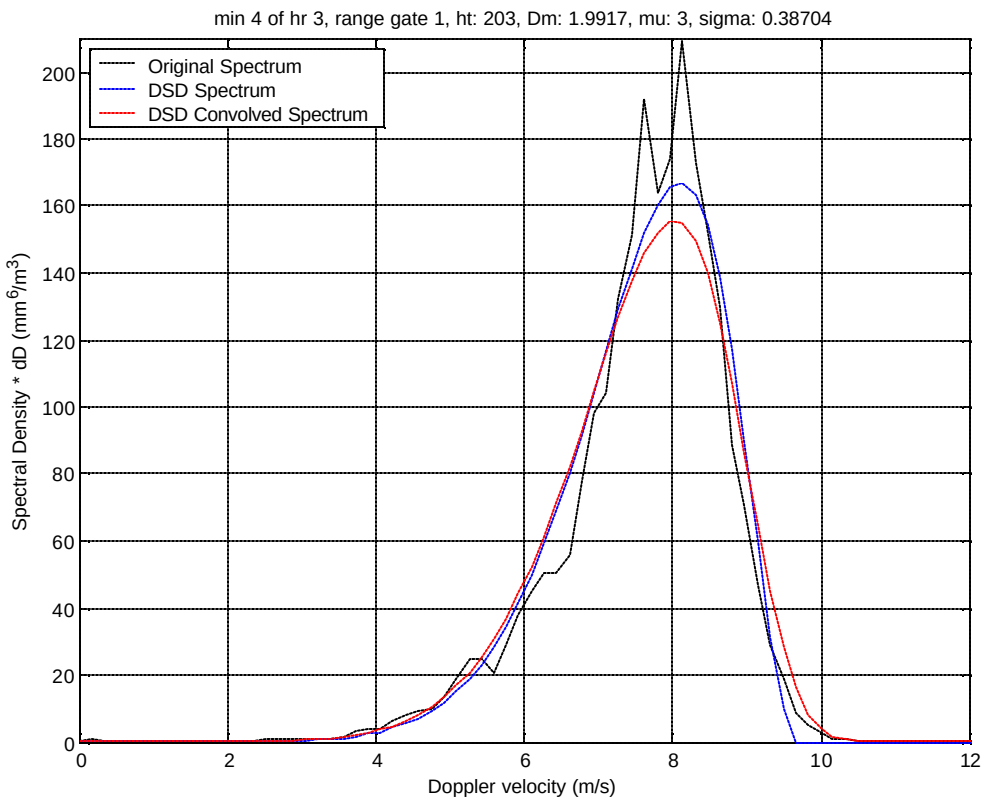
min 4 of hr 3, range gate 1, ht: 203, Dm: 1.9917, mu: 3, sigma: 0.38704
Original Spectrum
DSD Spectrum
DSD Convolved Spectrum
Spectral Density * dD (mm6/m3)
Doppler velocity (m/s)
0
20
40
60
80
100
120
140
160
180
200
0
2
4
6
8
10
12

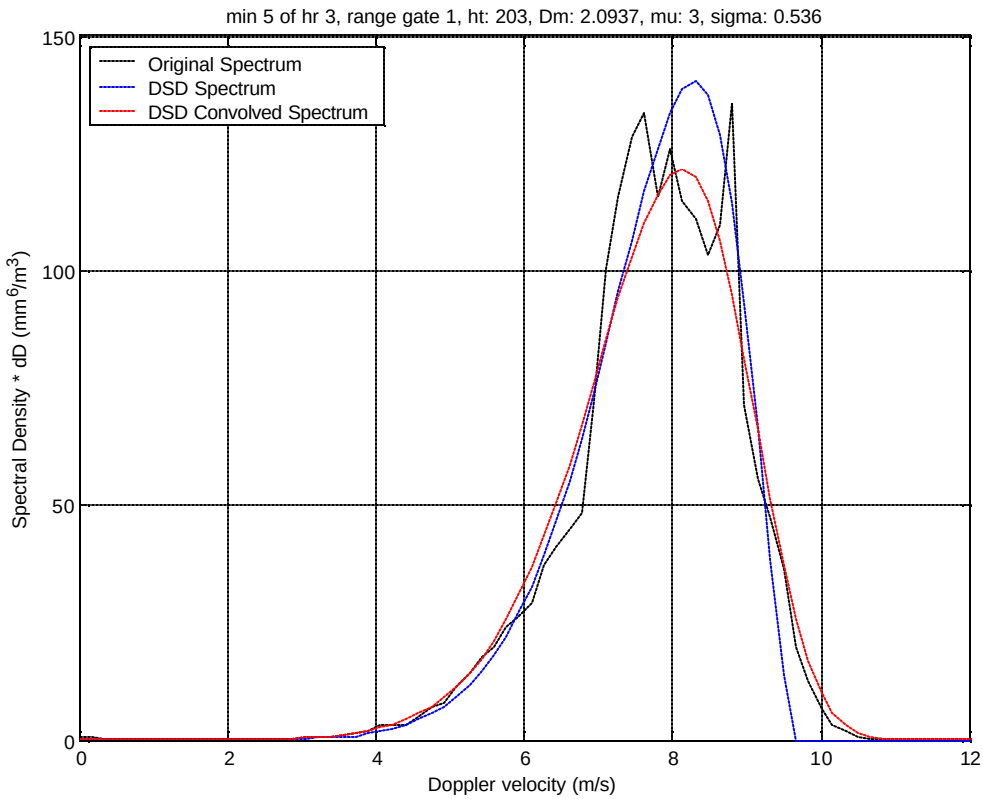
min 5 of hr 3, range gate 1, ht: 203, Dm: 2.0937, mu: 3, sigma: 0.536
Original Spectrum
DSD Spectrum
DSD Convolved Spectrum
Spectral Density * dD (mm6/m3)
Doppler velocity (m/s)
0
50
100
150
0
2
4
6
8
10
12

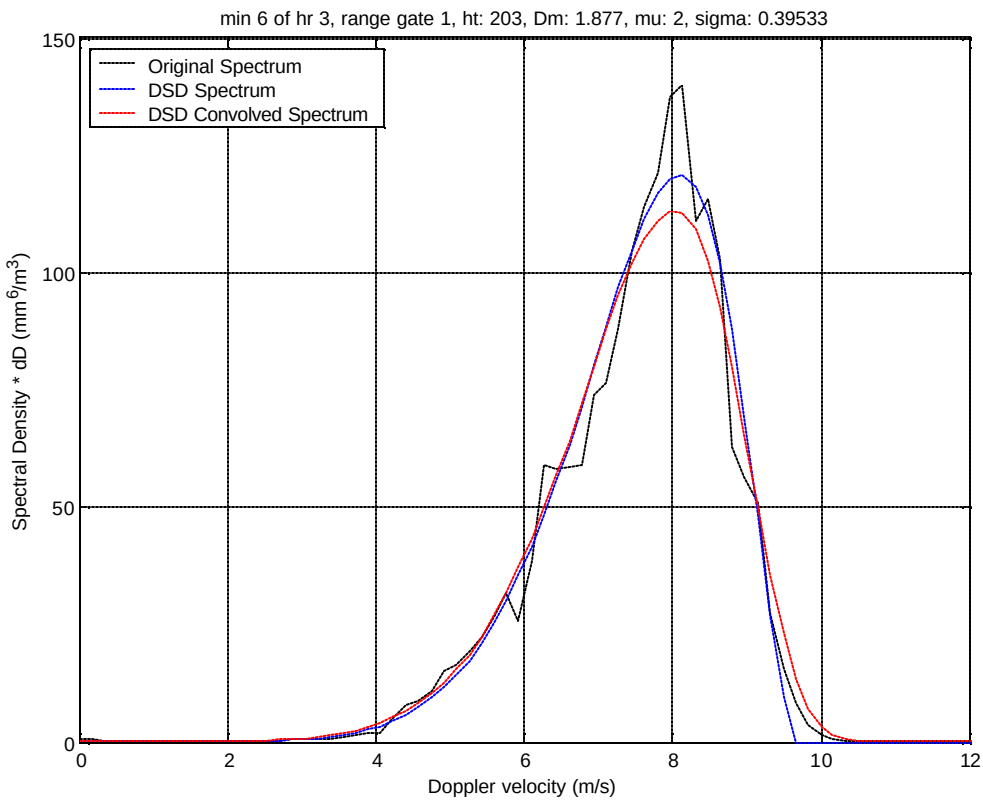
min 6 of hr 3, range gate 1, ht: 203, Dm: 1.877, mu: 2, sigma: 0.39533
Original Spectrum
DSD Spectrum
DSD Convolved Spectrum
Spectral Density * dD (mm6/m3)
Doppler velocity (m/s)
0
50
100
150
0
2
4
6
8
10
12

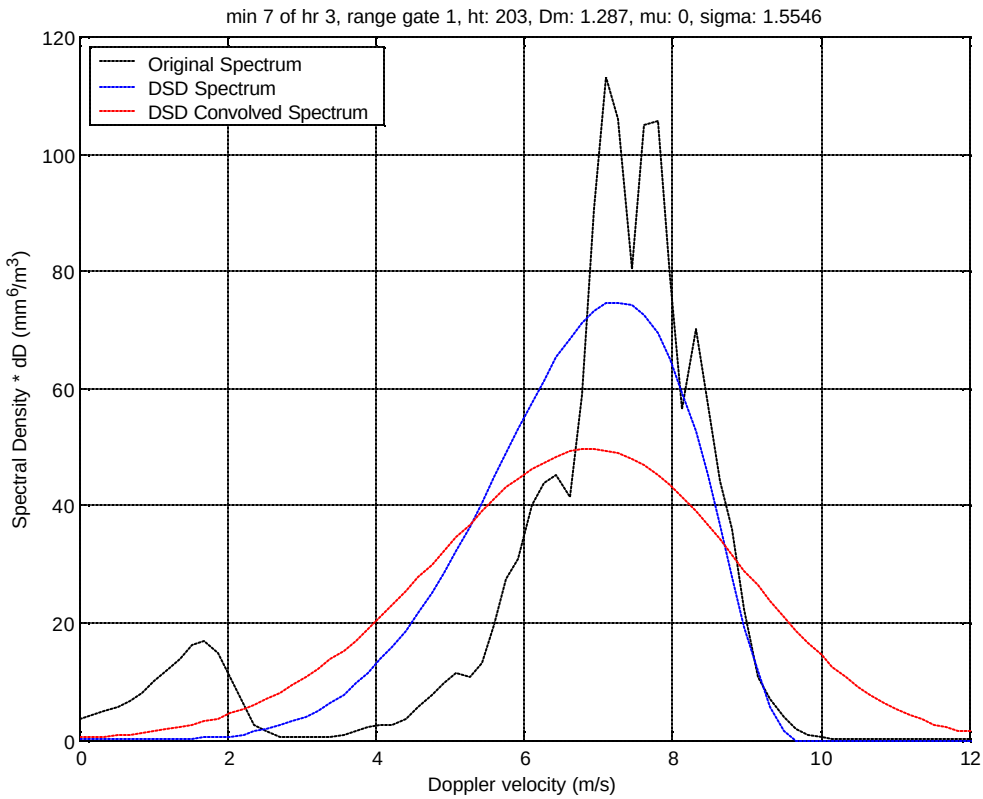
min 7 of hr 3, range gate 1, ht: 203, Dm: 1.287, mu: 0, sigma: 1.5546
Original Spectrum
DSD Spectrum
DSD Convolved Spectrum
Spectral Density * dD (mm6/m3)
Doppler velocity (m/s)
0
20
40
60
80
100
120
0
2
4
6
8
10
12

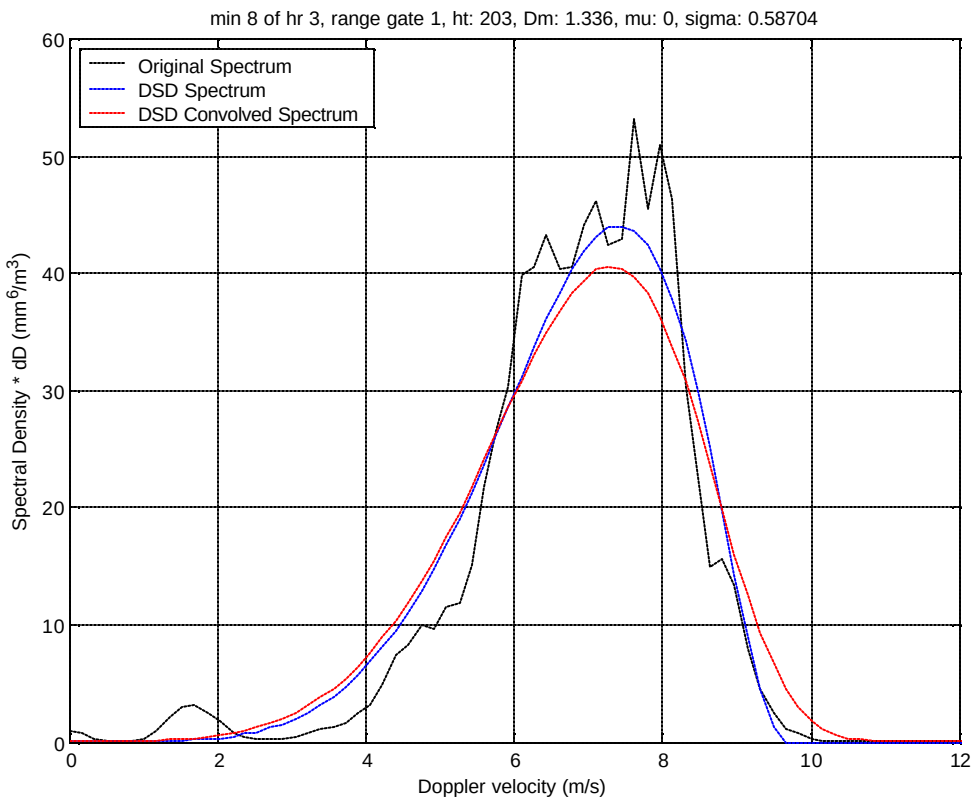
min 8 of hr 3, range gate 1, ht: 203, Dm: 1.336, mu: 0, sigma: 0.58704
Original Spectrum
DSD Spectrum
DSD Convolved Spectrum
Spectral Density * dD (mm6/m3)
Doppler velocity (m/s)
0
10
20
30
40
50
60
0
2
4
6
8
10
12

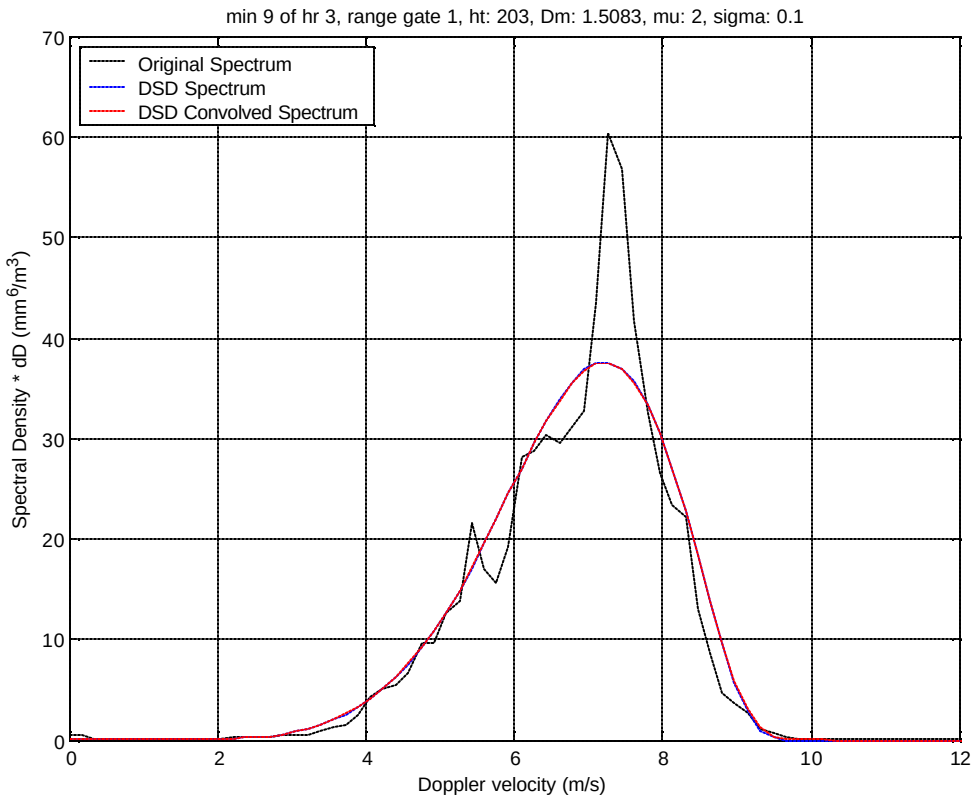
min 9 of hr 3, range gate 1, ht: 203, Dm: 1.5083, mu: 2, sigma: 0.1
Original Spectrum
DSD Spectrum
DSD Convolved Spectrum
Spectral Density * dD (mm6/m3)
Doppler velocity (m/s)
0
10
20
30
40
50
60
70
0
2
4
6
8
10
12

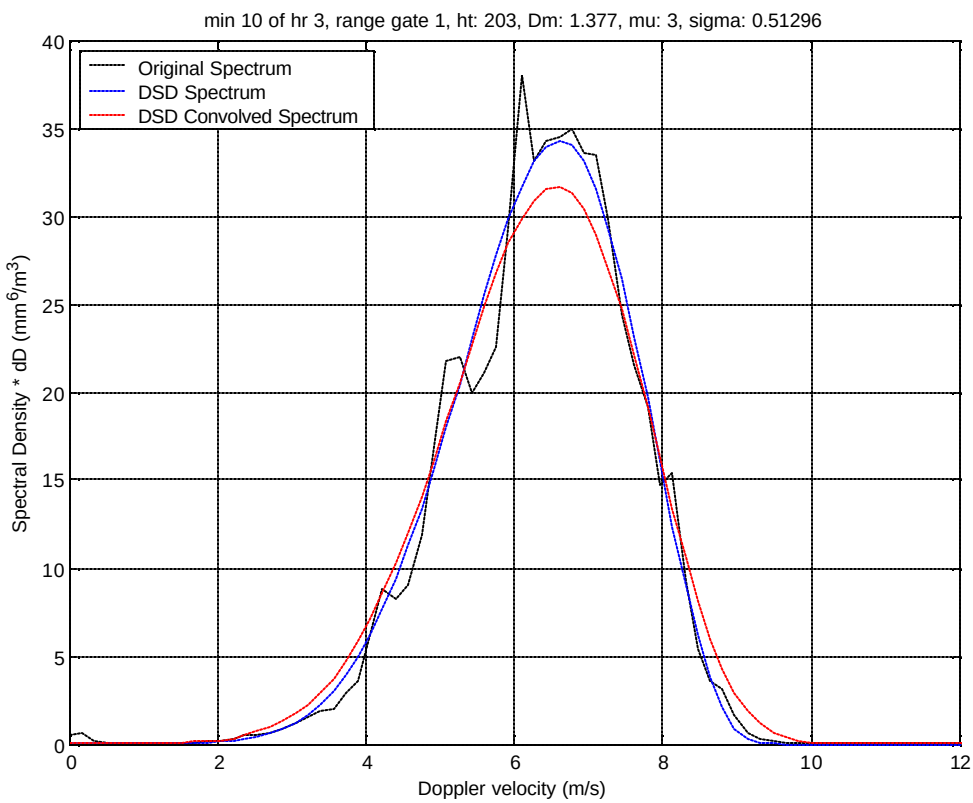
min 10 of hr 3, range gate 1, ht: 203, Dm: 1.377, mu: 3, sigma: 0.51296
Original Spectrum
DSD Spectrum
DSD Convolved Spectrum
Spectral Density * dD (mm6/m3)
Doppler velocity (m/s)
0
5
10
15
20
25
30
35
40
0
2
4
6
8
10
12

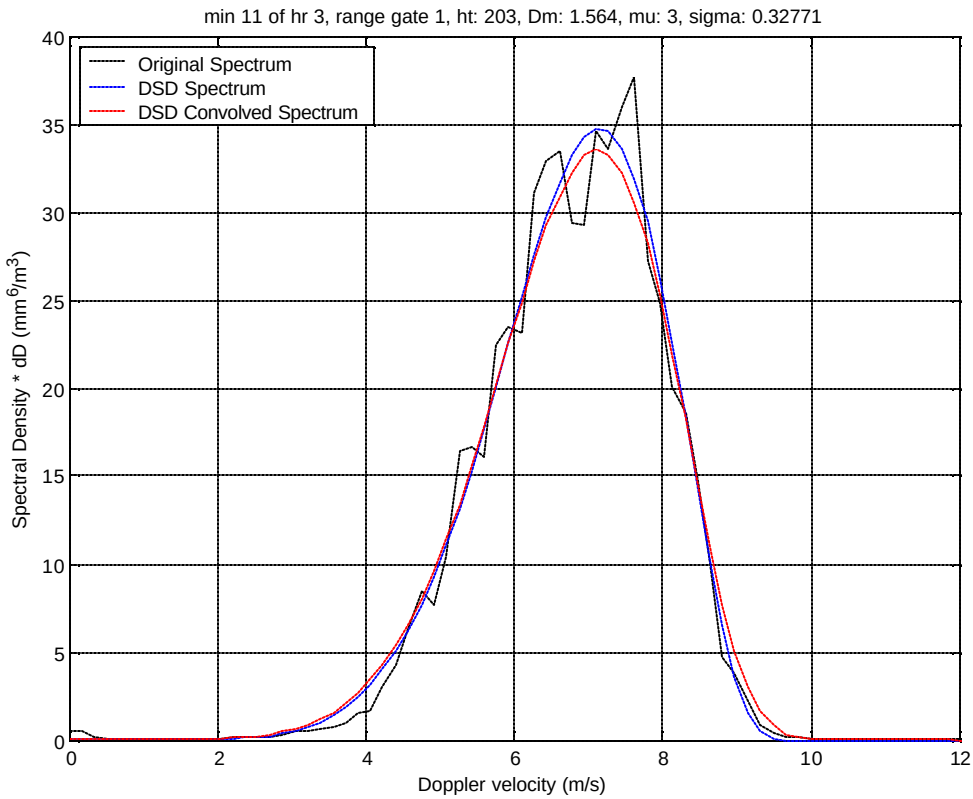
min 11 of hr 3, range gate 1, ht: 203, Dm: 1.564, mu: 3, sigma: 0.32771
Original Spectrum
DSD Spectrum
DSD Convolved Spectrum
Spectral Density * dD (mm6/m3)
Doppler velocity (m/s)
0
5
10
15
20
25
30
35
40
0
2
4
6
8
10
12

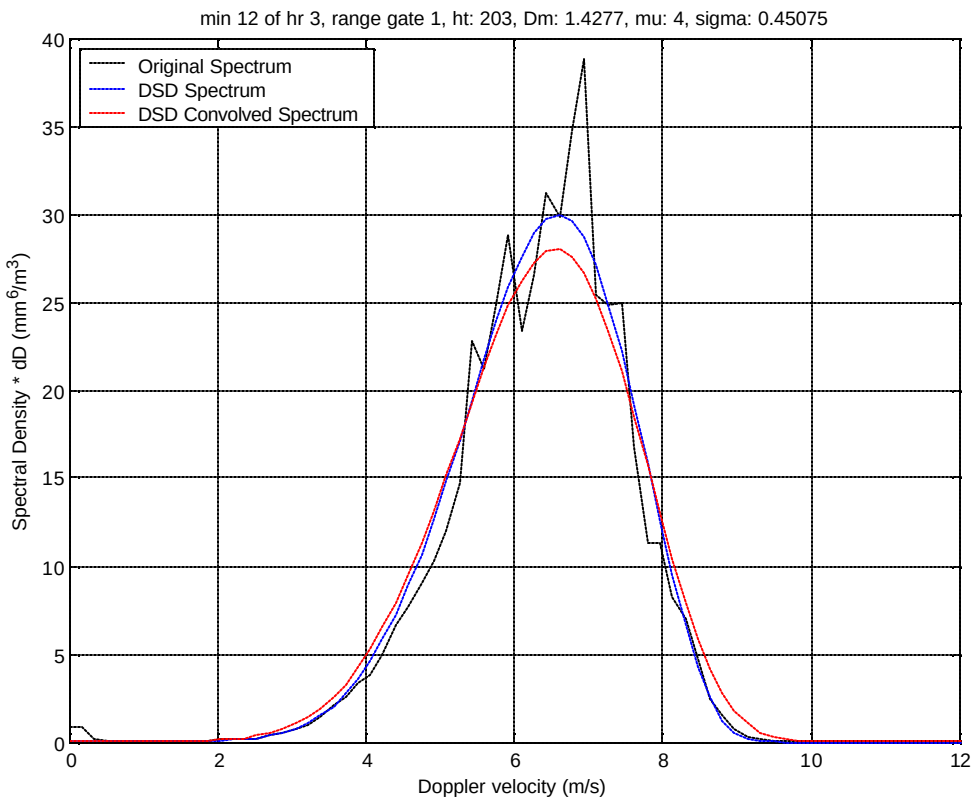
min 12 of hr 3, range gate 1, ht: 203, Dm: 1.4277, mu: 4, sigma: 0.45075
Original Spectrum
DSD Spectrum
DSD Convolved Spectrum
Spectral Density * dD (mm6/m3)
Doppler velocity (m/s)
0
5
10
15
20
25
30
35
40
0
2
4
6
8
10
12

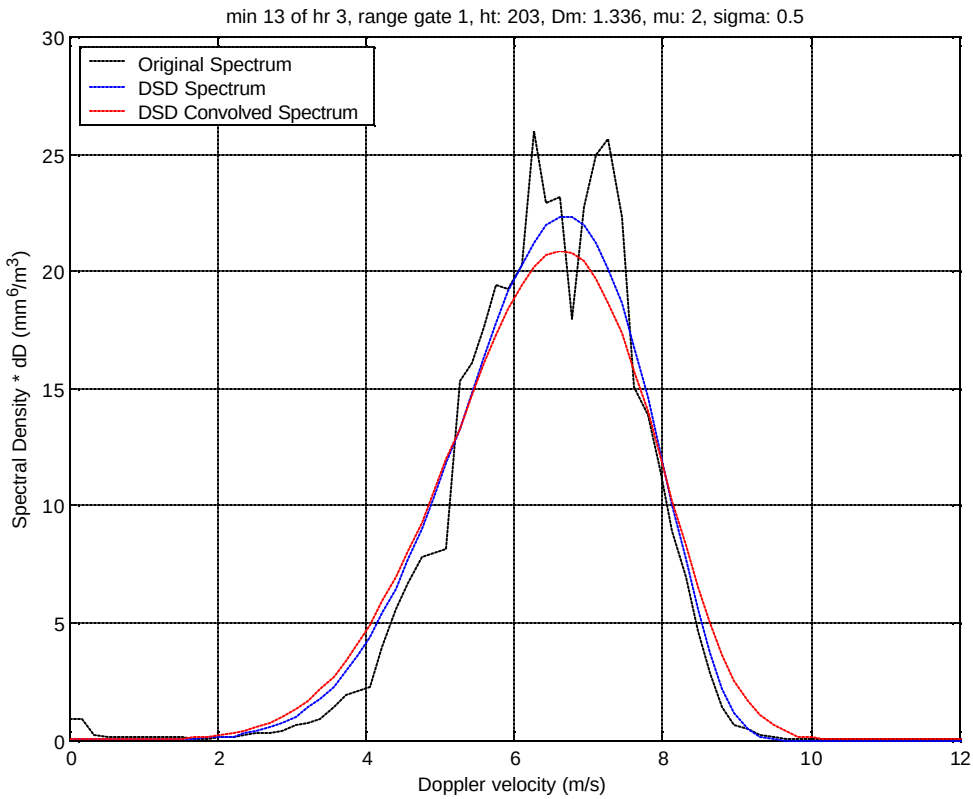
min 13 of hr 3, range gate 1, ht: 203, Dm: 1.336, mu: 2, sigma: 0.5
Original Spectrum
DSD Spectrum
DSD Convolved Spectrum
Spectral Density * dD (mm6/m3)
Doppler velocity (m/s)
0
5
10
15
20
25
30
0
2
4
6
8
10
12

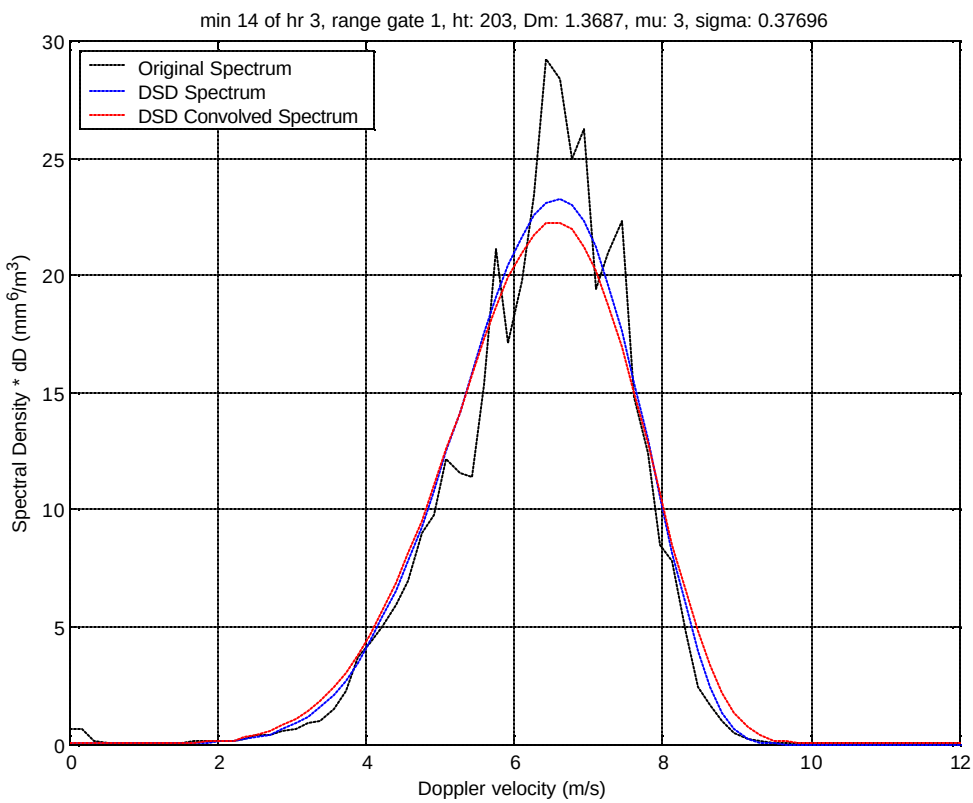
min 14 of hr 3, range gate 1, ht: 203, Dm: 1.3687, mu: 3, sigma: 0.37696
Original Spectrum
DSD Spectrum
DSD Convolved Spectrum
Spectral Density * dD (mm6/m3)
Doppler velocity (m/s)
0
5
10
15
20
25
30
0
2
4
6
8
10
12

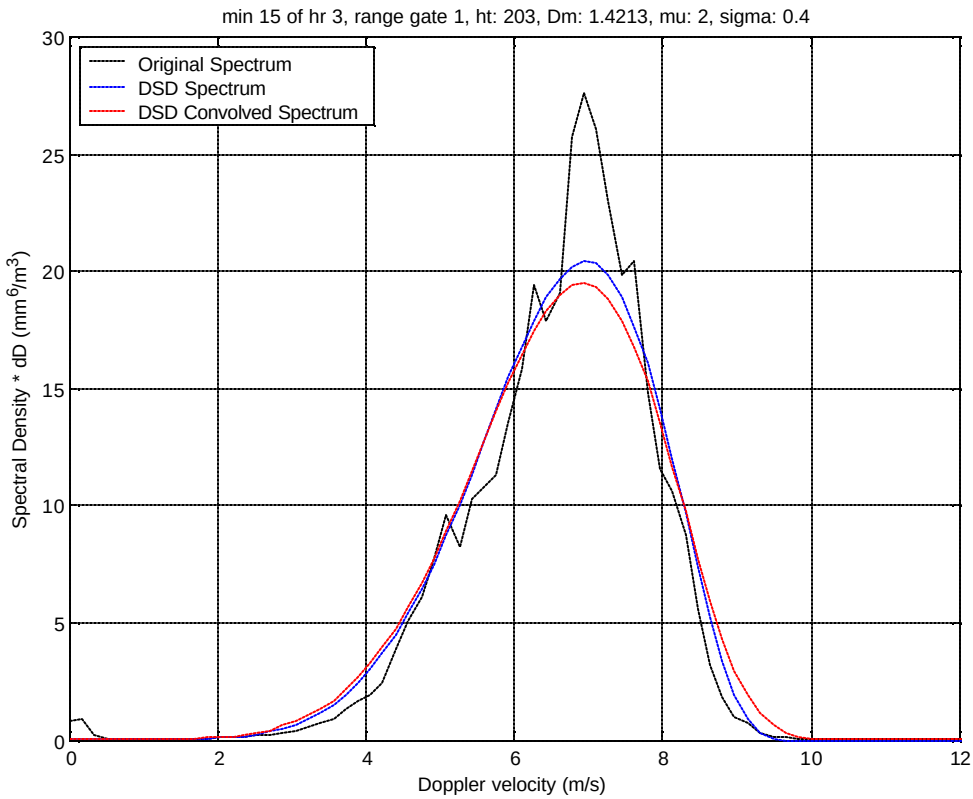
min 15 of hr 3, range gate 1, ht: 203, Dm: 1.4213, mu: 2, sigma: 0.4
Original Spectrum
DSD Spectrum
DSD Convolved Spectrum
Spectral Density * dD (mm6/m3)
Doppler velocity (m/s)
0
5
10
15
20
25
30
0
2
4
6
8
10
12

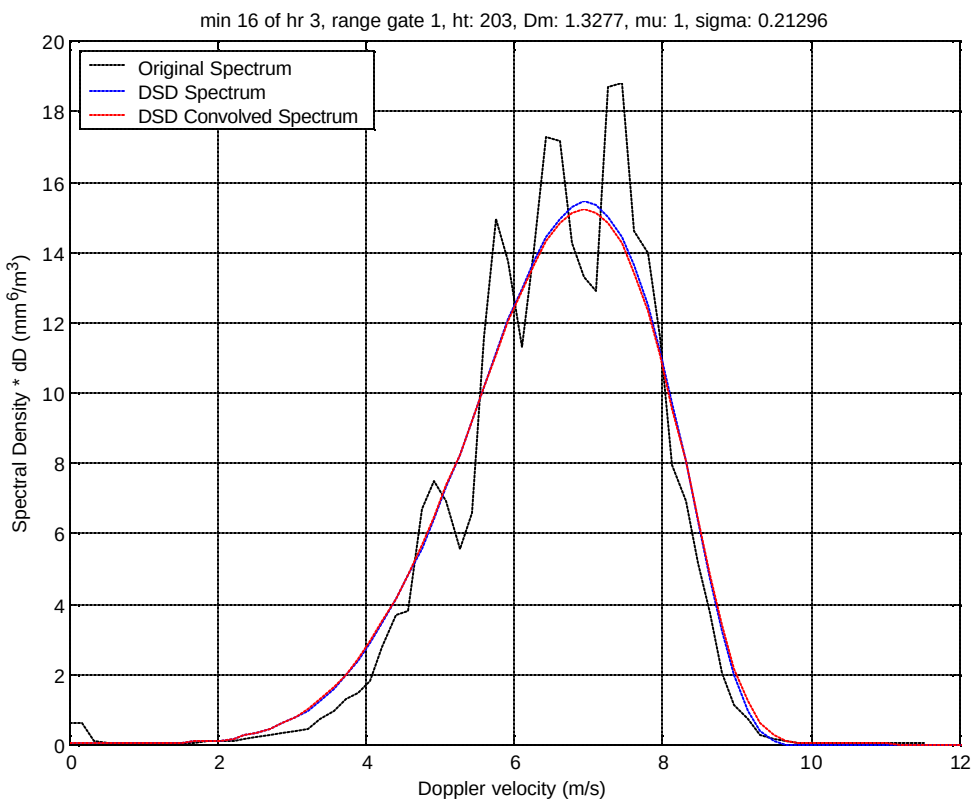
min 16 of hr 3, range gate 1, ht: 203, Dm: 1.3277, mu: 1, sigma: 0.21296
Original Spectrum
DSD Spectrum
DSD Convolved Spectrum
Spectral Density * dD (mm6/m3)
Doppler velocity (m/s)
0
2
4
6
8
10
12
14
16
18
20
0
2
4
6
8
10
12

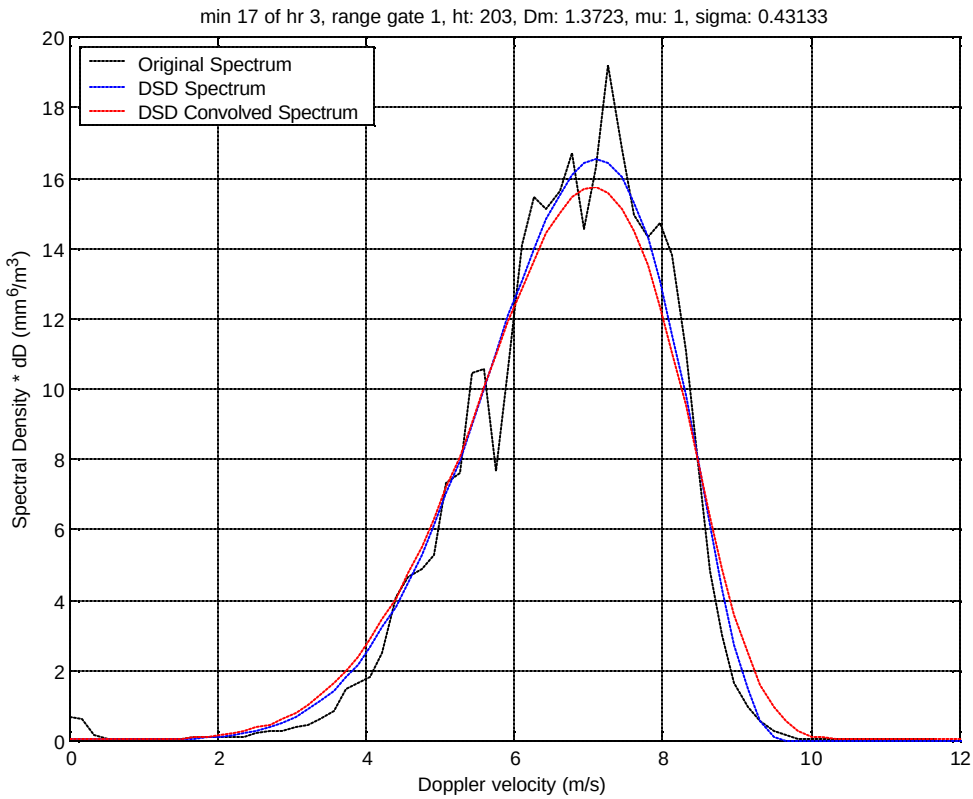
min 17 of hr 3, range gate 1, ht: 203, Dm: 1.3723, mu: 1, sigma: 0.43133
Original Spectrum
DSD Spectrum
DSD Convolved Spectrum
Spectral Density * dD (mm6/m3)
Doppler velocity (m/s)
0
2
4
6
8
10
12
14
16
18
20

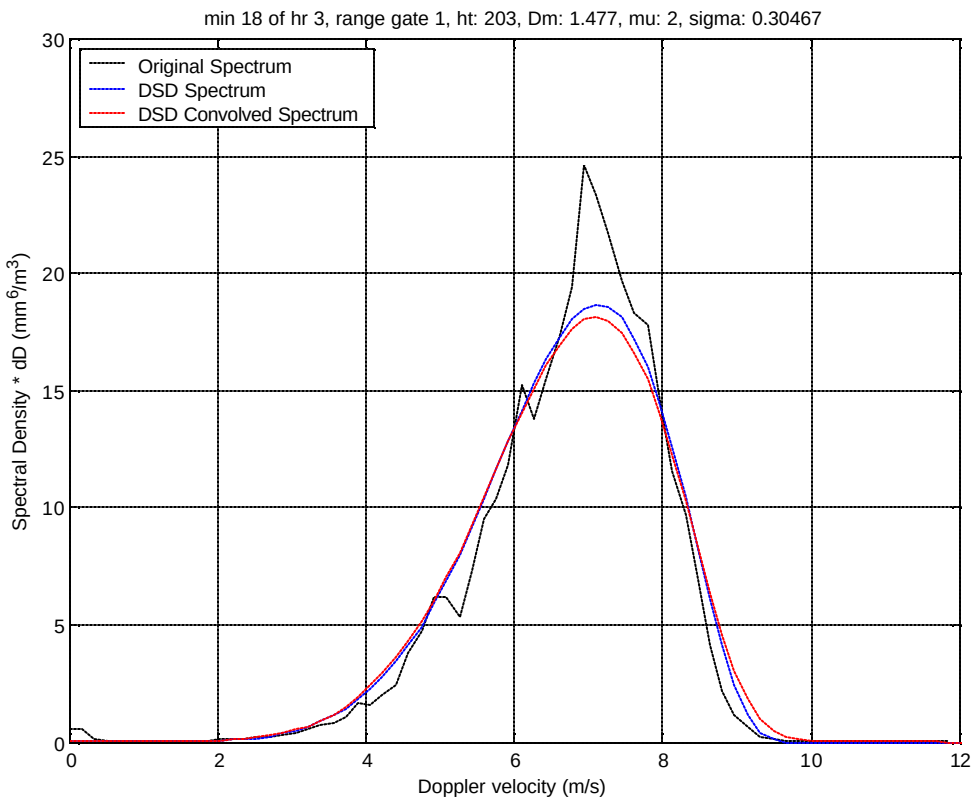
min 18 of hr 3, range gate 1, ht: 203, Dm: 1.477, mu: 2, sigma: 0.30467
Original Spectrum
DSD Spectrum
DSD Convolved Spectrum
Spectral Density * dD (mm6/m3)
Doppler velocity (m/s)
0
5
10
15
20
25
30

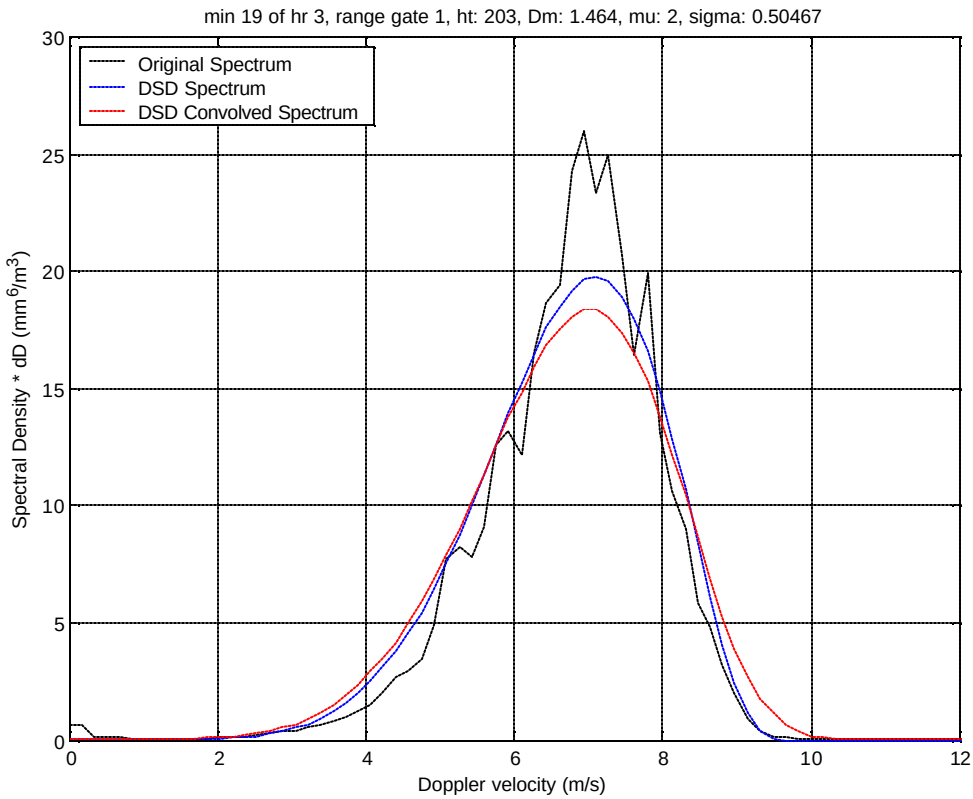
min 19 of hr 3, range gate 1, ht: 203, Dm: 1.464, mu: 2, sigma: 0.50467
Original Spectrum
DSD Spectrum
DSD Convolved Spectrum
Spectral Density * dD (mm6/m3)
Doppler velocity (m/s)
0
5
10
15
20
25
30
0
2
4
6
8
10
12

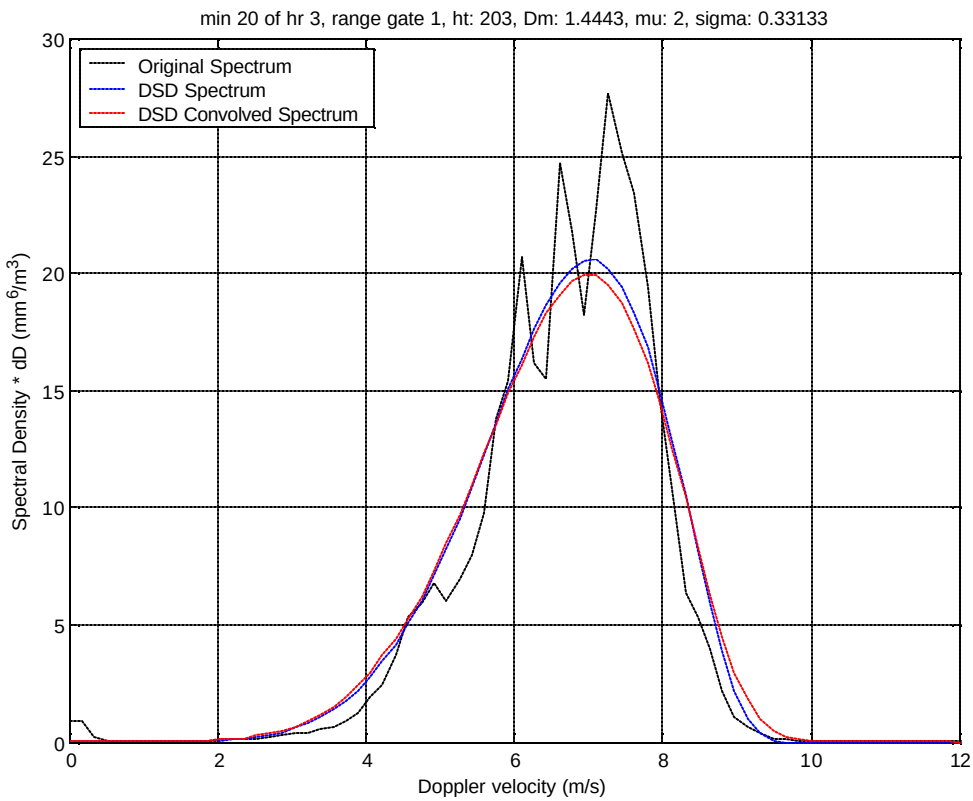
min 20 of hr 3, range gate 1, ht: 203, Dm: 1.4443, mu: 2, sigma: 0.33133
Original Spectrum
DSD Spectrum
DSD Convolved Spectrum
Spectral Density * dD (mm6/m3)
Doppler velocity (m/s)
0
5
10
15
20
25
30
0
2
4
6
8
10
12

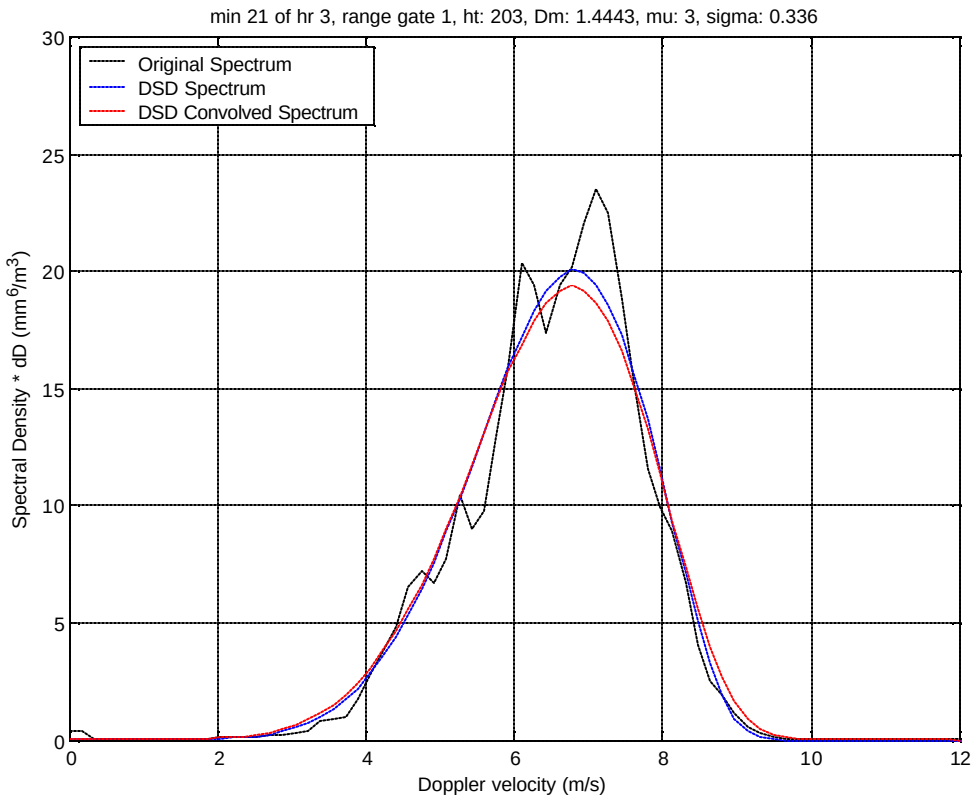
min 21 of hr 3, range gate 1, ht: 203, Dm: 1.4443, mu: 3, sigma: 0.336
Original Spectrum
DSD Spectrum
DSD Convolved Spectrum
Spectral Density * dD (mm6/m3)
Doppler velocity (m/s)
0
5
10
15
20
25
30
0
2
4
6
8
10
12

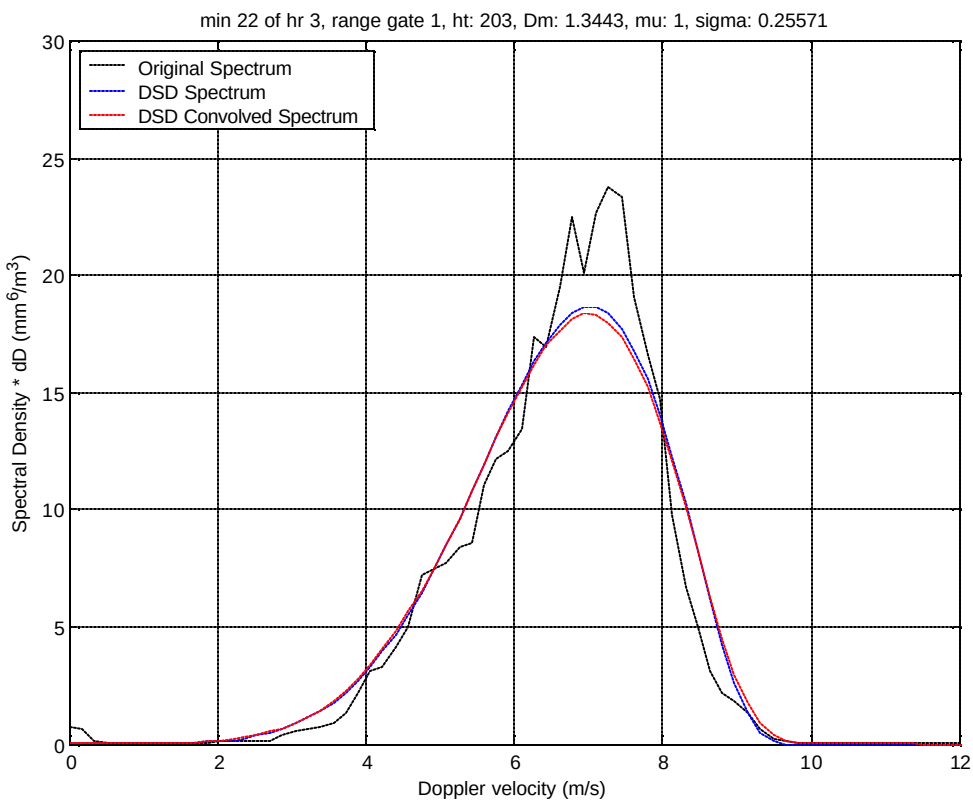
min 22 of hr 3, range gate 1, ht: 203, Dm: 1.3443, mu: 1, sigma: 0.25571
Original Spectrum
DSD Spectrum
DSD Convolved Spectrum
Spectral Density * dD (mm6/m3)
Doppler velocity (m/s)
0
5
10
15
20
25
30
0
2
4
6
8
10
12

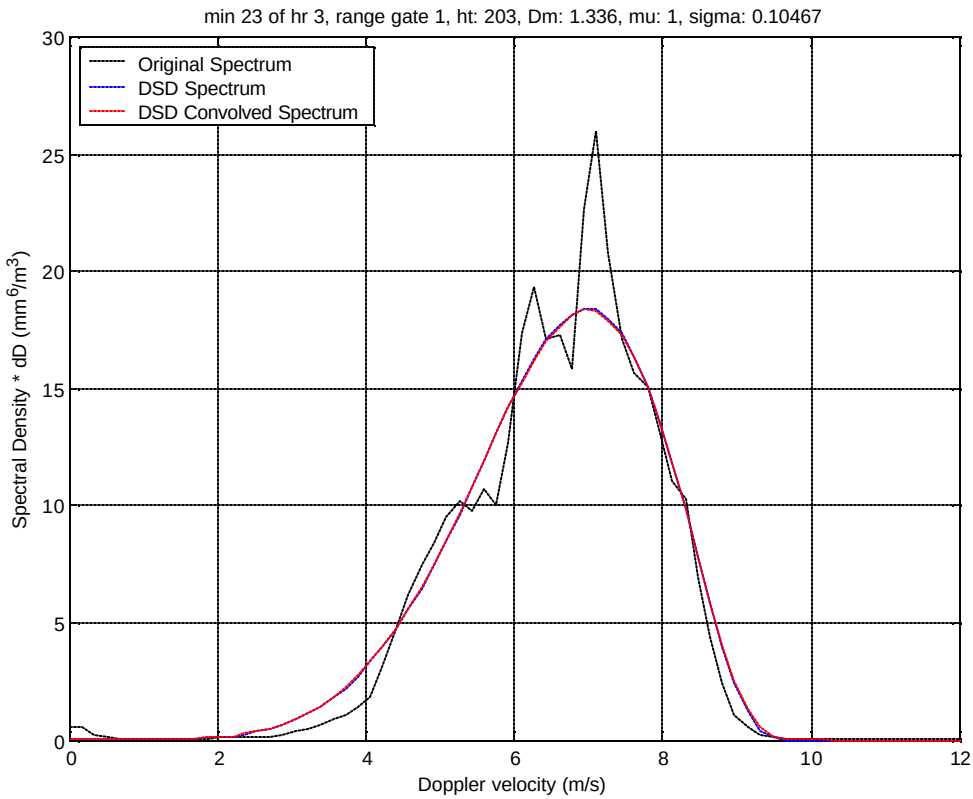
min 23 of hr 3, range gate 1, ht: 203, Dm: 1.336, mu: 1, sigma: 0.10467
Original Spectrum
DSD Spectrum
DSD Convolved Spectrum
Spectral Density * dD (mm6/m3)
Doppler velocity (m/s)
0
5
10
15
20
25
30
0
2
4
6
8
10
12

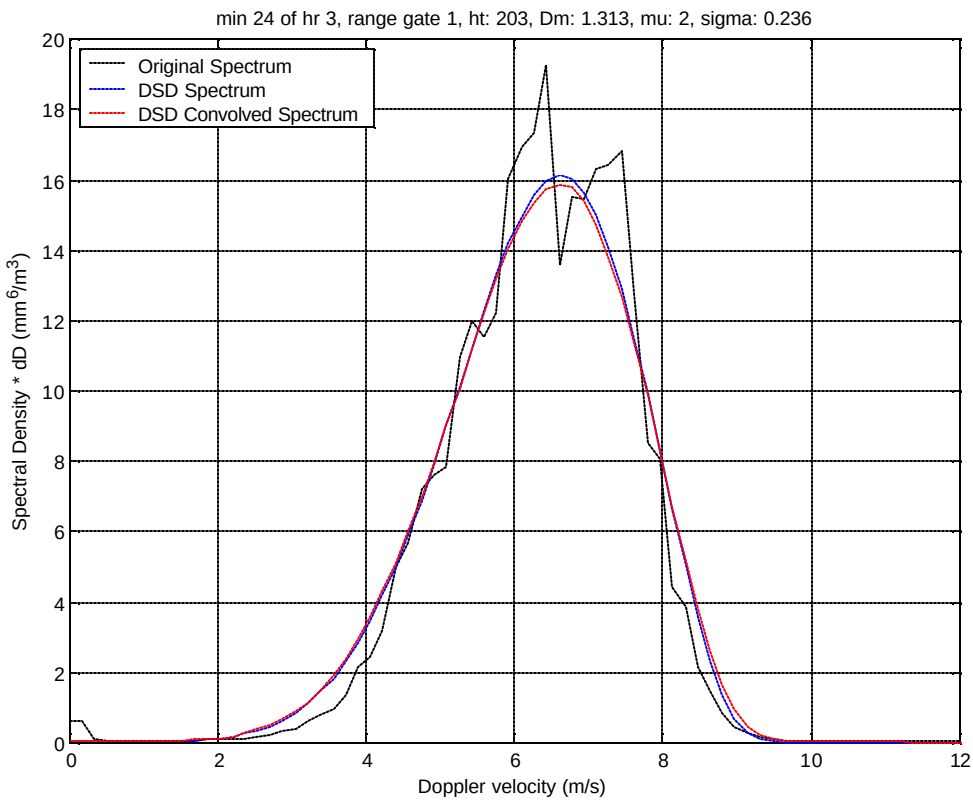
min 24 of hr 3, range gate 1, ht: 203, Dm: 1.313, mu: 2, sigma: 0.236
Original Spectrum
DSD Spectrum
DSD Convolved Spectrum
Spectral Density * dD (mm6/m3)
Doppler velocity (m/s)
0
2
4
6
8
10
12
14
16
18
20
0
2
4
6
8
10
12

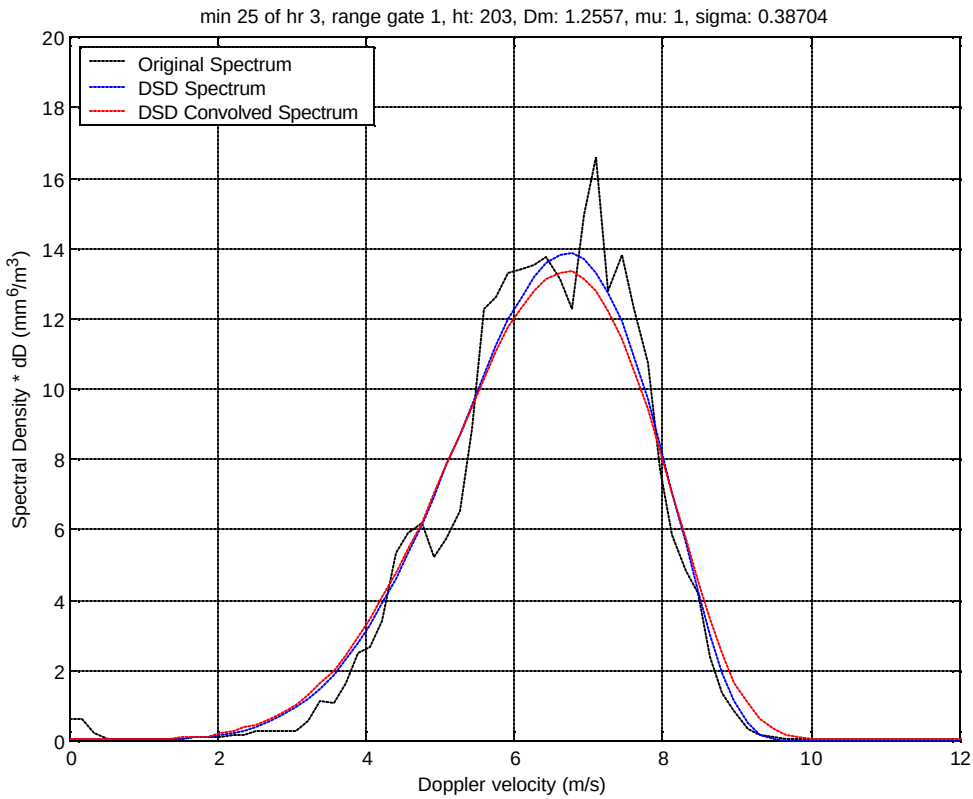
min 25 of hr 3, range gate 1, ht: 203, Dm: 1.2557, mu: 1, sigma: 0.38704
Original Spectrum
DSD Spectrum
DSD Convolved Spectrum
Spectral Density * dD (mm6/m3)
Doppler velocity (m/s)
0
2
4
6
8
10
12
14
16
18
20

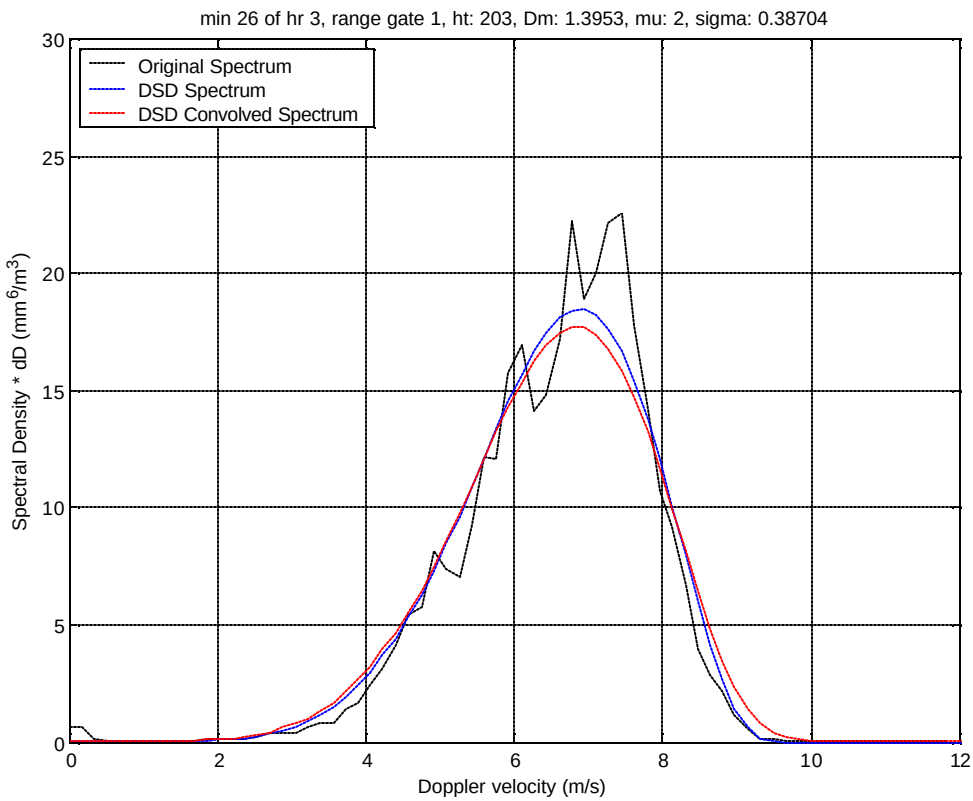
min 26 of hr 3, range gate 1, ht: 203, Dm: 1.3953, mu: 2, sigma: 0.38704
Original Spectrum
DSD Spectrum
DSD Convolved Spectrum
Spectral Density * dD (mm6/m3)
Doppler velocity (m/s)
0
5
10
15
20
25
30

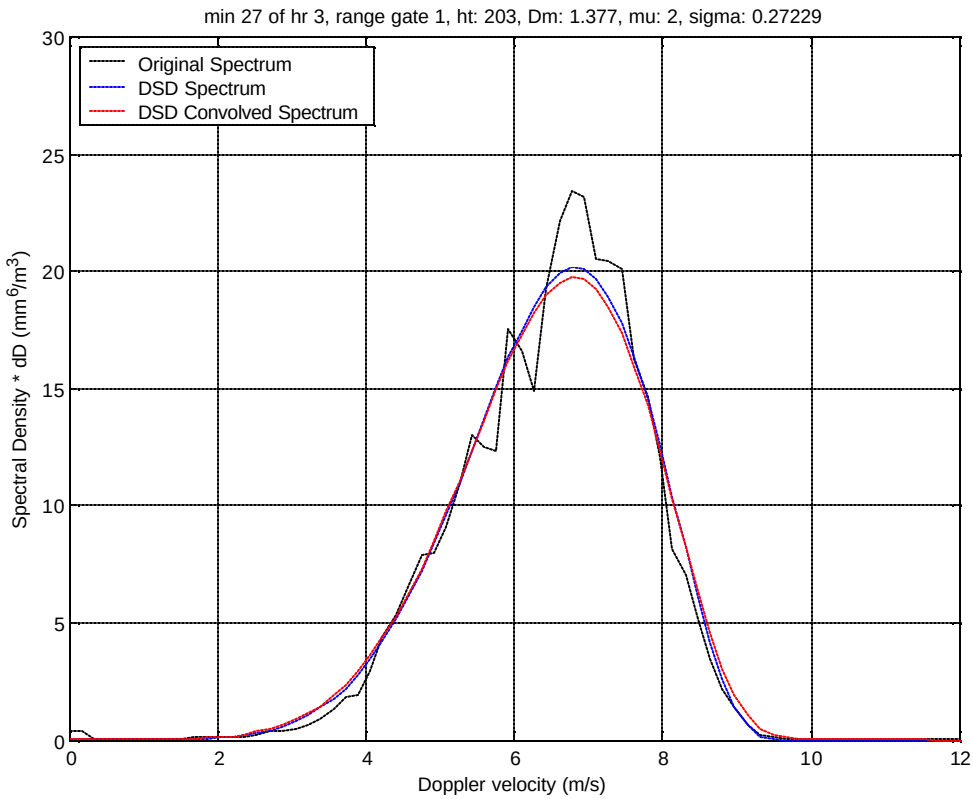
min 27 of hr 3, range gate 1, ht: 203, Dm: 1.377, mu: 2, sigma: 0.27229
Original Spectrum
DSD Spectrum
DSD Convolved Spectrum
Spectral Density * dD (mm6/m3)
Doppler velocity (m/s)
0
5
10
15
20
25
30
0
2
4
6
8
10
12

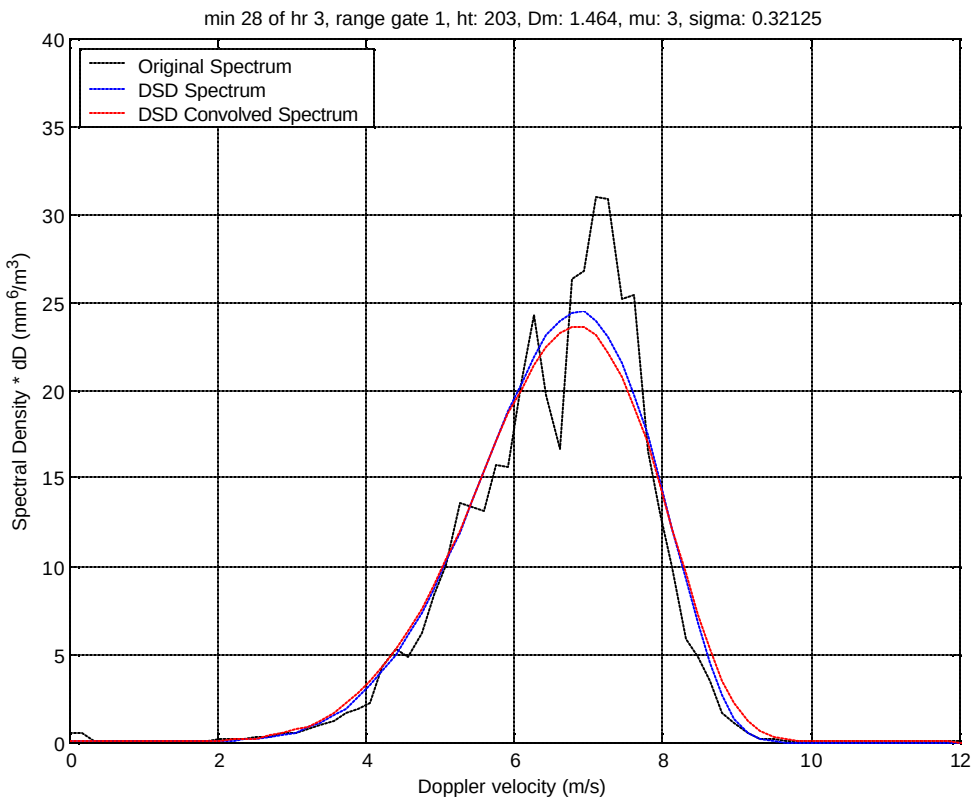
min 28 of hr 3, range gate 1, ht: 203, Dm: 1.464, mu: 3, sigma: 0.32125
Original Spectrum
DSD Spectrum
DSD Convolved Spectrum
Spectral Density * dD (mm6/m3)
Doppler velocity (m/s)
0
5
10
15
20
25
30
35
40
0
2
4
6
8
10
12

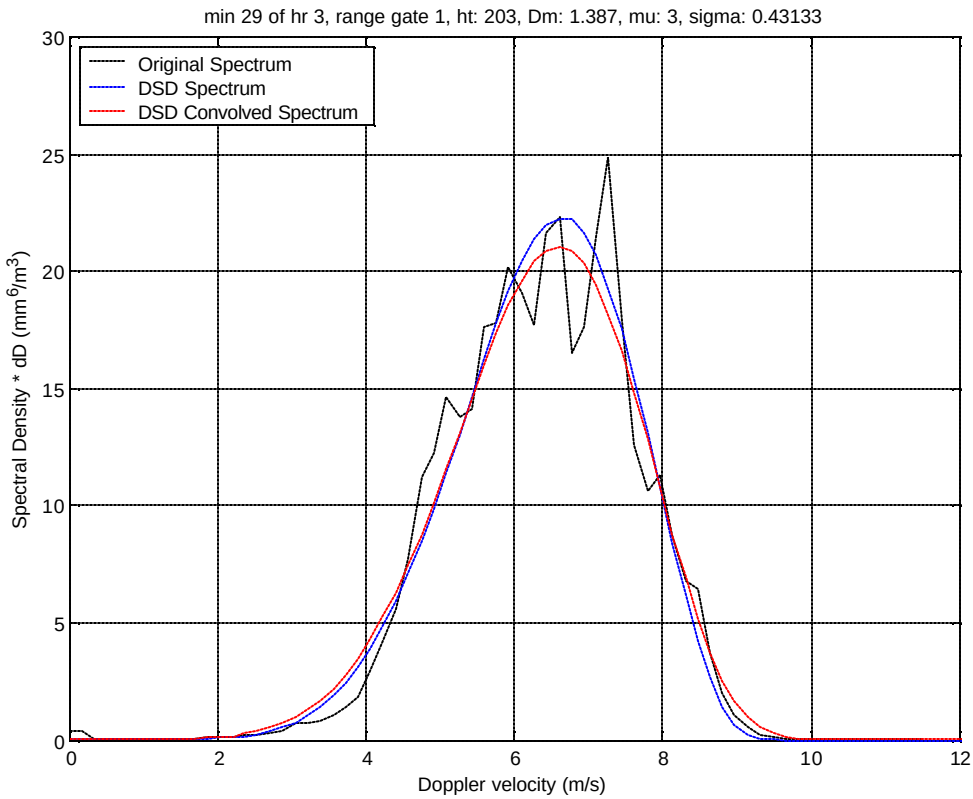
min 29 of hr 3, range gate 1, ht: 203, Dm: 1.387, mu: 3, sigma: 0.43133
Original Spectrum
DSD Spectrum
DSD Convolved Spectrum
Spectral Density * dD (mm6/m3)
Doppler velocity (m/s)
0
5
10
15
20
25
30
0
2
4
6
8
10
12

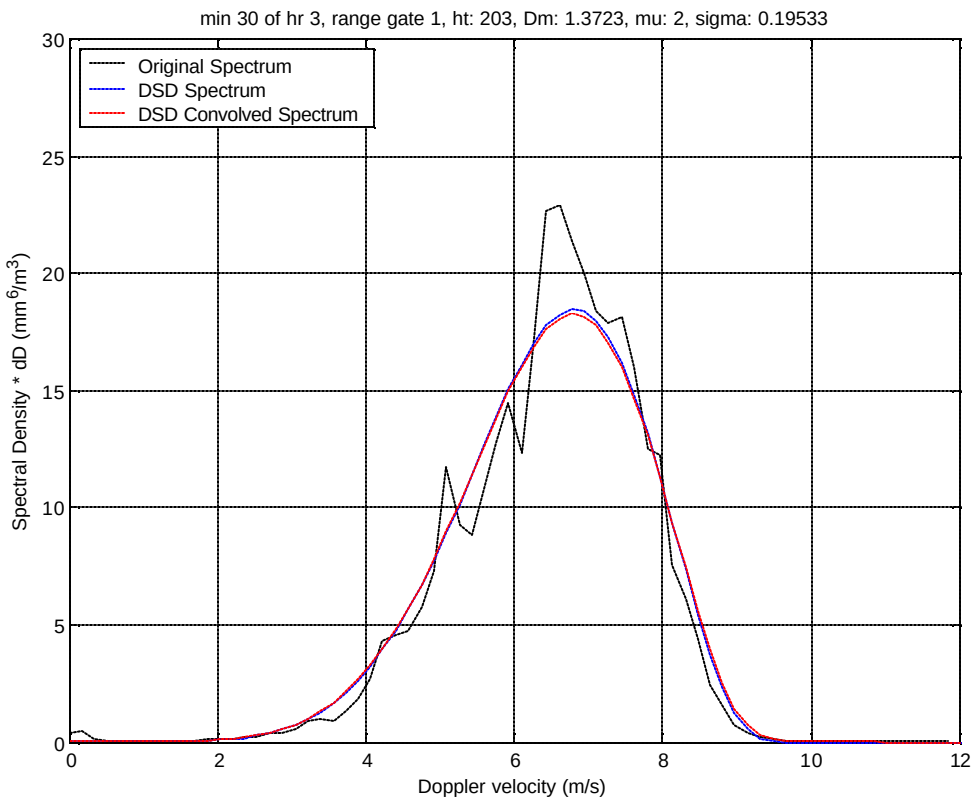
min 30 of hr 3, range gate 1, ht: 203, Dm: 1.3723, mu: 2, sigma: 0.19533
Original Spectrum
DSD Spectrum
DSD Convolved Spectrum
Spectral Density * dD (mm6/m3)
Doppler velocity (m/s)
0
5
10
15
20
25
30
0
2
4
6
8
10
12

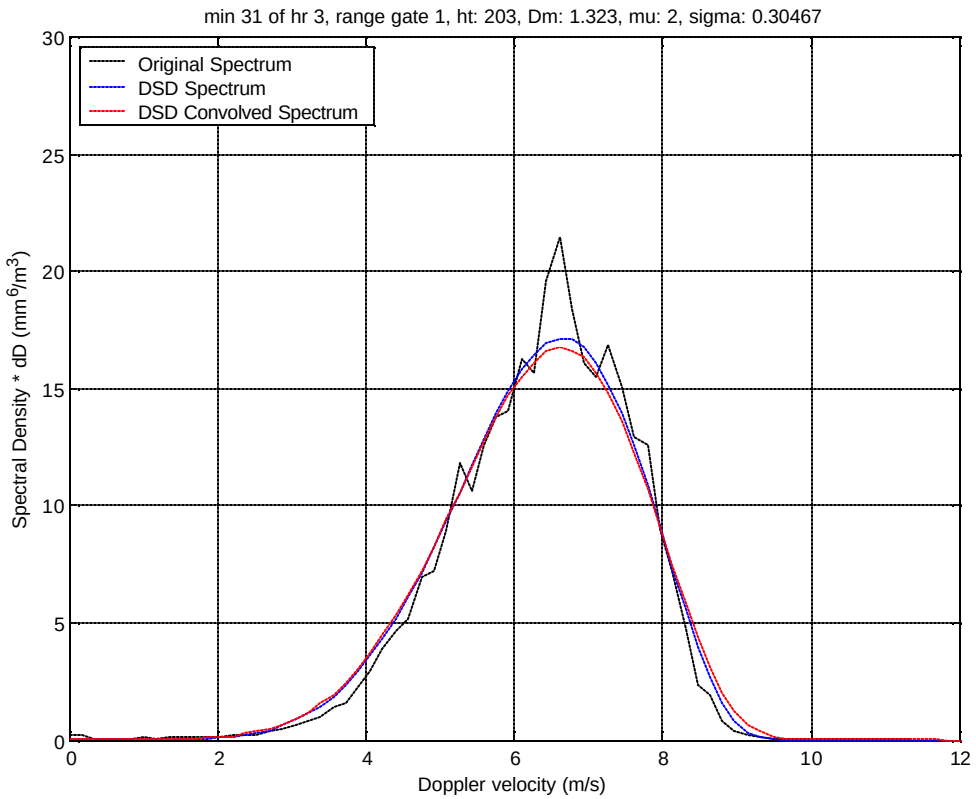
min 31 of hr 3, range gate 1, ht: 203, Dm: 1.323, mu: 2, sigma: 0.30467
Original Spectrum
DSD Spectrum
DSD Convolved Spectrum
Spectral Density * dD (mm6/m3)
Doppler velocity (m/s)
0
5
10
15
20
25
30
0
2
4
6
8
10
12

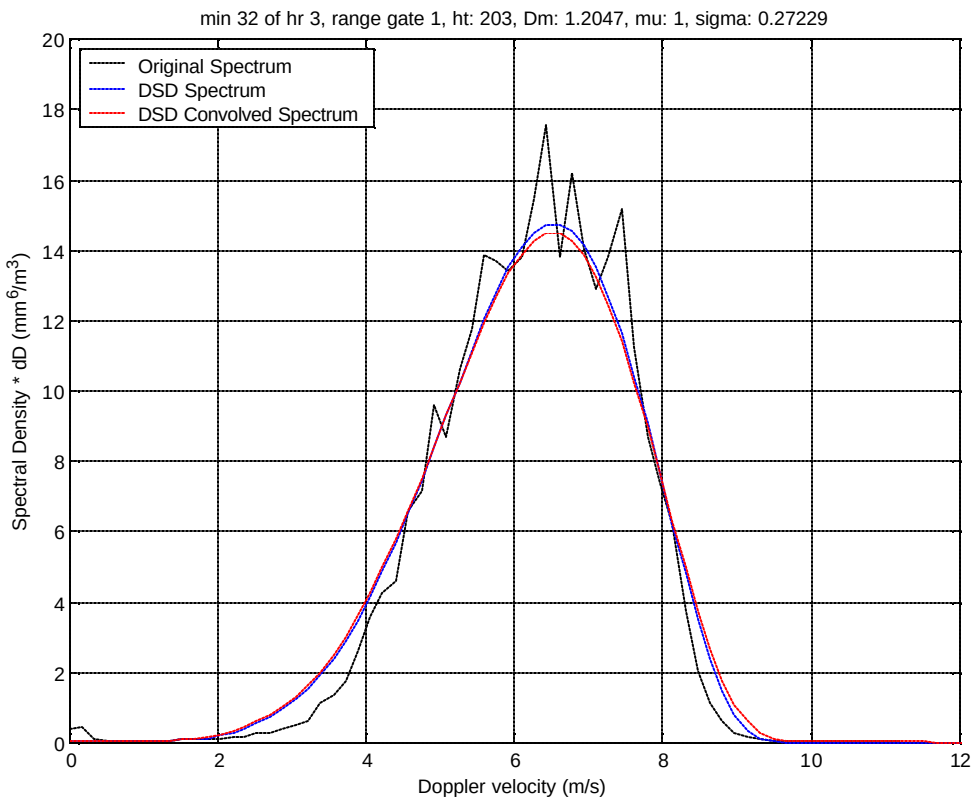
min 32 of hr 3, range gate 1, ht: 203, Dm: 1.2047, mu: 1, sigma: 0.27229
Original Spectrum
DSD Spectrum
DSD Convolved Spectrum
Spectral Density * dD (mm6/m3)
Doppler velocity (m/s)
0
2
4
6
8
10
12
14
16
18
20
0
2
4
6
8
10
12

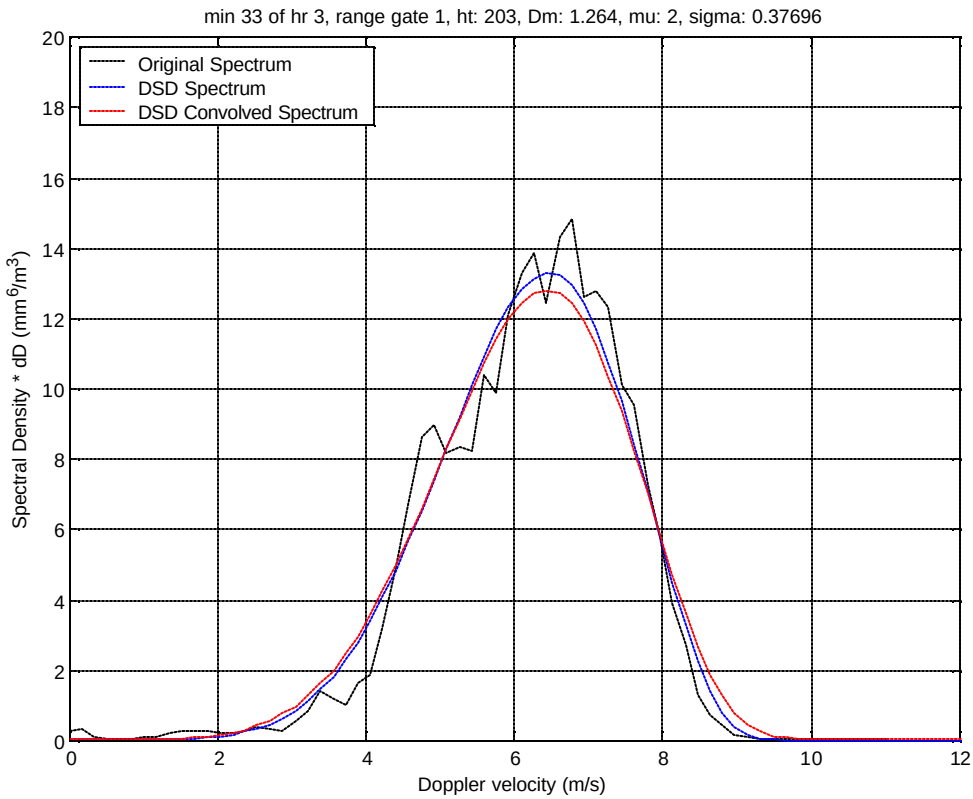
min 33 of hr 3, range gate 1, ht: 203, Dm: 1.264, mu: 2, sigma: 0.37696
Original Spectrum
DSD Spectrum
DSD Convolved Spectrum
Spectral Density * dD (mm6/m3)
Doppler velocity (m/s)
0
2
4
6
8
10
12
14
16
18
20

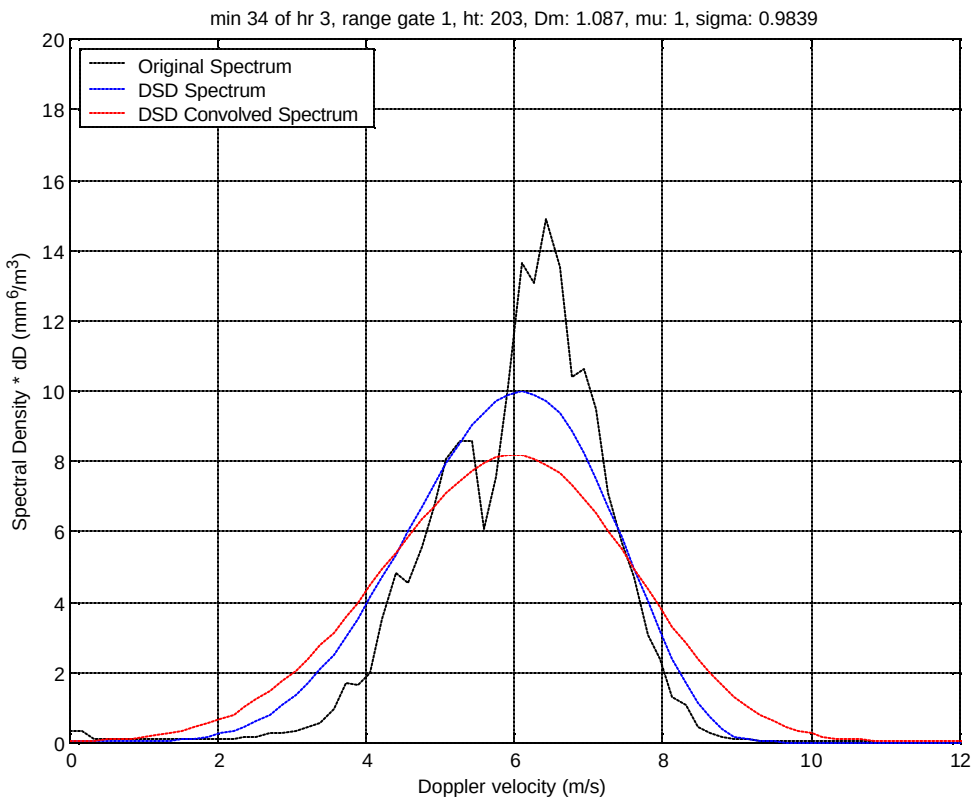
min 34 of hr 3, range gate 1, ht: 203, Dm: 1.087, mu: 1, sigma: 0.9839
Original Spectrum
DSD Spectrum
DSD Convolved Spectrum
Spectral Density * dD (mm6/m3)
Doppler velocity (m/s)
0
2
4
6
8
10
12
14
16
18
20

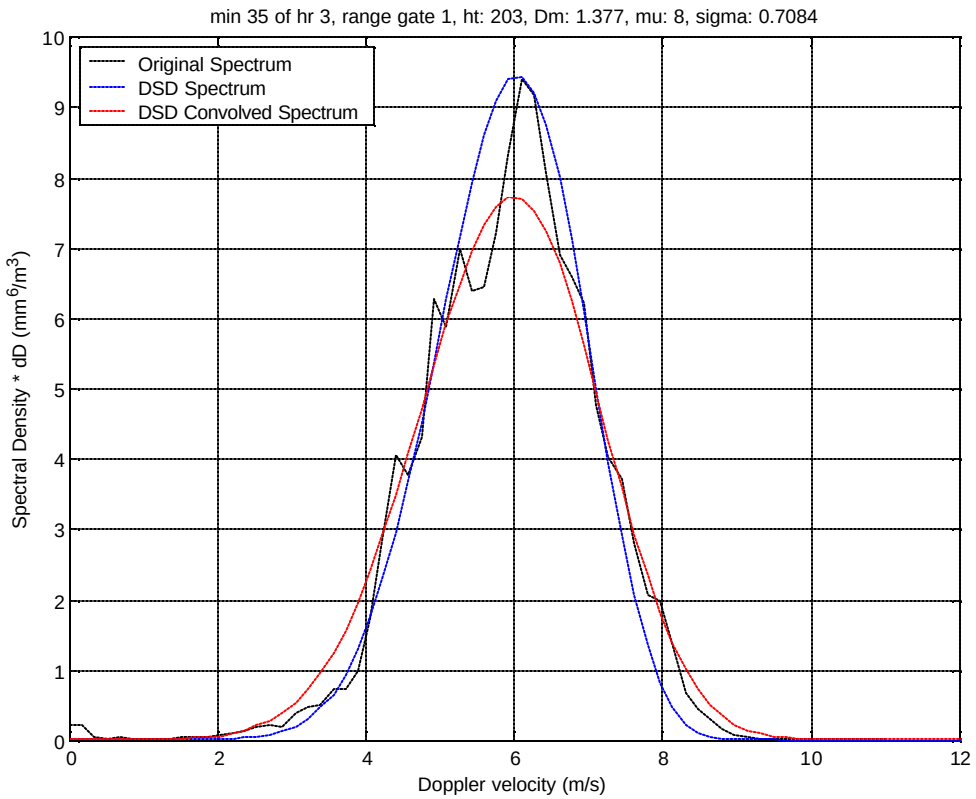
min 35 of hr 3, range gate 1, ht: 203, Dm: 1.377, mu: 8, sigma: 0.7084
Original Spectrum
DSD Spectrum
DSD Convolved Spectrum
Spectral Density * dD (mm6/m3)
Doppler velocity (m/s)
0
1
2
3
4
5
6
7
8
9
10
0
2
4
6
8
10
12

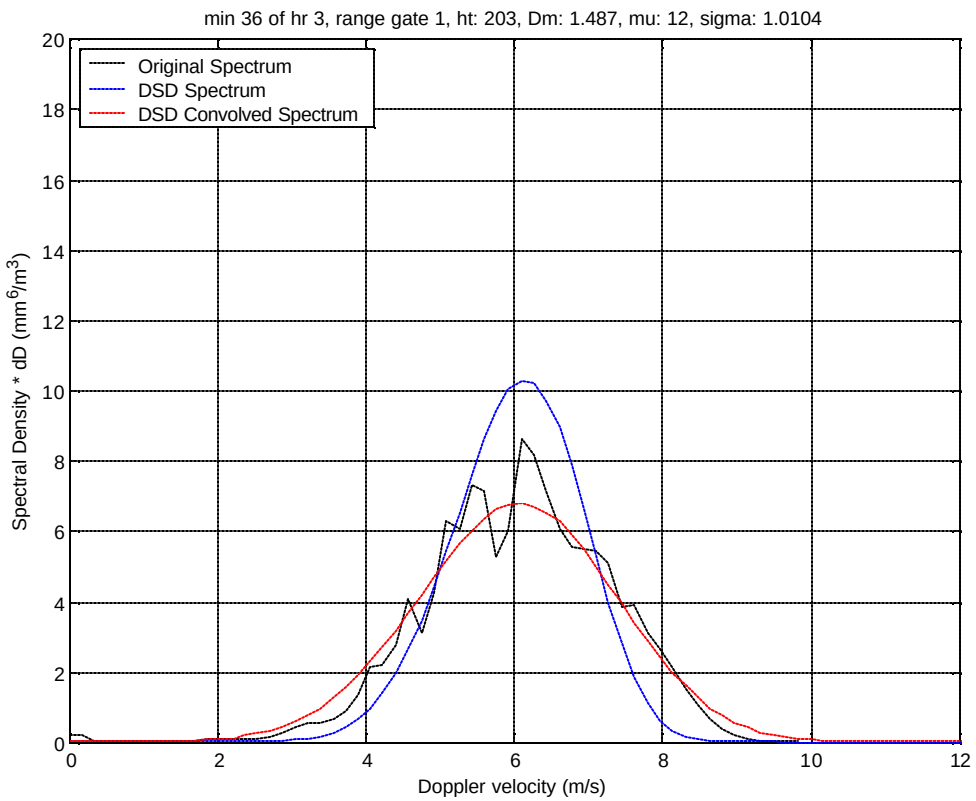
min 36 of hr 3, range gate 1, ht: 203, Dm: 1.487, mu: 12, sigma: 1.0104
Original Spectrum
DSD Spectrum
DSD Convolved Spectrum
Spectral Density * dD (mm6/m3)
Doppler velocity (m/s)
0
2
4
6
8
10
12
14
16
18
20
0
2
4
6
8
10
12

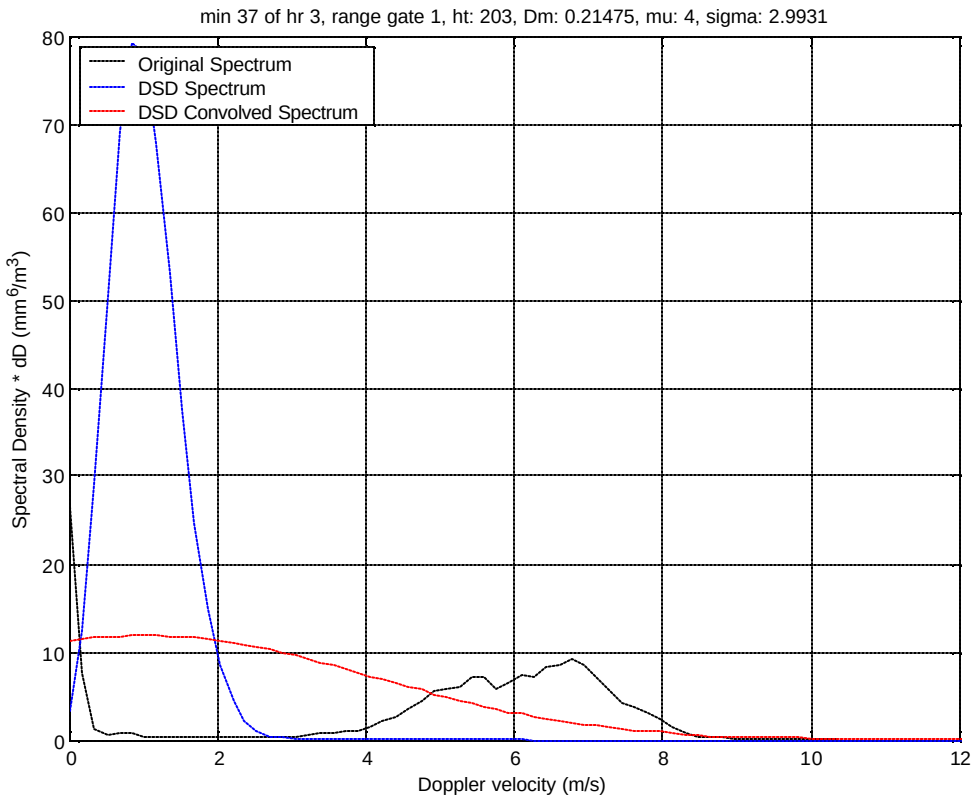
min 37 of hr 3, range gate 1, ht: 203, Dm: 0.21475, mu: 4, sigma: 2.9931
Original Spectrum
DSD Spectrum
DSD Convolved Spectrum
Spectral Density * dD (mm6/m3)
Doppler velocity (m/s)
0
10
20
30
40
50
60
70
80
0
2
4
6
8
10
12

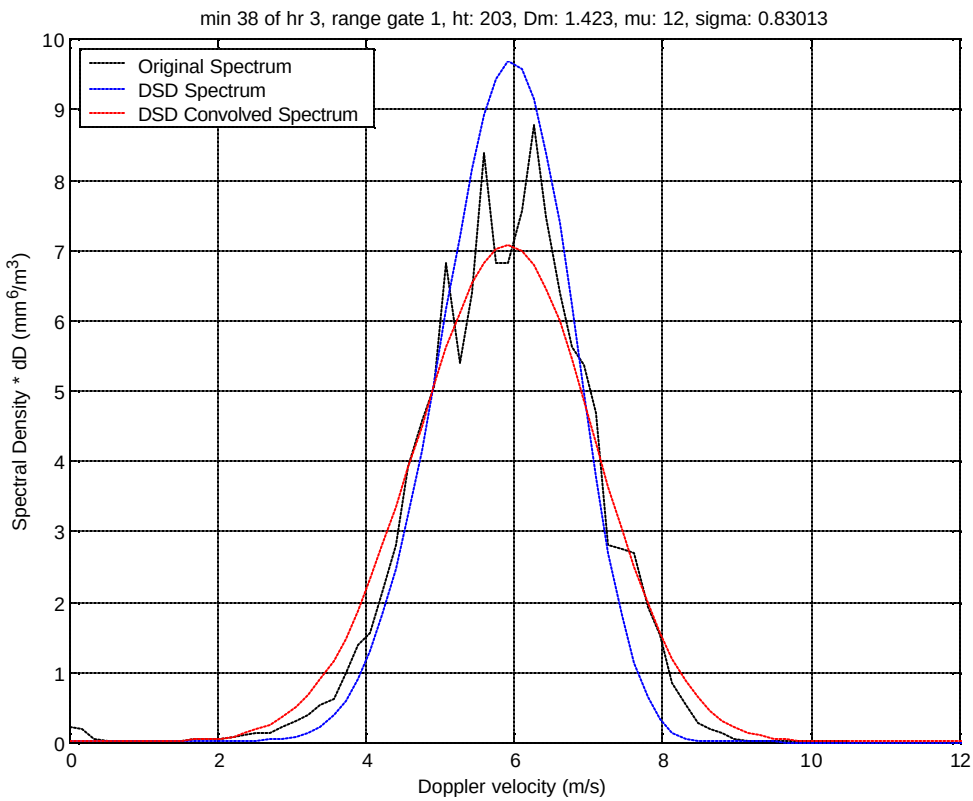
min 38 of hr 3, range gate 1, ht: 203, Dm: 1.423, mu: 12, sigma: 0.83013
Original Spectrum
DSD Spectrum
DSD Convolved Spectrum
Spectral Density * dD (mm6/m3)
Doppler velocity (m/s)
0
1
2
3
4
5
6
7
8
9
10
0
2
4
6
8
10
12

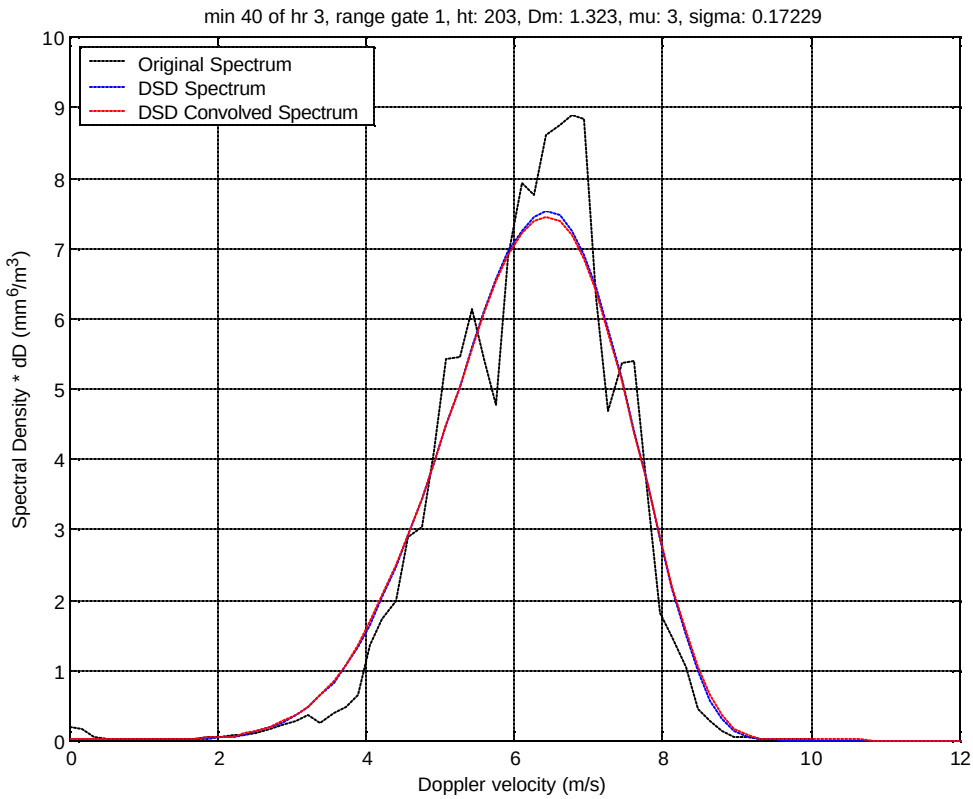
min 40 of hr 3, range gate 1, ht: 203, Dm: 1.323, mu: 3, sigma: 0.17229
Original Spectrum
DSD Spectrum
DSD Convolved Spectrum
Spectral Density * dD (mm6/m3)
Doppler velocity (m/s)
0
1
2
3
4
5
6
7
8
9
10
0
2
4
6
8
10
12

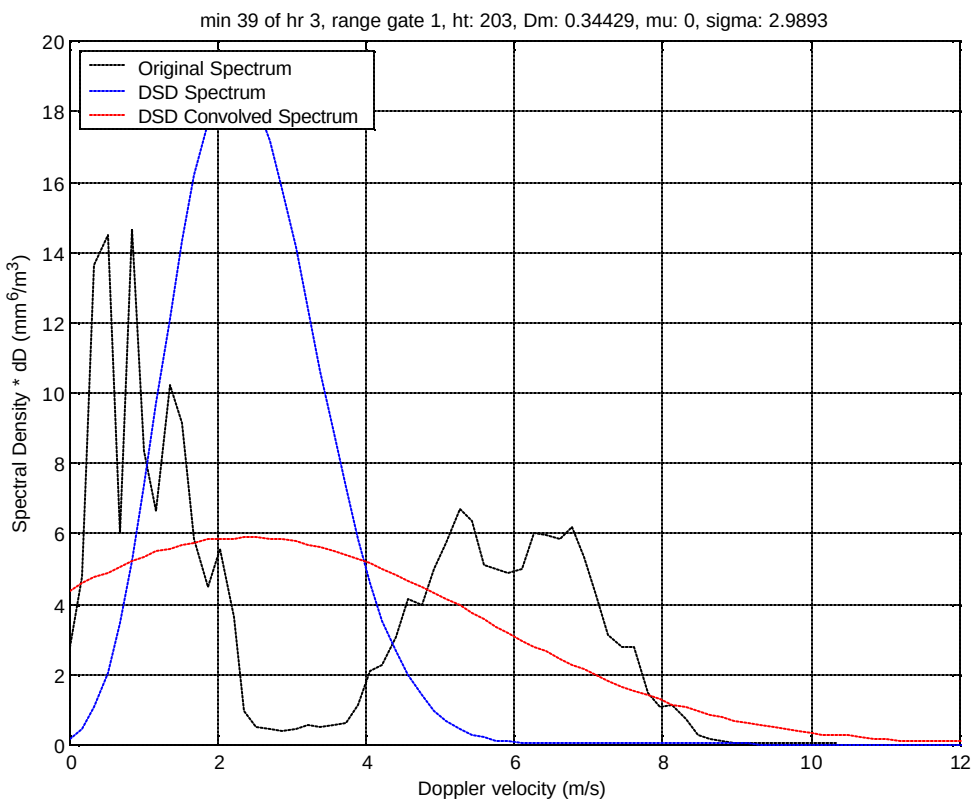
min 39 of hr 3, range gate 1, ht: 203, Dm: 0.34429, mu: 0, sigma: 2.9893
Original Spectrum
DSD Spectrum
DSD Convolved Spectrum
Spectral Density * dD (mm6/m3)
Doppler velocity (m/s)
0
2
4
6
8
10
12
14
16
18
20
0
2
4
6
8
10
12

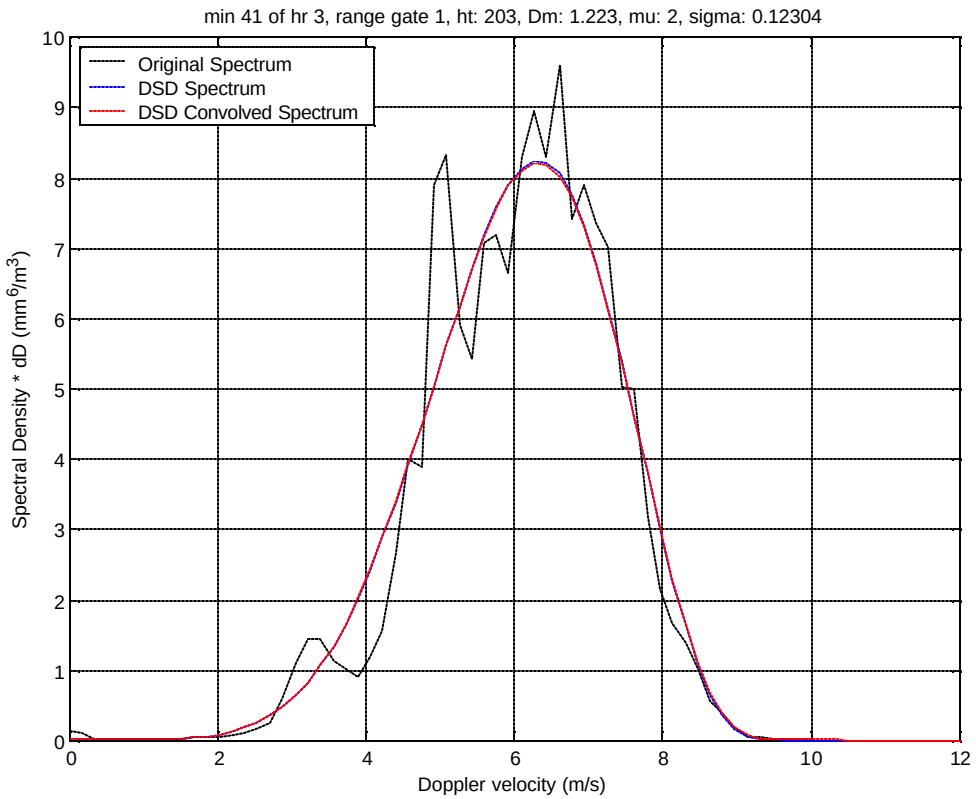
min 41 of hr 3, range gate 1, ht: 203, Dm: 1.223, mu: 2, sigma: 0.12304
Original Spectrum
DSD Spectrum
DSD Convolved Spectrum
Spectral Density * dD (mm6/m3)
Doppler velocity (m/s)
0
1
2
3
4
5
6
7
8
9
10
0
2
4
6
8
10
12

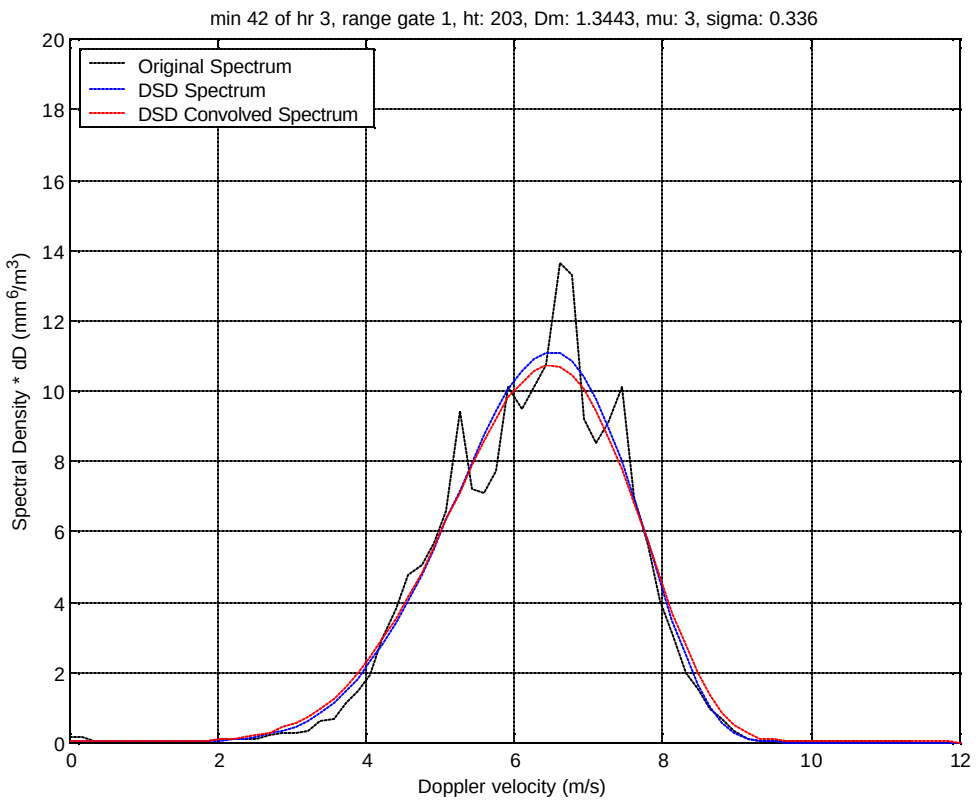
min 42 of hr 3, range gate 1, ht: 203, Dm: 1.3443, mu: 3, sigma: 0.336
Original Spectrum
DSD Spectrum
DSD Convolved Spectrum
Spectral Density * dD (mm6/m3)
Doppler velocity (m/s)
0
2
4
6
8
10
12
14
16
18
20
0
2
4
6
8
10
12

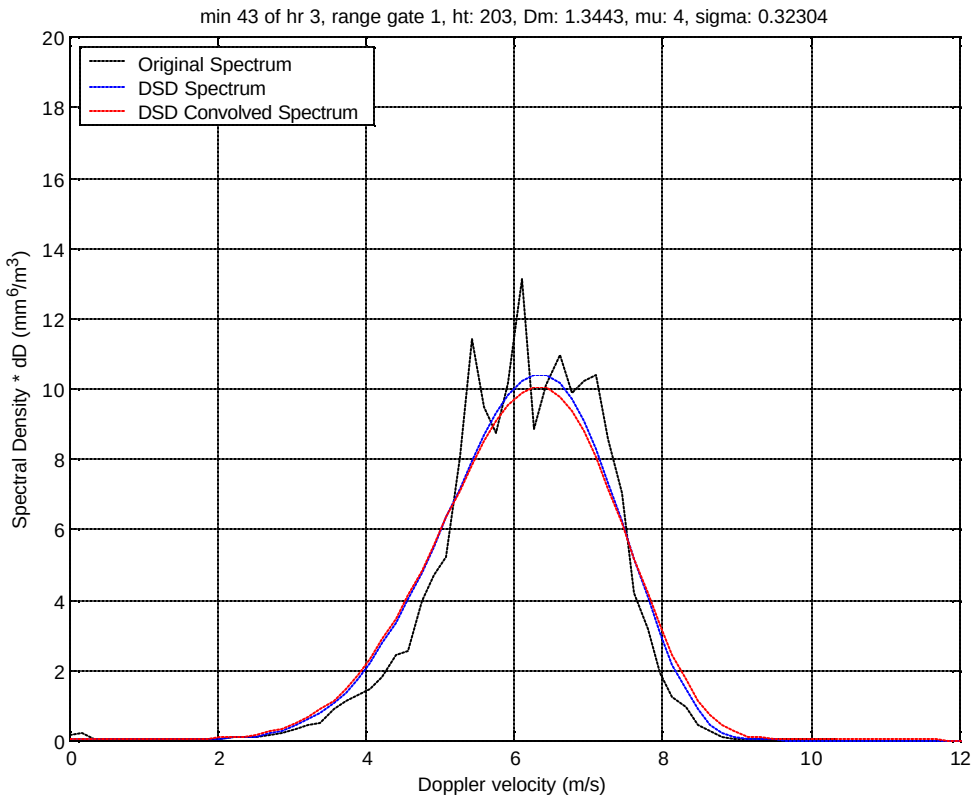
min 43 of hr 3, range gate 1, ht: 203, Dm: 1.3443, mu: 4, sigma: 0.32304
Original Spectrum
DSD Spectrum
DSD Convolved Spectrum
Spectral Density * dD (mm6/m3)
Doppler velocity (m/s)
0
2
4
6
8
10
12
14
16
18
20

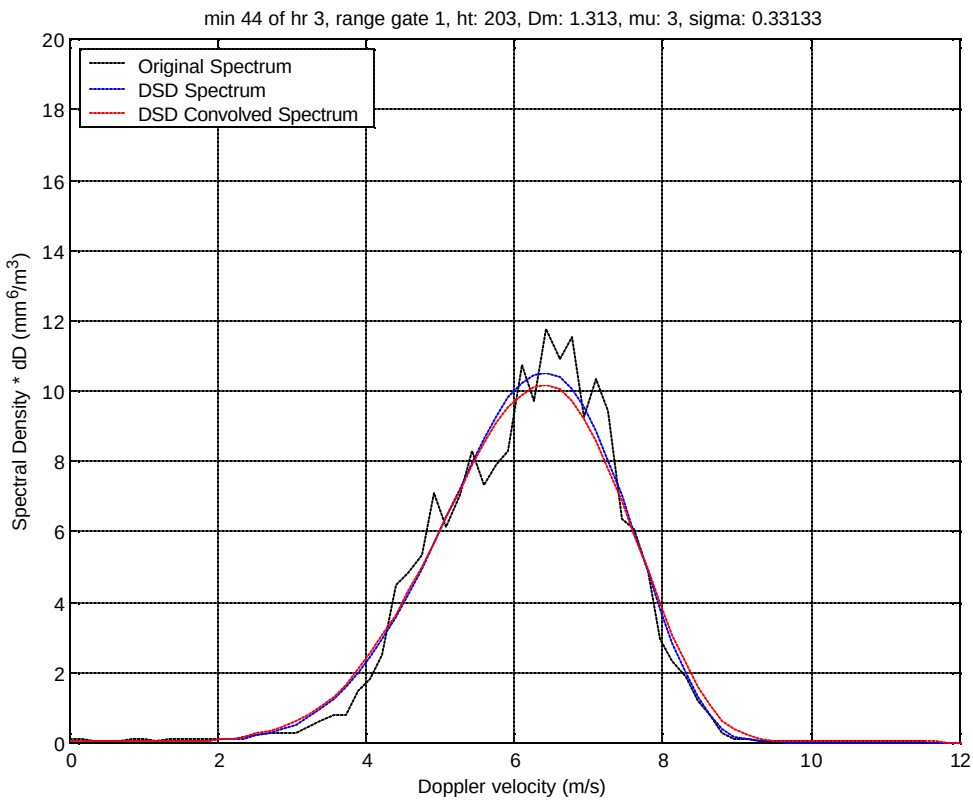
min 44 of hr 3, range gate 1, ht: 203, Dm: 1.313, mu: 3, sigma: 0.33133
Original Spectrum
DSD Spectrum
DSD Convolved Spectrum
Spectral Density * dD (mm6/m3)
Doppler velocity (m/s)
0
2
4
6
8
10
12
14
16
18
20

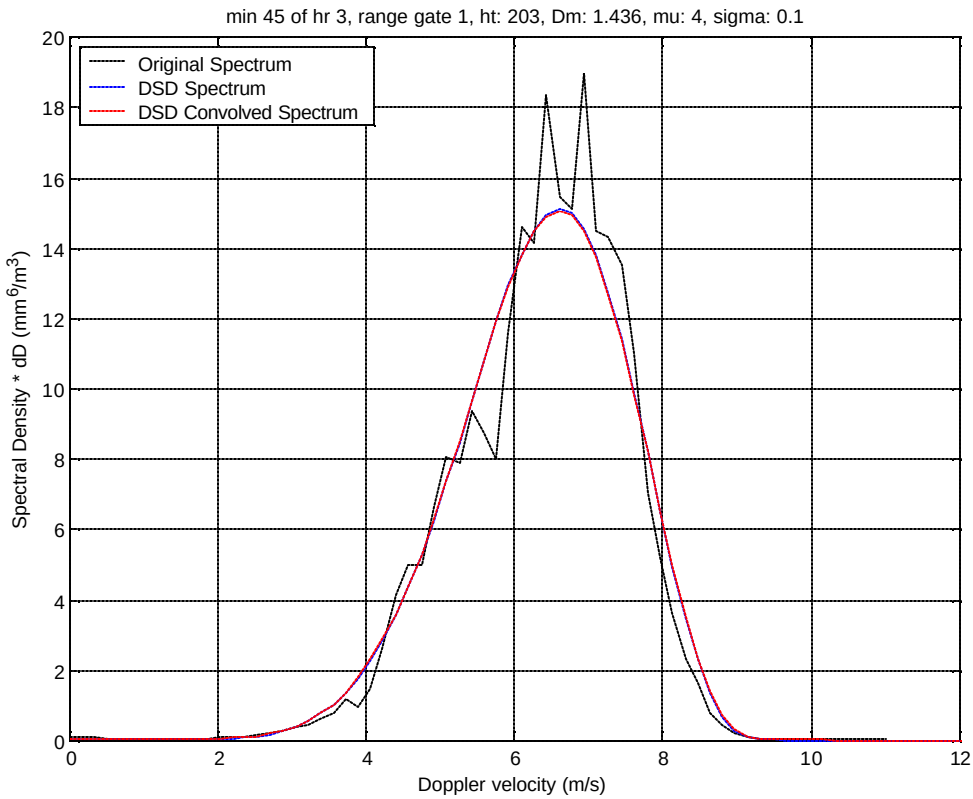
min 45 of hr 3, range gate 1, ht: 203, Dm: 1.436, mu: 4, sigma: 0.1
Original Spectrum
DSD Spectrum
DSD Convolved Spectrum
Spectral Density * dD (mm6/m3)
Doppler velocity (m/s)
0
2
4
6
8
10
12
14
16
18
20

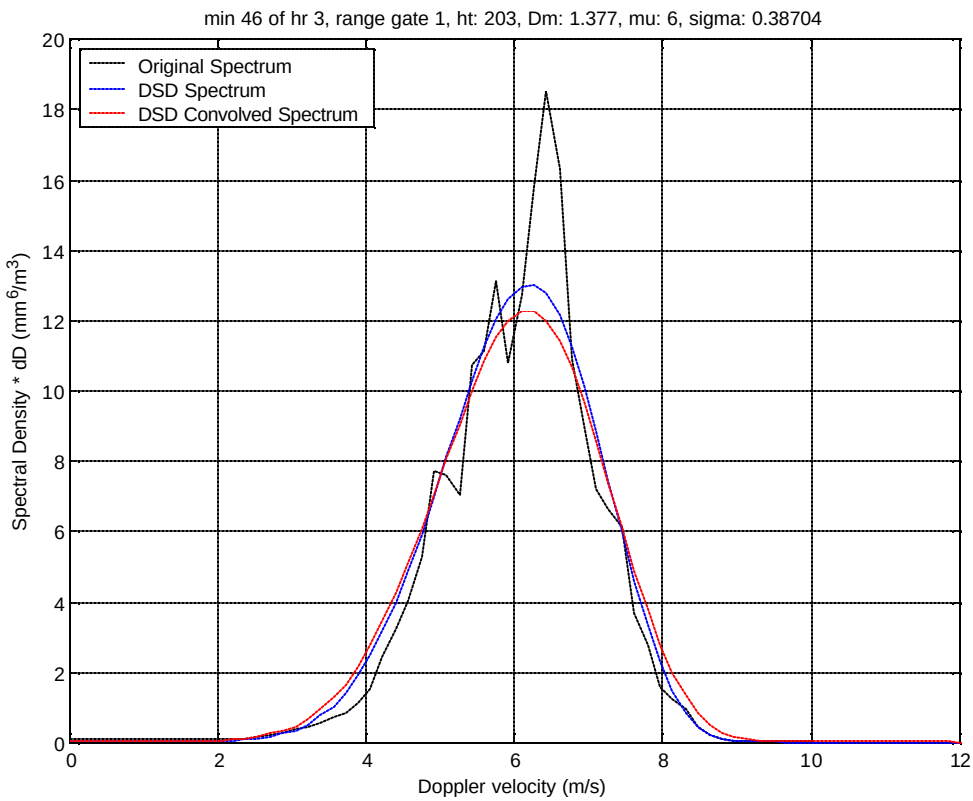
min 46 of hr 3, range gate 1, ht: 203, Dm: 1.377, mu: 6, sigma: 0.38704
Original Spectrum
DSD Spectrum
DSD Convolved Spectrum
Spectral Density * dD (mm6/m3)
Doppler velocity (m/s)
0
2
4
6
8
10
12
14
16
18
20

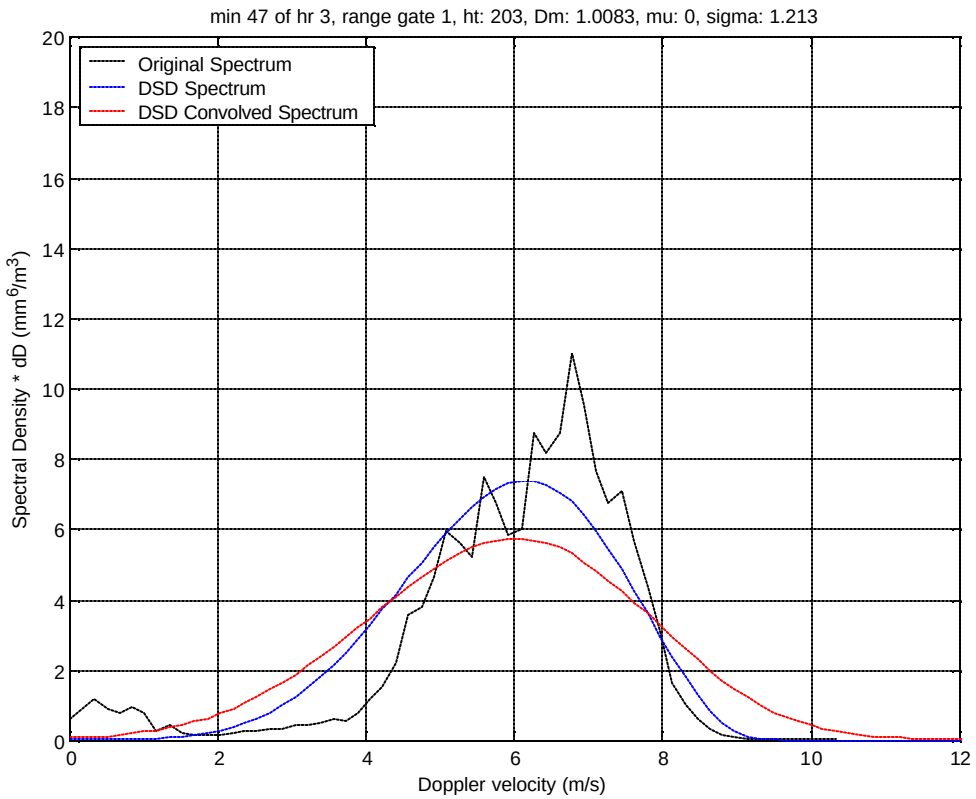
min 47 of hr 3, range gate 1, ht: 203, Dm: 1.0083, mu: 0, sigma: 1.213
Original Spectrum
DSD Spectrum
DSD Convolved Spectrum
Spectral Density * dD (mm6/m3)
Doppler velocity (m/s)
0
2
4
6
8
10
12
14
16
18
20

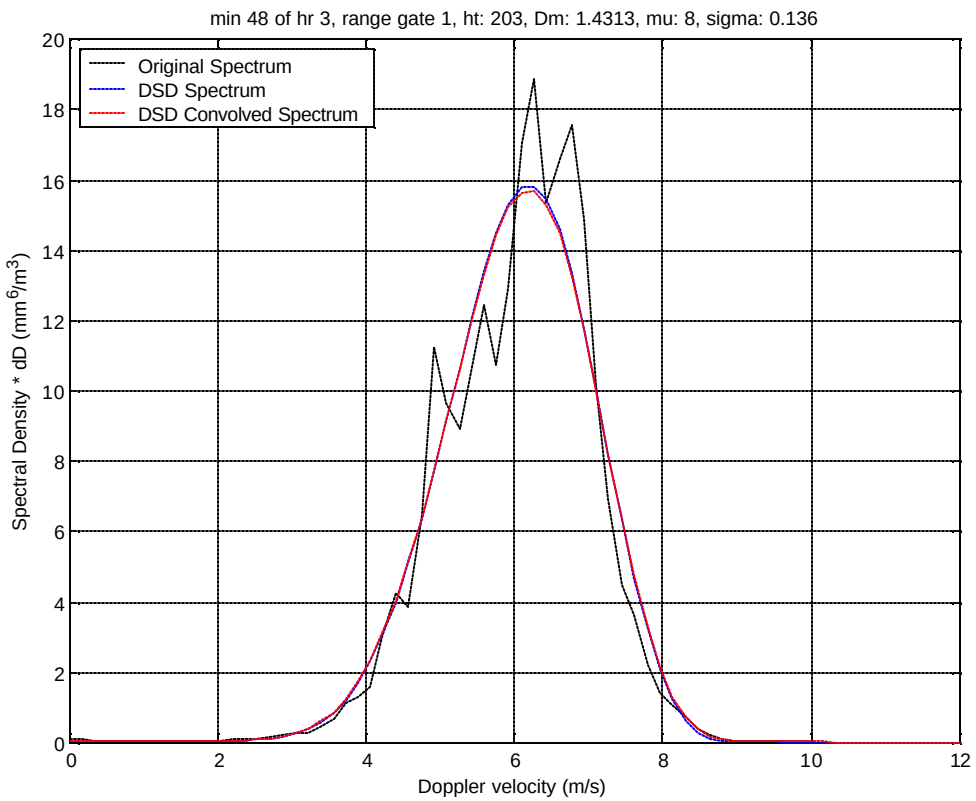
min 48 of hr 3, range gate 1, ht: 203, Dm: 1.4313, mu: 8, sigma: 0.136
Original Spectrum
DSD Spectrum
DSD Convolved Spectrum
Spectral Density * dD (mm6/m3)
Doppler velocity (m/s)
0
2
4
6
8
10
12
14
16
18
20

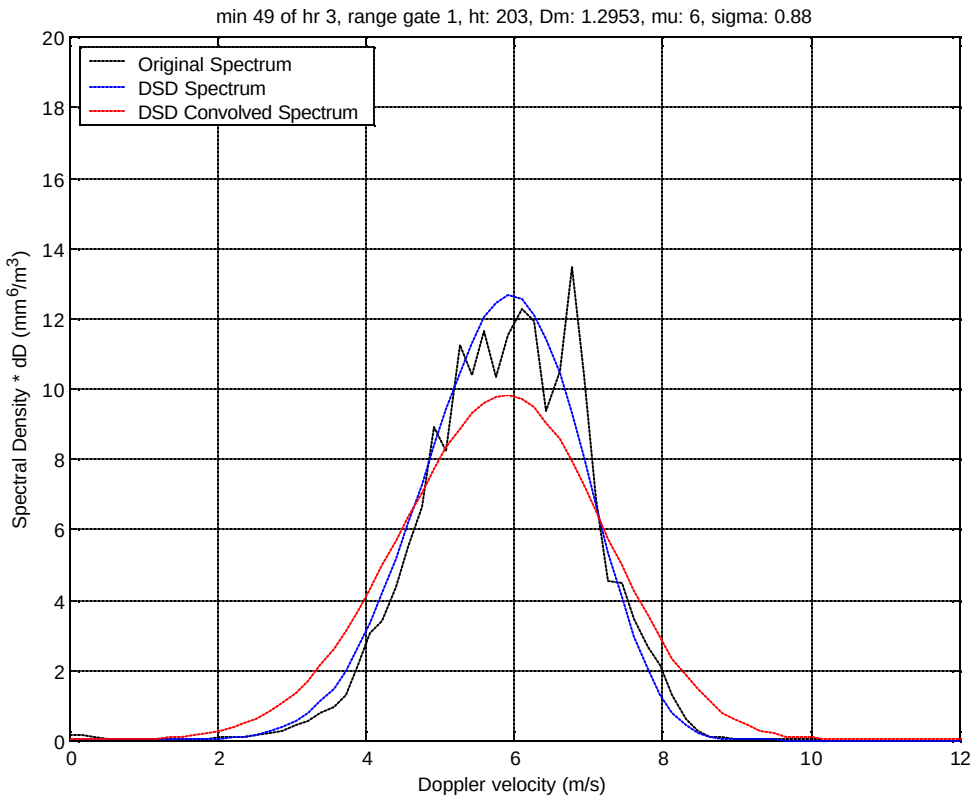
min 49 of hr 3, range gate 1, ht: 203, Dm: 1.2953, mu: 6, sigma: 0.88
Original Spectrum
DSD Spectrum
DSD Convolved Spectrum
Spectral Density * dD (mm6/m3)
Doppler velocity (m/s)
0
2
4
6
8
10
12
14
16
18
20

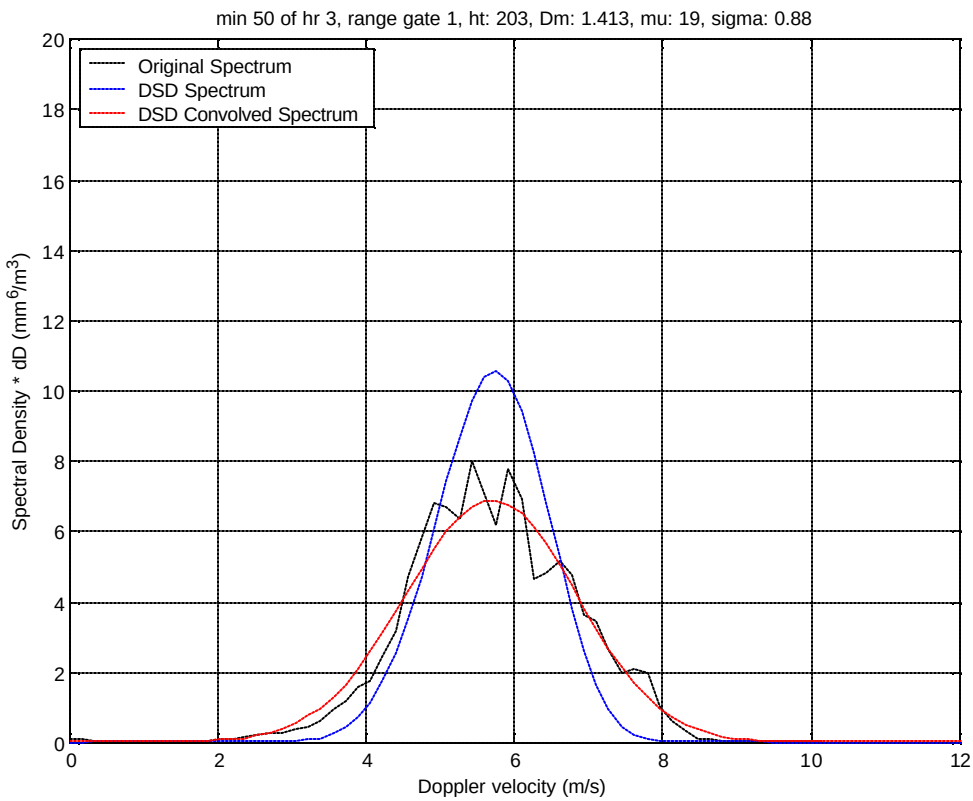
min 50 of hr 3, range gate 1, ht: 203, Dm: 1.413, mu: 19, sigma: 0.88
Original Spectrum
DSD Spectrum
DSD Convolved Spectrum
Spectral Density * dD (mm6/m3)
Doppler velocity (m/s)
0
2
4
6
8
10
12
14
16
18
20

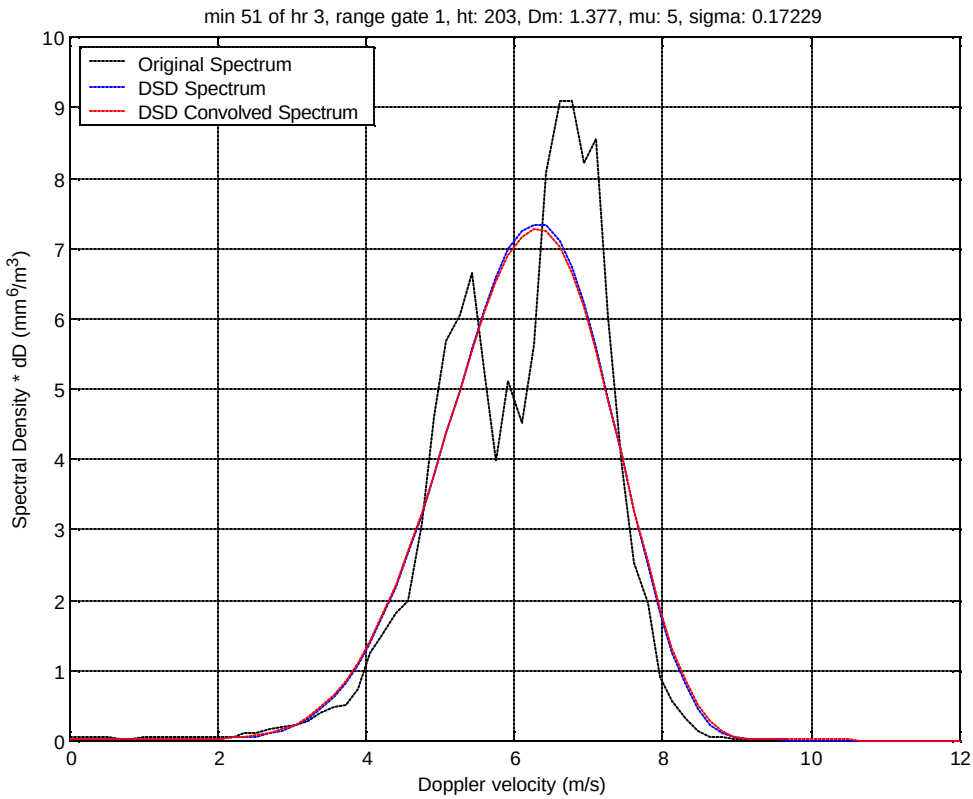
min 51 of hr 3, range gate 1, ht: 203, Dm: 1.377, mu: 5, sigma: 0.17229
Original Spectrum
DSD Spectrum
DSD Convolved Spectrum
Spectral Density * dD (mm6/m3)
Doppler velocity (m/s)
0
1
2
3
4
5
6
7
8
9
10
0
2
4
6
8
10
12

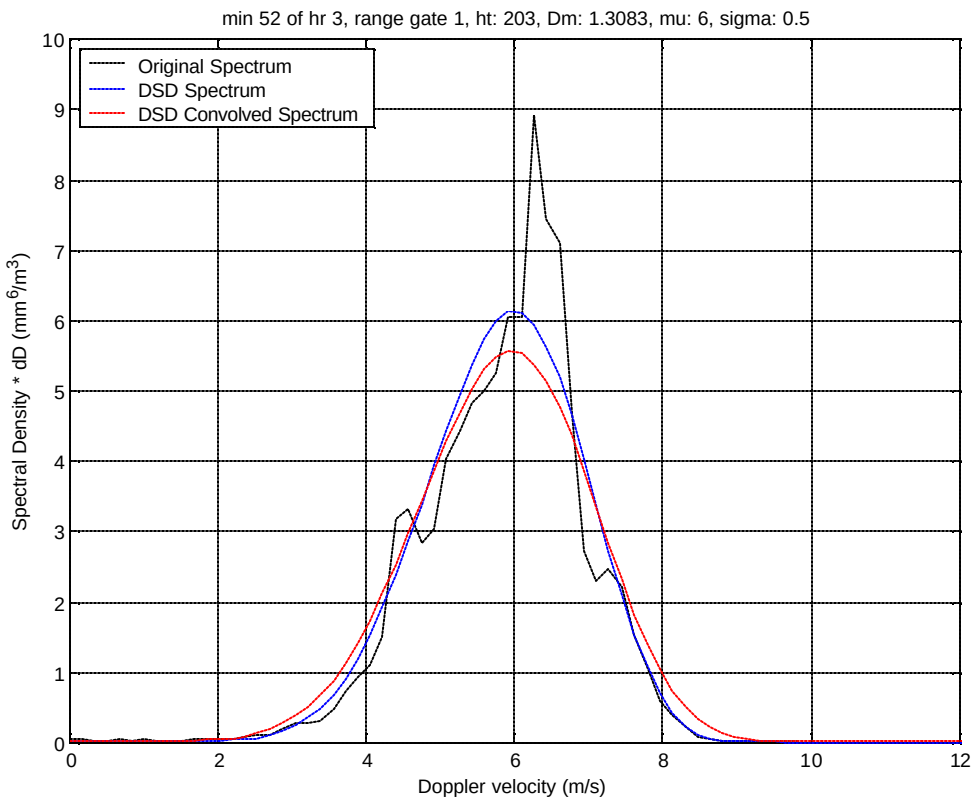
min 52 of hr 3, range gate 1, ht: 203, Dm: 1.3083, mu: 6, sigma: 0.5
Original Spectrum
DSD Spectrum
DSD Convolved Spectrum
Spectral Density * dD (mm6/m3)
Doppler velocity (m/s)
0
1
2
3
4
5
6
7
8
9
10
0
2
4
6
8
10
12

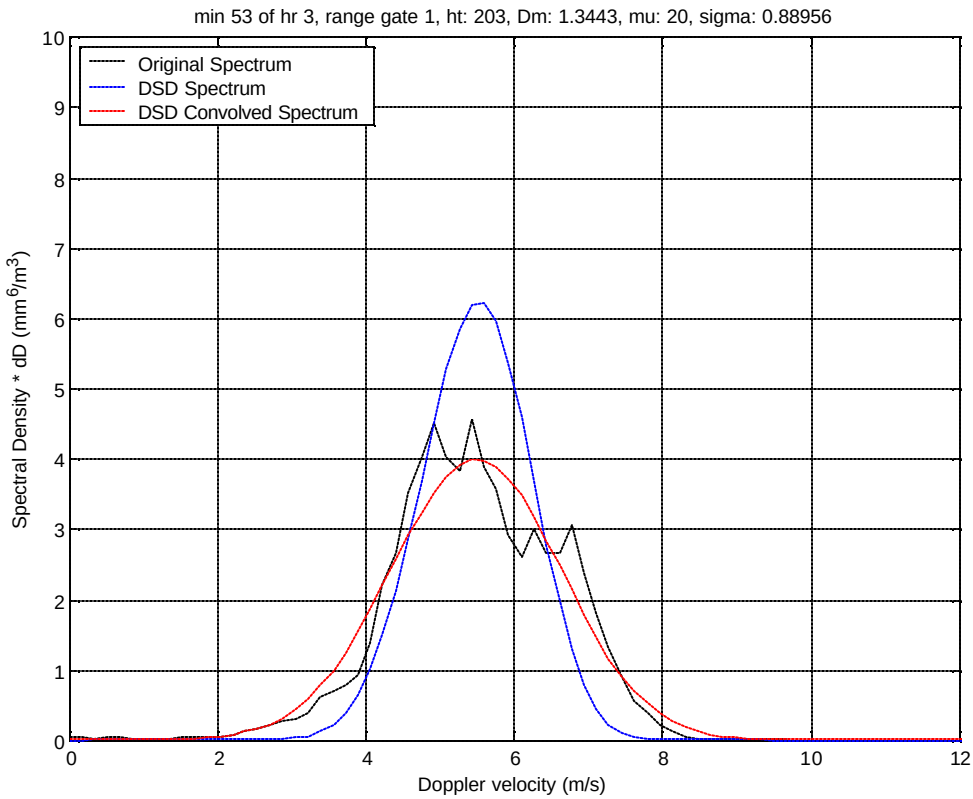
min 53 of hr 3, range gate 1, ht: 203, Dm: 1.3443, mu: 20, sigma: 0.88956
Original Spectrum
DSD Spectrum
DSD Convolved Spectrum
Spectral Density * dD (mm6/m3)
Doppler velocity (m/s)
0
1
2
3
4
5
6
7
8
9
10
0
2
4
6
8
10
12

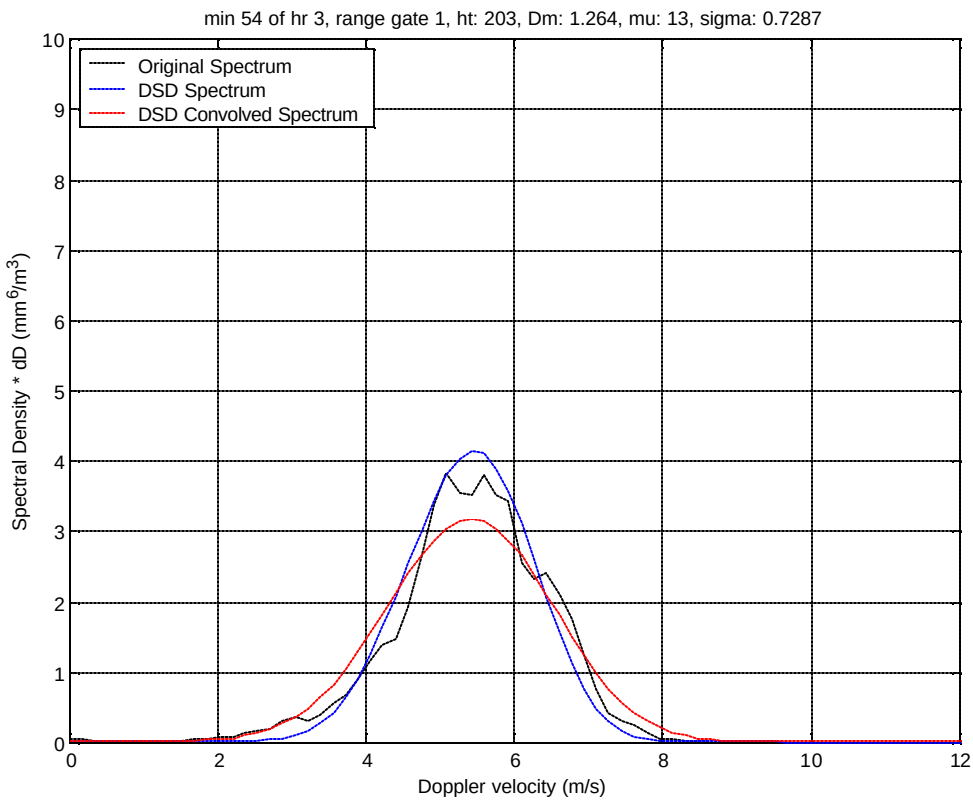
min 54 of hr 3, range gate 1, ht: 203, Dm: 1.264, mu: 13, sigma: 0.7287
Original Spectrum
DSD Spectrum
DSD Convolved Spectrum
Spectral Density * dD (mm6/m3)
Doppler velocity (m/s)
0
1
2
3
4
5
6
7
8
9
10
0
2
4
6
8
10
12

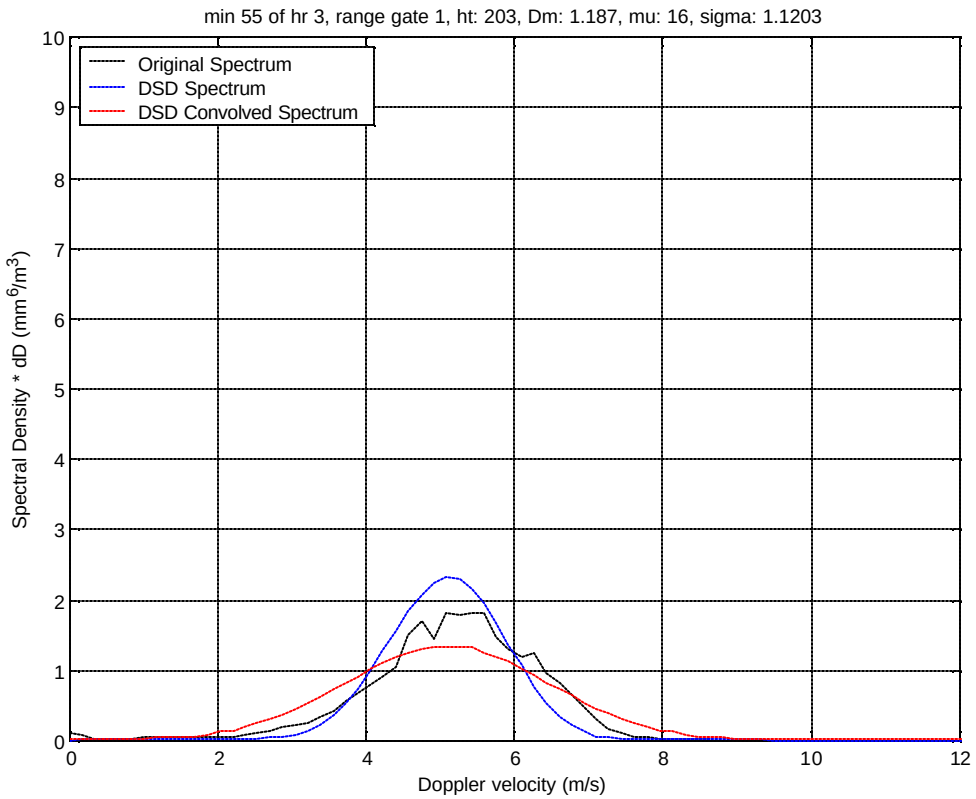
min 55 of hr 3, range gate 1, ht: 203, Dm: 1.187, mu: 16, sigma: 1.1203
Original Spectrum
DSD Spectrum
DSD Convolved Spectrum
Spectral Density * dD (mm6/m3)
Doppler velocity (m/s)
0
1
2
3
4
5
6
7
8
9
10
0
2
4
6
8
10
12

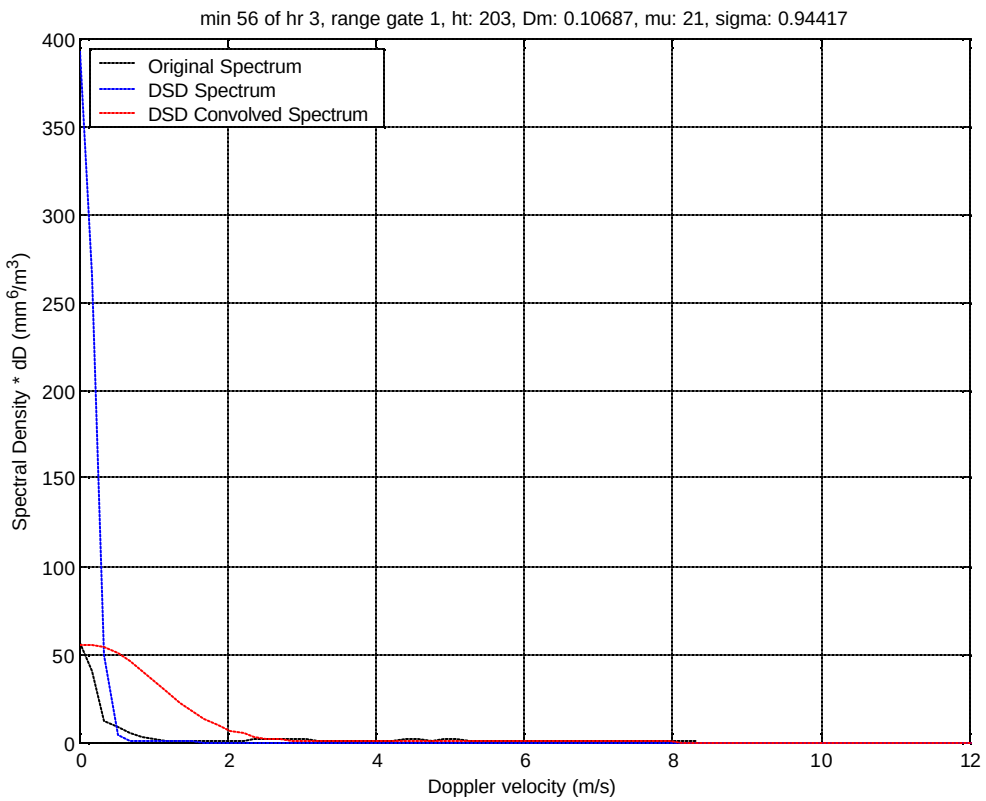
min 56 of hr 3, range gate 1, ht: 203, Dm: 0.10687, mu: 21, sigma: 0.94417
Original Spectrum
DSD Spectrum
DSD Convolved Spectrum
Spectral Density * dD (mm6/m3)
Doppler velocity (m/s)
0
50
100
150
200
250
300
350
400
0
2
4
6
8
10
12

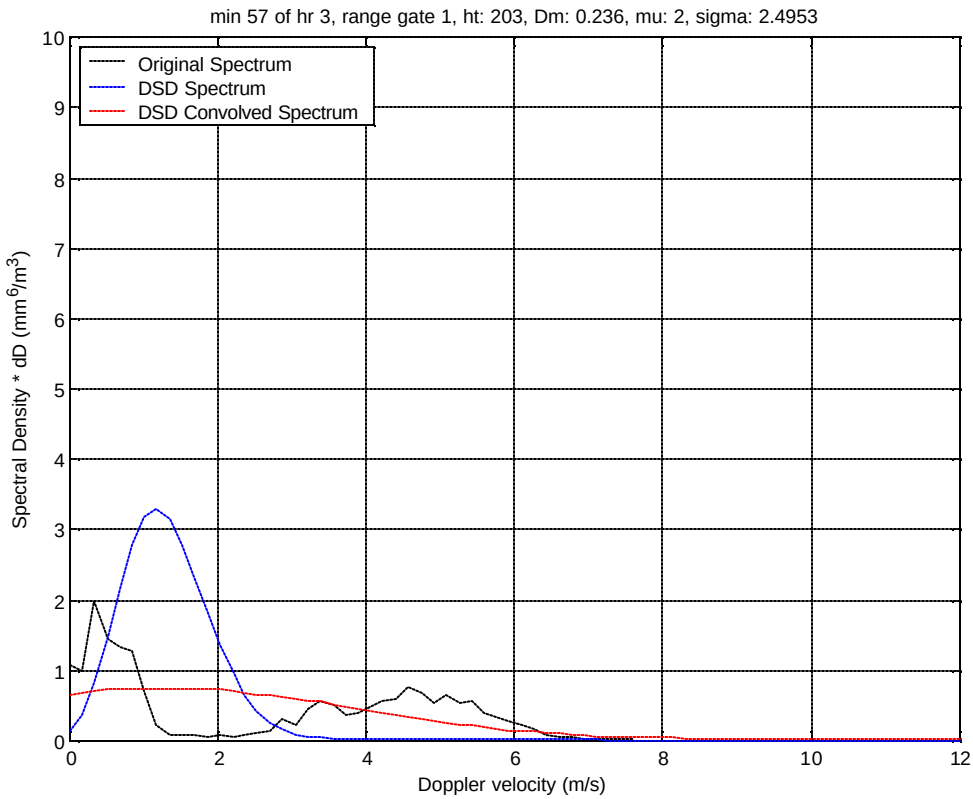
min 57 of hr 3, range gate 1, ht: 203, Dm: 0.236, mu: 2, sigma: 2.4953
Original Spectrum
DSD Spectrum
DSD Convolved Spectrum
Spectral Density * dD (mm6/m3)
Doppler velocity (m/s)
0
1
2
3
4
5
6
7
8
9
10
0
2
4
6
8
10
12

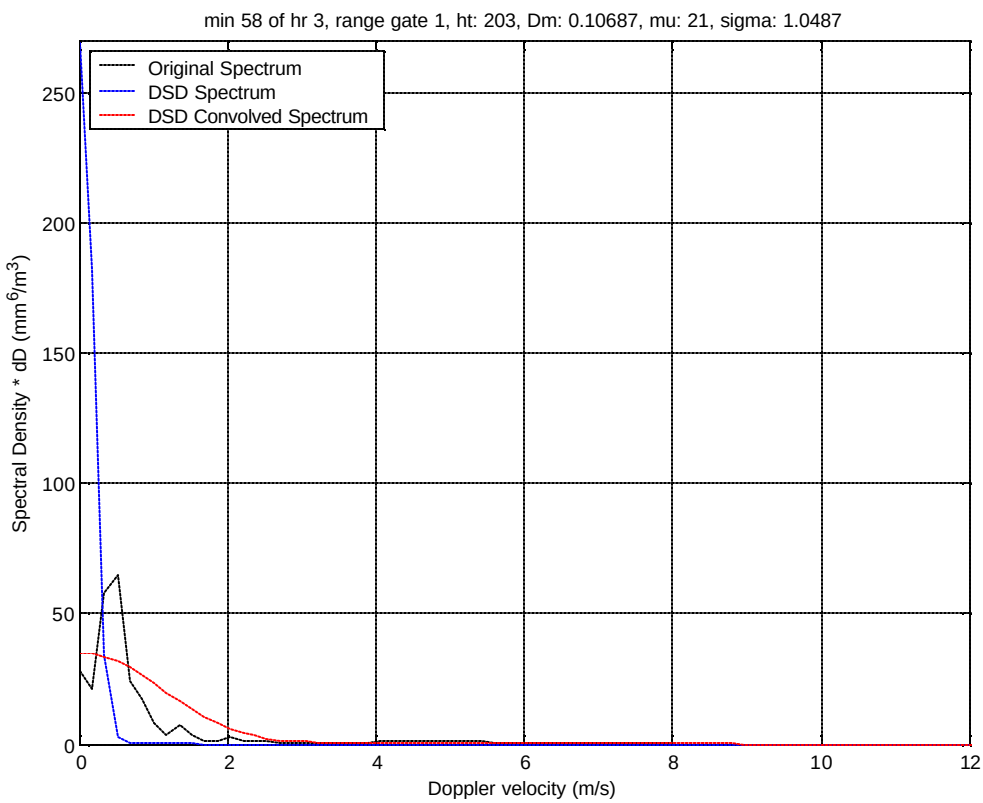
min 58 of hr 3, range gate 1, ht: 203, Dm: 0.10687, mu: 21, sigma: 1.0487
Original Spectrum
DSD Spectrum
DSD Convolved Spectrum
Spectral Density * dD (mm6/m3)
Doppler velocity (m/s)
0
50
100
150
200
250
0
2
4
6
8
10
12

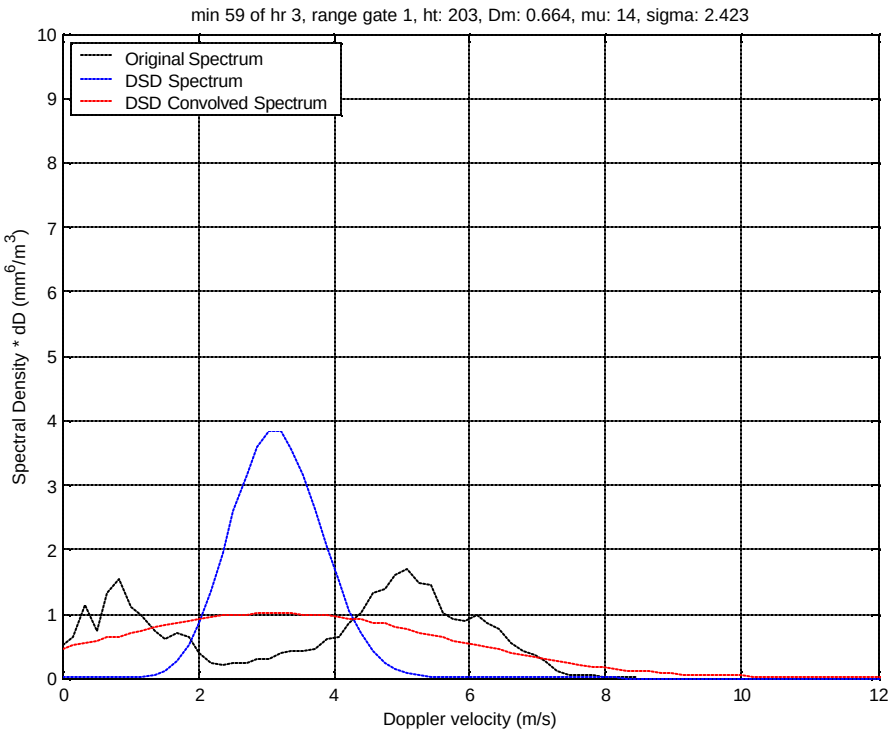

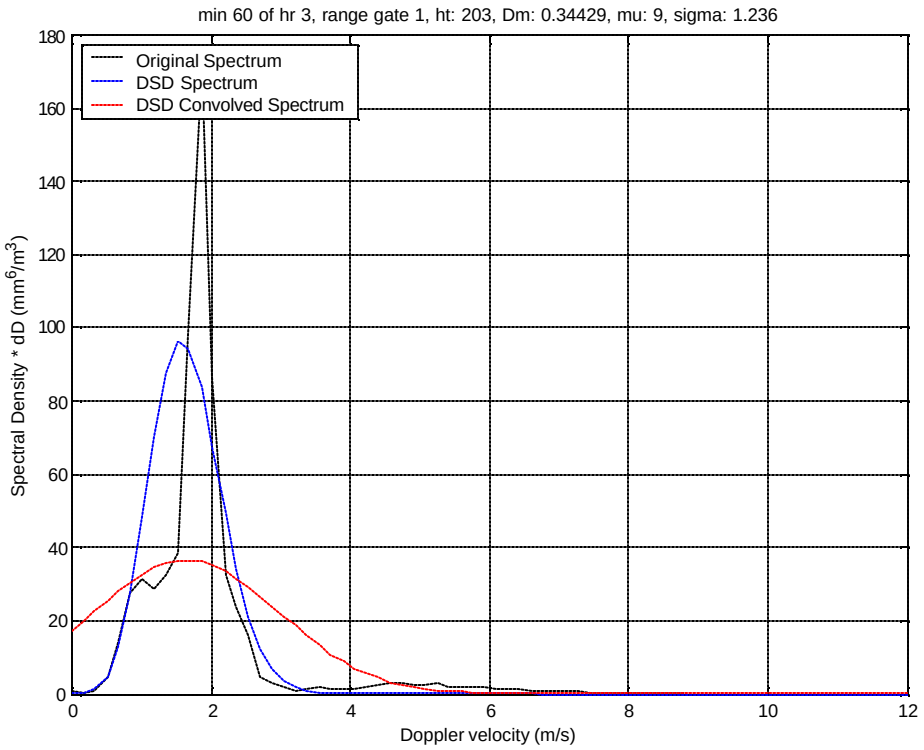

Figures C.2 (Sets) 60 minutes of Doppler spectra plots for hour 3

APPENDIX D

QUALITY CONTROL TEST

To identify the invalid Gamma parameter retrievals, a quality control test was developed based upon a subjective evaluation of the measured profiler spectra and the time series of rain parameters compared to the Joss disdrometer. Using these subjectively rejected spectra, the following objective test was developed. Below is an example of the algorithm for Hour 3.

First, 60 minutes of the Doppler spectral width are produced (Figure D.1). Plot the time series of spectra width (σ_v). Select a threshold (Figure D.2 Threshold=1.5), the retrievals for the minutes with the spectral width greater than 1.5 are discarded. (Minutes: 7, 34, 37, 39, 47, 57, 59) Secondly, identify the outliers from Table 5.1, values greater than 2 are discarded. (Minutes: 37, 39, 57, 59) Finally, compare the rain rate R, values less than 0.05 are discarded. (Minutes: 56, 58). Run through three steps of the test, the discarded minutes are found. In this case, they are minutes: 7, 34, 37, 39, 47, 56, 57, 58, and 59.

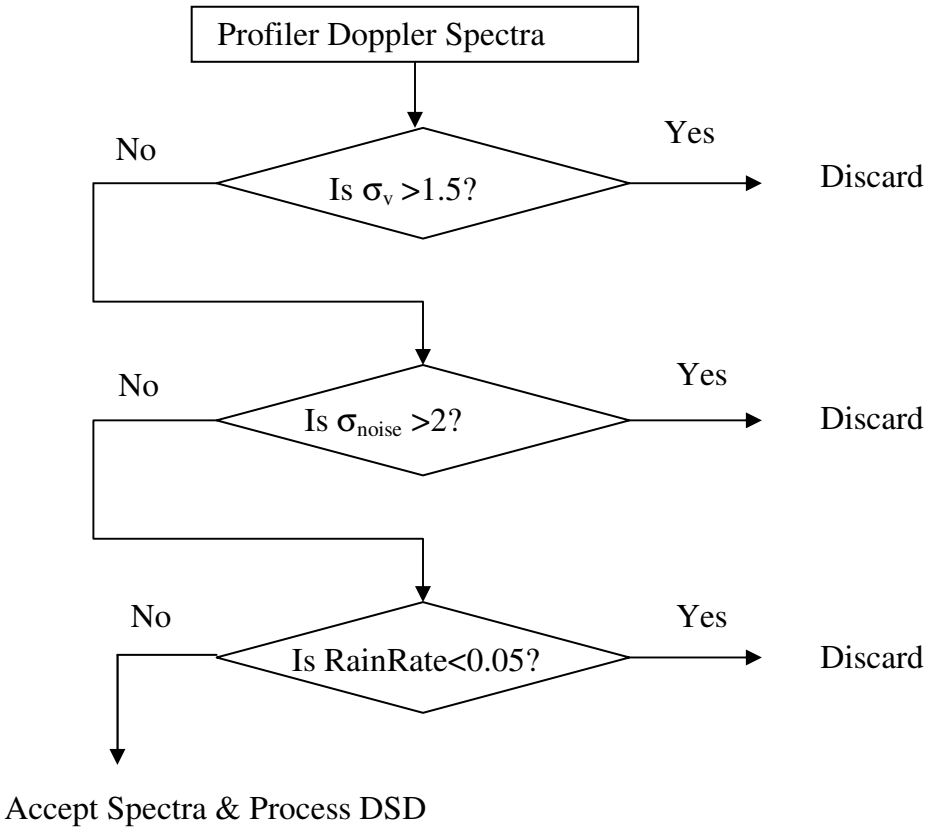

Figure D.1 Quality Control Flow Chart

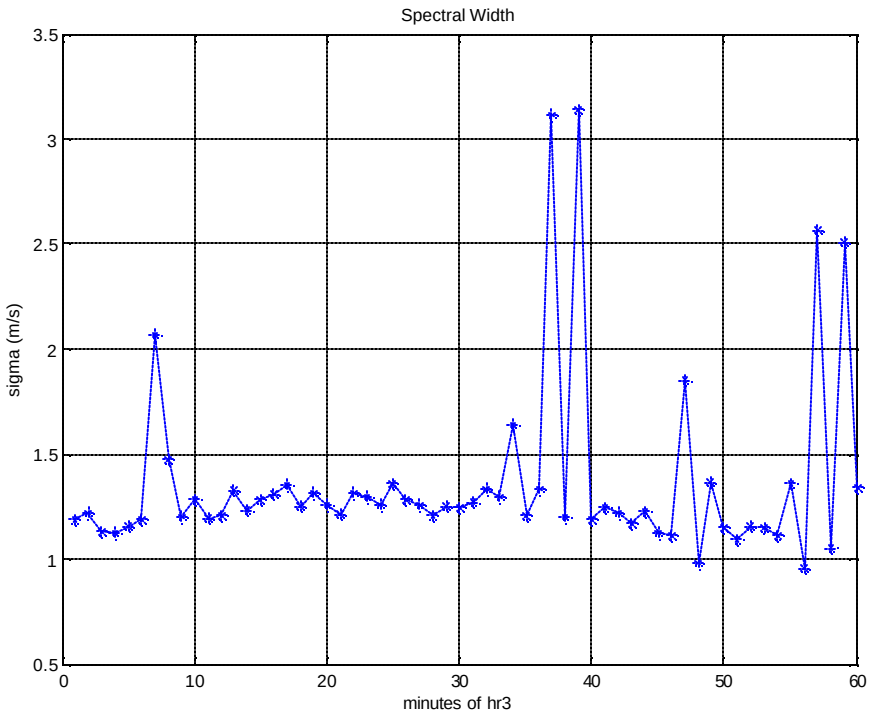

Figure D.2 Profiler spectral width for hour 3

APPENDIX E

FORWARD MODEL PROGRAM CODE

```
%assume Marshall-Palmer distribution, take raindrop diameter up to 7mm with 0.1mm interval
% clear;
% close all;
d=0.01:0.1:7;  %mm(total of 71values)
No=8*10^6; %m^-4
Rr1=1; %rainfall rate=1mm/hr
b1=4100*Rr1^-0.21;
p1=No*exp(-b1*d*1e-3);%number of drops per unit volume per unit dropsize diameter interval
v1 = d*1e-3.^3;%m^3 volume for one drop
V1 = p1.*v1;%total volume of drops w/ the same diameter

v1_original = d*1e-3.^3; % has units of mm*m^3
% is different than
v1_new      = (d*1e-3).^3; % has units of m^3
% These two estimates are different.
%
% And the (pi/6) factor that I'm talking about drops out with the normalziation below.
% I'm with you, now.
%
% My estimates using v1_orignal and v1_new are:
V1_new = p1.*v1_new;
percent1_new = V1_new/sum(V1_new)*100;
%
percent1 = V1/sum(V1)*100;
figure;
hold;grid;
plot(d,percent1,'b-');
plot(d,percent1_new,'r-');
xlabel('Raindrop Diameter (mm)');
% I would change this label to show that the percentage is with regard to volume
% or to mass (water has unity density, and it's just a change of units).
ylabel('Percent DSD Mass or Volume in 0.1mm intervals');
title('PDF of Marshal-Palmer DSD');


%2nd rain rate=5mm/hr
Rr2=5;%mm hr^-1
b2=4100*Rr2^-0.21;
p2=No*exp(-b2*d*1e-3);%number of drops per unit volume per unit dropsize diameter interval
v2 = d.^3;
V2 = p2.*v1;
percent2 = V2/sum(V2)*100;
plot(d,percent2,'b *-');
%
% how about these calculations?
V2_new = p2.*v2;
```

```
percent2_new = V2_new/sum(V2_new)*100;
plot(d,percent2_new,'r *-');


%3rd rain rate=25mm/hr
Rr3=25;%mm hr^-1
b3=4100*Rr3^-0.21;
p3=No*exp(-b3*d*1e-3);%number of drops per unit volume per unit dropsize diameter interval
v3 = d.^3;
V3 = p3.*v1;
percent3 = V3/sum(V3)*100;
%
plot(d,percent3,'b s-');
%
% And, how about these calculations?
V3_new = p3.*v3;
percent3_new = V3_new/sum(V3_new)*100;
plot(d,percent3_new,'r s-');

legend('rain rate=1mm/hr (old)','rain rate=1mm/hr (new)',...
    'rain rate=5mm/hr (old)','rain rate=5mm/hr (new)',...
    'rain rate=25mm/hr (old)','rain rate=25mm/hr (new)');

figure;
semilogy(d,0.001*p1,'-');
hold on;
grid;
semilogy(d,0.001*p2,'r *-');
semilogy(d,0.001*p3,'k .-');
legend('rain rate=1mm/hr','rain rate=5mm/hr','rain rate=25mm/hr');
xlabel('Raindrop Diameter (mm)');
ylabel('Number of drops per unit volume per DSD log(m^-3mm^-1)');
title('Marshal-Palmer DSD');
%produce doppler spectra
z1=d.^6.*p1;% reflectivity
z2=d.^6.*p2;
z3=d.^6.*p3;

pt=5;%  transmitted power 5watts
%taken an S-band profiler
c=3*10^8;%m s^-1
length=60;%m range resolution
%tao=length/c;
R=10.6*10^3;%m max height 10.6km
lamda=10.6*10^-2; %m wavelength 10.6cm
beamw=5*pi/180;%rad beamwidth
```

```
vol=pi*(R*beamw/2)^2*length;

sigmav1=10^-10*pi^5*0.93.*z1/(lamda*10^2)^4;%m^-1 backscattering cross section per unit
volume
sigma1=sigmav1*vol;%m^2 backscattering cross section
%calculate cross section for different rainrate
sigmav2=10^-10*pi^5*0.93.*z2/(lamda*10^2)^4;
sigma2=sigmav2*vol;
sigmav3=10^-10*pi^5*0.93.*z3/(lamda*10^2)^4;
sigma3=sigmav3*vol;

ant=1.2;%antenna dish 1.2meters
gain1=4*pi*(pi*ant^2/4)/(lamda^2);%antenna gain
pr1=5*gain1^2*lamda^2.*sigma1/(R^4*(4*pi)^3);%radar equation for received power
pr2=5*gain1^2*lamda^2.*sigma2/(R^4*(4*pi)^3);
pr3=5*gain1^2*lamda^2.*sigma3/(R^4*(4*pi)^3);
figure;%plot of rainfall drop vs Power spectrum
plot(d,log(pr1),'-');
hold;grid;
plot(d,log(pr2),'r *-');
plot(d,log(pr3), 'k .-');
title('Power Spectrum vs Dropsize');
xlabel('Raindrop Diameter (mm)');
ylabel('Radar received power in watts');
legend('rain rate=1mm/hr','rain rate=5mm/hr','rain rate=25mm/hr');
%Z=sum(z1);
%vm=3.8.*Z^(71e-3);%assume no downdraft wind
%Z=int(d^6.*p1,d,0,7e-3);
vt=9.65.*(1-1.067*exp(-0.6.*d));%terminal velocity approximation by Atlas
figure;
%plot([0 7],[vm vm],'*-');
%hold;
plot(d,vt,'r');
grid;
title('Raindrop Diameter vs Terminal Velocity');
xlabel('Raindrop Diameter (mm)');
ylabel('Terminal velocity (m/s)');
%doppler frequency shift for terminal velocity
freqs=2*vt/lamda;
figure;
plot(freqs,log10(pr1),'.-');
grid;hold;
plot(freqs,log10(pr2),'r *-');
plot(freqs,log10(pr3),'k .-');
% plot(freqs,pr1,'.-');
% grid;hold;
```

```
% plot(freqs,pr2,'r *-');
% plot(freqs,pr3,'k .-');
title('Power vs doppler frequency');
xlabel('doppler frequency of terminal velocity (Hz)');
ylabel('Radar received power in watts');
legend('rain rate=1mm/hr','rain rate=5mm/hr','rain rate=25mm/hr');
%hold;
%plot(vt,pr1);
%title('power vs terminal fall velocity','r');
figure;
semilogy(vt,pr1,'-');
hold;grid;
semilogy(vt,pr2,'r *-');
semilogy(vt,pr3,'k .-');
title('Radar received power vs terminal fall velocity');
xlabel('Terminal velocity (m/s)');
ylabel('Radar received power in watts');
legend('rain rate=1mm/hr','rain rate=5mm/hr','rain rate=25mm/hr');
```

APPENDIX F

MAIN PROGRAM CODE

F.1

```
filename     = ['spc_p_1998234_'];
start_hour = 3; %%choose any hour from 1 to 5:input the start number of hour data
end_hour= 3; %input the end number of hour data
start_min=48; %input the starting minute of the hour
end_min=50; %input the ending minute of the hour
min_gate=1; %input the start of the range gate
max_gate=1; %input the end of the range gate, the max is up to 40
Zs = []; % initial reflectivity variable
        for hour_num = start_hour:end_hour,
           filename = [filename,'hr',num2str(hour_num),'_v1.mat'];
              disp(['loading: ',filename]);
              load(filename);
              % pspc--reflectivity spectral density[mm^6/m^3/(m/s)]
              [m,n,p] = size(pspc);
                  % for i = 1:max_i, max_i is 60 minute
                  % change i for a different minute
         for i = start_min:end_min,
                 % Get the time information from the phed variable
                 day    = phed(i,7);
                 hour   = floor(phed(i,8)/(60*60));
                 minute = floor((phed(i,8) - hour*(60*60)) / 60);
                 second = phed(i,8) - hour*(60*60) - minute*60;
                 % Assign the moments to vectors:
                 zdb_moment = pzdb(i,:); %all rangegate zdb in a minute
                 vel_moment = (-1)*pvel(i,:); % sign convention needs to be reversed
                 wid_moment = pwid(i,:);%all moments 1x100
                 Vd = pV(i,:);%velocity of each spectral point in spectra [m/s]60x256independant of
hight/rangegate
                 % For each height range, estimate the DSD
                 % Look only at range gates below the freezing level
                 % which is around 4.4 km.(or first 40 rangegate)
                            for j = min_gate:max_gate,
                    % The diameter-to-fallspeed relationship is
                    % dependent on the atmospheric density.
                    ht = prange(i,j);%ran 1st time get 1st minute, j=1 first range gate
                    [Ds,dDs] = VD_relationship_test(Vd,ht);
                    % Load the particular spectrum into an array.
                    spc(1,:) = squeeze(pspc(i,j,:))';
                    thres    = pthr(i,j);
                    % Clean up the Doppler velocity sepectra to keep
                    % only the points above the noise floor.
                    left_min_dB =  120;% set to large value to turn off.
                    right_min_dB = 120;% set to large value to turn off.
                    [spk] = clean_spk_v1_test(Vd,spc,thres,left_min_dB,right_min_dB);
                    % The spectrum in spk does not have any noise values
```

```
                if(zdb_moment(j) >= 0),
                    [Dm, mu, sigma, SSE] = find_mu_Dm_D6_test(Vd, Ds, dDs, spk);
                    f = ~isnan(spk) & (spk > 0);
                    %No = sum(spk(f).*dVd) * (((4+mu)/Dm).^(7+mu))  / gamma(7+mu);
                    No = sum(spk(f)) * (((4+mu)/Dm).^(7+mu))  / gamma(7+mu);
                    Z=[];
                    R=[];
                    [Z,M,R] = My_find_ZMR_v1 (No, Dm, mu);
                    Zs = [Zs;Z];
                    figure;
                      plot(Vd,spk,'k');
                      hold on;grid on;
                       ND = No .* Ds.^(6+mu) .* exp( -((4+mu)./Dm) .* Ds);
                       DSD = ND .* dDs;
                       % Convolve spectra with noise
                       Sv = exp(-((Vd).^2)/(2*sigma^2));
                        Sv = Sv ./ sum(Sv); % normalize to unity area
                       C = conv(DSD,Sv);
                       DSD_conv(1,:) = C((length(Vd)/2)+1:3*(length(Vd)/2));
                       plot(Vd,DSD,'b');
                       plot(Vd,DSD_conv,'r');
                       legend('Original Spectrum','DSD Spectrum','DSD Convolved Spectrum',2);
                        axis([0 12 0 max([ceil(max(spk(f))/10)*10 ceil(max(DSD)/10)*10])]);
                        title(['hr: ',num2str(hour),', min: ',num2str(minute),', rangegate: ',num2str(j),',
ht: ',num2str(ht),', Dm: ',num2str(Dm),', mu: ',num2str(mu),', sigma: ',num2str(sigma)]);
                        xlabel(['Doppler velocity (m/s)'])
                        ylabel(['Spectral Density * dD (mm^6/m^3)']);
                end,% end if(zdb_moment(j) >= 0)
            end,% end for j loop
        end,% end for i loop
    end,% end for hour_num loop

    save Zs_new Zs; %save Zs to any name and compare with corresponding observed
reflectivity "pzdb"
```

F 2

```
function [Ds,dDs,Do,dDo,DSDtrans,density_correction] =
beard_VD_relationship_lba_v2(Vd,ht);
% Adjust the velocity to density corrected terminal velocity (Potential terminal velocity)
% for a fixed range of diameters, find the fallspeed
%Atlas_fallspeed
   xD = [0.01:0.01:20];
   as  =  9.65;
   bs  = 10.3;
   cs  =  0.6;
   Vfall = (as - bs.*exp(-cs.*xD));
```

```
% Vfall is the terminal fallspeed at the surface. Density correction
load density_calc_lba_v1_new
% The density is the variable density_mean.
% Use the range2 (above ground) to determine which density to use.
[x_difference x_index] = min(abs(ht - range2));
density_aloft = density_mean(x_index);
density_surface = density_mean(1);
density_ratio = density_surface / density_aloft;
density_correction = (1/(density_ratio^0.4));
f = isnan(Ds);
if(sum(f)>0),
   Ds(f) = zeros(1,sum(f));
end,% end if(sum(f)>0)
f = isnan(dDs);
if(sum(f)>0),
   dDs(f) = zeros(1,sum(f));
end,% end if(sum(f)>0)
f = isnan(Do);
if(sum(f)>0),
   Do(f) = zeros(1,sum(f));
end,% end if(sum(f)>0)
f = isnan(dDo);
if(sum(f)>0),
   dDo(f) = zeros(1,sum(f));
end,% end if(sum(f)>0)
```

F3

```
function [spk_clean] = clean_spk_test(V,spk,thres,left_min_dB,right_min_dB);
% Clean the spectra assuming that only Rayleigh components are present
[index_zero] = find(V == 0);
if(~isnan(spk(index_zero-1)) & ~isnan(spk(index_zero+1))),
    spk(index_zero) = (spk(index_zero-1)+spk(index_zero+1))/2;
else
    spk(index_zero) = spk(index_zero)*NaN;
end,% end if(~isnan(spk(index_zero-1)) | ~isnan(spk(index_zero+1)),
f = spk < thres;
if(sum(f)>0),
   spk(f) = spk(f)*NaN;
end,% end if(sum(f)>0)
[max_mag i_max] = max(10*log10(spk));
left_min_mag    = max_mag - left_min_dB;
right_min_mag   = max_mag - right_min_dB;
% keep only the values from the peak to the first NaN which should be the noise floor
% Move to the left of the max value
f = ~isnan(spk);
spk(~f) = spk(~f)*NaN;
```

```
good_value = 1;
for k = i_max:-1:1,
  if(isnan(spk(k))),
    good_value = 0;
  end,% end if(isnan(spk(k)))
  if(10*log10(spk(k)) < left_min_mag),
    good_value = 0;
  end,% end if 10*log10(spk(k)) < left_min_mag)
  % If the value is not a keeper, set the spectra value to NaN
  if(good_value == 0)
    spk(k) = NaN;
  end,% end if(good_value == 0)
end,% end for k loop
good_value = 1; % Move to the right of the max value
for k = i_max:1:length(V),
  if(isnan(spk(k))),
    good_value = 0;
  end,% end if(isnan(spk(k)))
  if(10*log10(spk(k)) < right_min_mag),
    good_value = 0;
  end,% end if 10*log10(spk(k)) < right_min_mag)
  % If the value is not a keeper, set the spectra value to NaN
  if(good_value == 0)
    spk(k) = NaN;
  end,% end if(good_value == 0)
end,% end for k loop
spk_clean = spk; % spk has the spectral values that should be fitted.
```

F.4

```
function [Dm, mu, sigma, SSE] = find_mu_Dm_D6_test(Vd, Ds, dDs, spk)
% This routine finds the best mu of a gamma DSD for the inputed D^6 spectrum.
f = ~isnan(spk) & (spk > 0);%index f
z_total = sum(spk(f));
log10_z = log10(spk(f));
Vdoppler_obs = sum(Vd(f) .* spk(f)) / sum(spk(f));%second moment
Wdoppler_obs = sum((Vd(f) - Vdoppler_obs).^2 .* spk(f)) / sum(spk(f));%third moment
mu_range     = [0:1:21];
sigma_range  = [1.0];
row = 0;
for k = 1:length(mu_range),
   mu = mu_range(k);
   % Given the Vdoppler_obs value for this spectra.  For this mu value, find
   % the Dm value that produces the same Vdoppler value.  Call it Dm_z.
   [Dm_z, SSE_Dm_z] = find_Dz_test(Vd, Ds, dDs, mu, Vdoppler_obs);
   [sigma_z, SSE_sigma_z] = find_sigma_z_test(Vd, Ds, dDs, mu, Dm_z, Wdoppler_obs);
   % Construct the spectrum
```

```
    ND = Ds.^(6+mu) .* exp( -((4+mu)./Dm_z) .* Ds);    %
    DSD = ND .* dDs;
    DSD = DSD .* (z_total ./ sum(DSD));% normalize to have the correct total reflectivity    %
    Sv = exp(-((Vd).^2)/(2*sigma_z^2));
    Sv = Sv ./ sum(Sv); % normalize to unity area
    C = conv(DSD,Sv);
    DSD(1,:) = C((length(Vd)/2)+1:3*(length(Vd)/2));
    g = (DSD > 0);
    log10_DSD = DSD.*0;
    log10_DSD(g) = log10(DSD(g));
    Z_SSE = sum((spk(f) - DSD(f)) .^2);
    keep_Dm_z(k)          = Dm_z;
    keep_sigma_z(k)       = sigma_z;
    keep_Z_SSE(k)         = Z_SSE;
    keep_sigma_SSE(k)     = SSE_sigma_z;
    keep_Dm_SSE(k)        = SSE_Dm_z;
end,
% Find the solution with the smallest Dm difference
[sort_value sort_index] = sort(keep_Z_SSE);
% sort_index(1) has the index to the best solution
Dm    = keep_Dm_z(sort_index(1));
mu    = mu_range(sort_index(1));
sigma = keep_sigma_z(sort_index(1));
SSE   = keep_Z_SSE(sort_index(1));
```

F.5

```
function [Z, M, R] = My_find_ZMR_v1(No, Dm, mu)
% Estimate the slope parameter of the gamma DSD
lamda = (4 + mu) / Dm;
% Estimate the Z, M, and R
if(mu > -4),%mu must be greater than -4 in this program
    z = No .* gamma(mu+7) ./ (lamda.^(mu+7));
    Z = 10*log10(z);
    M = No.*(pi/(6*10^3)).*gamma(mu+4)./(lamda.^(mu+4));
    a =  9.65;b = 10.3;c =  0.6;
    term1 = (6 .* pi .* No) .* (gamma(mu+4))./(10000.*lamda.^(mu+4));
    term2         = (a - b .* (1 + c ./lamda).^(-(mu+4)));
    R = term1*term2;
    if(imag(R) > 0),
        R = NaN;
    end,% end if(imag(R) > 0)
else
    Z = NaN;
    M = NaN;
    R = NaN;
end,% end if(mu > -4)
```

LIST OF REFERENCES

[1] Gage, K.S., W.L. Ecklund, W.L. Clark Jr., D.A. Carter, C.R. Williams, P.E. Johnson, 2003, "A low-powered S-band precipitation profiler for hydrological applications," 12th Symposium on Meteorological Observations and Instrumentation, 10.6.

[2] Kollias, P. and Albrecht, B.A., 2003, "Overview of the use of Doppler spectra from profiling radars for cloud and precipitation studies". Atmospheric Science, 3.2.

[3] Collier, C.G., 1996, "Applications of weather Radar systems," Jone Wiley and Sons, 2nd Edition, 24, 14-18.

[4] Williams, C. R., 2002, "Simultaneous ambient air motion and raindrop size distributions retrieved from UHF vertical incident profiler observations," Radio Sci., Vol. 37, No. 2.

[5] Gage, K. S., C. R. Williams, P. E. Johnston, and W. L. Ecklund, 2000, "Doppler Radar Profilers as Calibration Tools for Scanning Radars,"American Meteorological Society, Vol. 39, 2209-2222.

[6] Doviak, R.J., and D.S. Zrnic, 1993, "Doppler radar and weather observations," Acad. Press., 2nd Edition.

[7] Battan, L.J., 1981, "Radar observation of the atmosphere," The University of Chicago Press, Ch4: 29-44, Ch7,8: 84-145.

[8] Williams, C.R., NOAA Aeronomy Laboratory, private communication.

[9] Skolnik, M.L., 2001, "Introduction to radar systems," 3rd edition, 6.

[10] Ulaby, F.T., Moore, R.K. and Fung, A.K., 1981, "Microwave remote sensing: active and passive," Vol.1, Artech House, Norwood, Ch5:256-337.

[11] Steiner, M. and R.A. Houze Jr.,1997, "Sensitivity of estimated monthly convective rain fraction to the choice of Z-R relation," Journal of Applied Meteorology, 36, 452-462.

[12] Marshall, J. S.,and Palmer, W.M.K, 1948, "The distribution of raindrops with size," J. Meteor. 5: 165-66.

[13] Atlas, D. (Ed.), 1990, "Radar in Meteorology," Amer. Meteor. Soc., 11, 1-35.

[14] Uijlenhoet, R., 2001, "Raindrop size distributions and radar reflectivity-rain rate relationships for radar hydrology," Hydrology and Earth Sys. Sci., 5(4), 615-627.

[15] Han, Q, Eubanks, C, Jones, W. L. and T. Kasparis, April 24-29, 2000, "Comparison of TRMM precipitation radar with NEXRAD and in situ Rain Gauges in Central and South Florida", SPIE Proc. AeroSense, Orlando, FL.

[16] Kumar, N.V.P.K. and Rao, D.N., 2000, "Deriving drop size distribution from VHF and UHF Radar spectra," National MST Radar Facility, Gadanki, India.

[17] Ulbrich, C.W., 1983, "Natural variations in the analytical form of the raindrop size distribution," J. Clim. Appl. Meteorol., 22, 1764-1775.

[18] Waldvogel, A., 1974, "The N0 Jump of Raindrop Spectra." Journal of the Atmospheric Sciences, 31, 1067-1978.

[19] Ulbrich, C.W., and P.B.Chilson, 1994, "Effects of variations in precipitation size distribution and fall speed low parameters on relations between mean Doppler fall speed and reflectivity factor," J.Atmos. Oceanic Technol.,11, 1656-1663.

[20] Raghavan, S., 2003, "Meteorology." Kluwer Academic Publishers, 433-435.

[21] Wind Profiler Database: Determination of Moments from Doppler Spectra, 1998. Available on the website:
http://www.al.noaa.gov/wwwhd/pubdocs/tropdyn/msttoga/text/determine_moments.html

[22] Lane, J.E., 1998, "Numerical, Image, and signal processing algorithms applied to radar rainfall estimation," Orlando, FL.